2024-08

Potential use of zero-valent iron in enhancing performance and resource recovery during the anaerobic digestion of domestic sewage

Bakari, Omari

NM-AIST

POTENTIAL USE OF ZERO-VALENT IRON IN ENHANCING PERFORMANCE AND RESOURCE RECOVERY DURING THE ANAEROBIC DIGESTION OF DOMESTIC SEWAGE

Omari Bakari

A Dissertation Submitted in Fulfilment of the Requirements for the Degree of Doctor of Philosophy in Environmental Sciences and Engineering of the Nelson Mandela African Institution of Science and Technology

Arusha, Tanzania

August, 2024

ABSTRACT

Incorporating metallic iron (Fe^0) into anaerobic digesters can improve organics (chemical oxygen demand (COD)), phosphorus, and nitrogen from contaminated water. However, no study has systematically assessed Fe^0-supported anaerobic digestion (AD) systems for removing organic compounds and nutrients from domestic sewage (DS), limiting our understanding of their potential to replace tertiary treatment units. Besides, existing studies often focus on single contaminants at high concentrations, which may not reflect real-world effluents with multiple pollutants. Variations in experimental conditions and the type of wastewater effluent treated complicate comparisons across studies. Additionally, there is a lack of comprehensive evaluations of predictive models for methane (CH_4) yields in Fe^0-supported AD systems, hindering the identification of the most effective model and affecting future research and applications. Moreover, there is little information on sludge characteristics from Fe^0-aided AD systems and their potential applications. This research focused on three primary objectives: (i) assessing the impact of Fe^0 type and dosage in AD systems for the simultaneous removal of COD and nutrients (orthophosphate (PO_4^{3-}), ammonium (NH_4^+), nitrate (NO_3^-)), and (ii) characterizing the solids and biogas in Fe^0-supported AD of DS, and (iii) evaluating the Gompertz, Logistic, and Richard models for methane yield prediction. Two distinct experiments were conducted at various scales. In the first experiment, lab-scale reactors containing DS were subjected to varying dosages of Fe^0 (0 to 30 g/L) over 32 experimental runs conducted for 76 days at a constant temperature of $37 \pm 0.5°C$. In the second experiment, bench-scale reactors with DS were fed with Fe^0 and operated over 15 experimental runs for 53 days at $24 \pm 3°C$ temperature. Iron scraps (SI) and steel wool (SW) were used as the Fe^0 sources. A control experiment was also conducted. It was found out that: (a) the optimal Fe^0 dosage for organic and nutrient removal was 10 g/L SI, (b) NH_4^+ and NO_3^- removal showed the lowest removal efficiency, and (c) maximum removal efficiencies for COD, PO_4^{3-}, and $NH_4^+ + NO_3^-$ were 88.0%, 98.0%, and 40.0% for 10 g/L SI; 88.2%, 99.9%, and 25.1% for 10 g/L SW; and 68.9%, 7.3%, and 0.7% for the control system. Fe^0 significantly enriched nutrients in the sludge, improved settling characteristics, and increased the percentage of methane content in biogas by over 12%. All tested methane prediction models showed good accuracy (error < 10%), with the Richard model demonstrating the highest level of fit (error < 1.6%). These findings confirm the effectiveness of Fe^0-supported AD in removing organics and nutrients from DS, producing agriculturally suitable sludge, and enhancing biogas methane content for potential energy recovery.

DECLARATION

I, Omari Bakari, do hereby declare to the Senate of the Nelson Mandela African Institution of Science and Technology that this dissertation is my original work and that it has neither been submitted nor being concurrently submitted for degree award in any other institution.

Omari Bakari   16/08/2024

Name of Candidate   **Signature**   **Date**

The above declaration is confirmed by:

Prof. Karoli Njau   16/08/2024

Name of Supervisor 1   **Signature**   **Date**

Prof. Chicgoua Noubactep   16/08/2024

Name of Supervisor 2   **Signature**   **Date**

COPYRIGHT

CERTIFICATION

The undersigned certify that they have read and hereby recommend for acceptance by the Nelson Mandela African Institution of Science and Technology, a dissertation titled "**Potential Use of Zero-Valent Iron in Enhancing Performance and Resource Recovery During the Anaerobic Digestion of Domestic Sewage"** in partial fulfillment of the requirements for the award of the Degree of Doctor of Philosophy in Environmental Sciences and Engineering of the Nelson Mandela African Institution of Science and Technology.

Prof. Karoli Njau   16/08/2024

Name of Supervisor 1   **Signature**   **Date**

Prof. Chicgoua Noubactep   16/08/2024

Name of Supervisor 2   **Signature**   **Date**

ACKNOWLEDGEMENTS

DEDICATION

This work is dedicated to the Almighty God, with deep gratitude for His merciful blessings upon me and my family and his continued benevolence in maintaining the prevailing peace and tranquility among all Tanzanians.

TABLE OF CONTENTS

LIST OF TABLES

LIST OF FIGURES

LIST OF PLATES

LIST OF ABBREVIATIONS AND ACRONYMS

AD	Anaerobic Digestion
AK	Acetate Kinase
BK	Butyrate Kinase
Ca	Calcium
CO_2	Carbon Dioxide
COD	Chemical Oxygen Demand
Cr	Chromium
Cr^{3+}	Trivalent Chromium
Cr^{6+}	Hexavalent Chromium
Cu	Copper
DS	Domestic Sewage
Fe	Iron
Fe^0	Zero Valent Iron (ZVI)
H_2O	Water
H_2O_2	Hydrogen Peroxide
K	Potassium
Mg	Magnesium
Mn	Manganese
NH_3	Ammonia
NH_4^+	Ammonium
Ni	Nickel
NO_3^-	Nitrate
ORP	Oxidation Reduction Potential
P	Phosphorus
Pb	Lead
pH	Potential of Hydrogen
PO_4^{3-}	Orthophosphate
PTA	Phosphotransacetylase
S	Sulfur
SI	Iron Scraps
SO_4^{2-}	Sulfate
SW	Steel Wool

T	Temperature
TKN	Total Kjeldahl Nitrogen
TOC	Total Organic Carbon
TP	Total Phosphorus
TS	Total Solids
TSS	Total Suspended Solids
TVS	Total Volatile Solids
TVSS	Total Volatile Suspended Solids
VSS	Volatile Suspended Solids
WAS	Waste-Activated Sludge
Zn	Zinc

CHAPTER ONE

INTRODUCTION

1.1 Background of the Problem

This study highlights the essential role of anaerobic wastewater treatment systems in addressing significant global challenges outlined by the Sustainable Development Goals (SDGs) and Tanzania Development Vision 2025, especially in pollution control and environmental sustainability (Tandari, 2004; Chitonge *et al.,* 2020; Pereira & Marques, 2021). Anaerobic systems are increasingly favored in developing countries for their effective extraction of resources from waste and cost-effectiveness in construction, operation, and maintenance. Despite these advantages, conventional anaerobic systems often yield effluents of inadequate quality and require extended start-up periods to establish and stabilize the biological processes within the system. Meeting regulatory effluent standards requires additional treatment to reduce residual Chemical Oxygen Demand (COD), posing challenges to environmental compliance (Moran, 2018; Show & Lee, 2017). These challenges underscore the urgent need for innovative wastewater treatment approaches to mitigate environmental pollution and ensure sustainable water resource management. The SDGs, particularly Goal 6 (Clean Water and Sanitation) and Goal 14 (Life Below Water), prioritize efficient water use and pollution reduction, aligning closely with Tanzania's Development Vision 2025 focus on sustainable development and environmental protection (Tandari, 2004; Chitonge *et al.,* 2020; Pereira & Marques, 2021). By enhancing the efficiency of anaerobic wastewater treatment systems, this study aims to support these global and national objectives by improving effluent quality, minimizing environmental impacts, and facilitating resource recovery from sewage. This contributes to advancing sustainable water management practices on both local and global scales.

In domestic sewage, nitrogen (N) and phosphorus (P) are commonly found at significant concentrations (Li *et al.,* 2020), which can lead to the eutrophication of surface water sources when not adequately treated (Diatta *et al.,* 2020; Riffat & Husnain, 2022). Several studies have examined and proposed innovative approaches to enhance the efficiency of anaerobic digestion. These approaches encompass pretreatment, co-digestion, digester design (Karki *et al.,* 2021; Nguyen *et al.,* 2021; Shah *et al.,* 2015), and the application of additives (Romero-Güiza *et al.,* 2016). Additives come in various forms, including: (a) ashes from waste

incineration, (b) supplements of macro- (e.g., P, N, and sulfur (S)) and micro- (cobalt (Co), iron (Fe), molybdenum (Mo), nickel (Ni), selenium (Se), and tungsten (W)) nutrients, (c) compounds (bentonite, glauconite, phosphorite, and zeolites) capable of mitigating ammonia inhibition, (d) bioaugmentation, and (e) compounds (e.g., Fe^0 and Fe^{III}) known for their high biomass immobilization capacity (Romero-Güiza *et al.,* 2016).

The Fe^0 materials, in particular, have gained recognition as effective additives for enhancing the performance of anaerobic digestion reactors due to their abundance, ease of manufacturing, cost-effectiveness, non-toxicity, and environmental friendliness (Farooqi *et al.,* 2022; Izadi *et al.,* 2022; Li *et al.,* 2018; Liu & Wang, 2019; Mucha, 2016; Yamada *et al.,* 2015; Zhou *et al.,* 2014).

The Fe^0 materials have demonstrated their performance in several applications, including: (a) Enhancing anaerobic digestion for diverse effluents like domestic wastewater, waste-activated sludge, food waste, palm oil mill wastewater, swine wastewater, and azo dye wastewater (Domrongpokkaphan *et al.,* 2021; Feng *et al.,* 2014; Kong *et al.,* 2016; Wu *et al.,* 2015; Yuan *et al.*, 2020; Zang *et al.,* 2020; Zhang *et al.,* 2011), (b) Improving AD reactors' capability to remove nitrogen and phosphorus from different wastewaters (Deng *et al*., 2020; Florea *et al.,* 2022; Hua *et al*., 2016; Konadu-Amoah *et al.,* 2022b; Till *et al.,* 1998), (c) Improving particular phases within the anaerobic digestion (AD) process, which encompass hydrolysis, acidogenesis, acetogenesis, and Methanogenesis (Feng *et al.*, 2014; Liu *et al.*, 2012; Meng *et al*., 2013; Zhang *et al.,* 2020; Zhang *et al.,* 2015), (d) Regulating pH in specific AD contexts, such as food waste AD (Kong *et al.,* 2016; Yuan *et al.,* 2020), and (e) Increasing the methane (CH_4) content in biogas produced from palm oil mill wastewater, swine wastewater, and activated sludge (Domrongpokkaphan *et al.,* 2021; Feng *et al.,* 2014; Wu *et al.,* 2015).

The Fe^0 materials exhibit their wastewater treatment improvement potentials in various ways, functioning as enzymatic cofactors and facilitating fermentation during hydrolysis. They also effectively alleviate the inhibition of hydrogen sulphide (H_2S) on various microorganisms, including acetogenic, methanogenic, and sulfate-reducing bacteria (SRB), through mechanisms involving pH buffering and iron sulphide precipitation (Liu *et al.,* 2015; Zhong *et al.,* 2022). Furthermore, incorporating Fe^0 materials into wastewater treatment systems promotes bacterial growth, thereby enhancing the efficiency of biological wastewater treatment (Bensaida *et al.,* 2021; Eljamal *et al.,* 2022).

In addition to the intrinsic attributes of Fe^0 materials, operational parameters such as pH, dissolved oxygen (DO), iron dosage, iron pretreatment, mixing conditions, reactor volume, added solution volume, contact time, and temperature exert a significant influence on the performance of Fe^0 materials in pollutant removal (Konadu-Amoah *et al.,* 2022a; Sun *et al.,* 2016; Xiao *et al.*, 2022; Xu *et al.,* 2017). For instance, pH has been reported as a pivotal factor in pollutant removal, with various contaminants displaying specific optimum pH ranges for Fe^0-supported biological wastewater treatment, as observed in studies conducted by Deng *et al.* (2016) and Bai *et al.* (2013).

In the context of anaerobic digestion, Fe^0 materials have been primarily studied for the mechanisms and improvement of various stages in the anaerobic digestion process (hydrolysis, acidogenesis, acetogenesis, and Methanogenesis) for various types of organic waste (Boontian, 2015b; Liu *et al.*, 2012; Xu *et al.*, 2017). Limited research has focused on nitrate or phosphorus removal by Fe^0 in different wastewaters. Notably, most studies involving Fe^0 in anaerobic digestion focused on a single pollutant type with relatively high concentrations, making it challenging to compare results due to variations in experimental conditions (Xu *et al.,* 2017).

By introducing more reactive Fe^0 materials or increasing their amounts, more Fe^0 corrosion products (FeCPs) precipitates are formed. These FeCPs adsorb pollutants while settling, leading to more contaminants entrapped into sludge. In addition to organic and nutrient elements, the sludge may contain macro-nutrients (calcium, magnesium, nitrogen, phosphorus, potassium, sulfur), micro-nutrients (copper, iron, manganese, zinc), carbon, and toxic elements like chromium, nickel, and lead, which must comply to the acceptable limits for agricultural land application (Metcalf *et al.,* 2014; Part, 1994; Wiśniowska *et al.,* 2019b).

The precipitation of sulfur as Fe_2S and nitrogen as $FeNH_4PO_4 \cdot H_2O$ may reduce and inhibit the concentration of gaseous impurities (H_2S and NH_3) in the biogas produced, enhancing the biogas' energy recovery potential with higher methane (CH_4) content and fewer impurities (Akunna, 2018; Pullen, 2015). Biogas emissions must be controlled because CH_4 is approximately 21 times more potent than carbon dioxide (CO_2), which induces the greenhouse effect (McCarty *et al.,* 2011; Pullen, 2015).

The kinetic modelling of CH_4 production is a valuable approach for determining the dominant parameters for the optimum operation of the anaerobic digestion systems, including cumulative specific CH_4 production, maximum specific CH_4 production potential, specific rate of CH_4

production, and phase delay time (Ali *et al.*, 2018; Pererva *et al.,* 2020; Ware & Power, 2017). Globally, there is limited information on kinetic modelling for predicting CH_4 yield from Fe^0-aided anaerobic digestion of domestic sewage.

The variability in the reactivity of different Fe^0 materials is crucial in anaerobic digestion systems. Each Fe^0 material possesses distinct inherent reactivity, meaning they have different abilities to participate in chemical reactions and influence anaerobic digestion (Hu *et al.,* 2019; Lufingo *et al.,* 2019). This intrinsic reactivity of Fe^0 materials is well-documented in the scientific literature, as reported by Hu *et al.* (2019), Lufingo *et al.* (2019) and Noubactep *et al.* (2005). Due to these inherent differences in reactivity, it is expected that different Fe^0 materials will yield varying outcomes in pollutant removal, biogas production, and sludge characteristics when used in effluent treatment systems. The expected differences lead to several aspects, including pollutant removal performances, quantities, and quantity of biogas and sludge produced. However, it is essential to note that while these differences are expected due to the intrinsic reactivity of Fe^0 materials, the significance of these variations is challenging to compare directly. This difficulty arises because past experiments and studies have been conducted under different experimental designs, operating conditions, and specific Fe^0 materials (Xu *et al.,* 2017).

The Fe^0 materials have demonstrated their effectiveness in several applications. However, several challenges remain. Standardized reference material has been lacking in serving as a benchmark. Additionally, the absence of a systematic investigation characterizing the impact of Fe^0 intrinsic reactivity compounds the difficulty of comparing results from different studies (Lufingo *et al.,* 2019). Potential challenges include variations in material properties, inconsistencies in experimental conditions, and differences in measurement techniques.

Consequently, the significance of the differences in the performance of Fe^0-supported anaerobic digestion systems for domestic sewage, including pollutant removal, biogas production, and sludge characteristics, remains a subject of investigation. This study seeks to fill the knowledge gap created by the absence of a systematic investigation characterizing the impact of Fe^0 intrinsic reactivity. It systematically assesses the influence of different types and dosages of Fe^0 materials (specifically SI and SW) on anaerobic digestion, providing insights into their varying effects and implications for effluent treatment systems.

This research explored the potential of Fe^0-aided anaerobic digestion to enhance domestic wastewater treatment by removing organics (COD) and nutrients (PO_4^{3-}, and $NO_3^-+NH_4^+$). It also assessed the effectiveness of Fe^0 in enriching nutrients (nitrogen and phosphorus) in sludge and increasing CH_4 production in biogas reactors. The ultimate goal was to contribute to adopting anaerobic digesters as comprehensive units for both organics and nutrient removal.

1.2   Statement of the Problem

Effluents from anaerobic digestion (AD) processes often require additional treatment to meet regulatory standards due to residual Chemical Oxygen Demand (COD) (Moran, 2018; Show & Lee, 2017; Metcalf *et al.,* 2014). Although AD effectively decomposes organic matter, the remaining effluent frequently contains significant levels of COD, necessitating further treatment to comply with environmental regulations. Additionally, the removal of nitrogen (N) and phosphorus (P) during secondary AD poses considerable challenges, potentially leading to eutrophication in water bodies (Metcalf *et al.,* 2014; Riffat, 2012).

To address these challenges, tertiary treatment methods such as constructed wetlands and sequencing batch reactors (SBRs) are commonly employed (Othman *et al.,* 2010; Riffat, 2012). However, these systems often require substantial space and funding, highlighting the need to enhance AD systems to provide a comprehensive solution for COD and nutrient removal from domestic sewage.

One promising strategy to enhance anaerobic digesters is the incorporation of zero-valent iron (ZVI), which has demonstrated potential for improving COD and nutrient removal by facilitating microbial processes and chemically reacting with contaminants (Boontian, 2015; Xu *et al.,* 2017; Farooqi *et al.,* 2022). However, despite extensive research in the field, no study has systematically assessed the significance of Fe^0-supported anaerobic digestion systems in simultaneously removing organic compounds and nutrients from domestic sewage. This gap hinders our understanding of the potential for anaerobic digesters to serve as comprehensive solutions for both organic and nutrient removal, thereby eliminating the need for tertiary treatment units. Furthermore, existing studies on ZVI supported anaerobic digestion often focus on single contaminants at high concentrations, which may not accurately reflect the complexities of real-world effluents containing multiple contaminants at varying levels (Xu *et al.,* 2017). Many investigations also overlook the impact of different types of zero-valent iron materials on treatment efficiency. Variations in experimental conditions, including

temperature, pH, reactor design, and the type of wastewater effluent treated, complicate comparisons across studies. Additionally, comprehensive evaluations of predictive models for methane (CH_4) yields in Fe^0-supported anaerobic digestion systems are notably lacking. Addressing this gap will help identify the most suitable model for predicting methane yield in Fe^0-aided anaerobic digestion of domestic sewage, thereby saving time and funding in future research and applications.

This comprehensive study seeks to address essential research gaps by systematically comparing different types and dosages of Fe^0 to assess their effectiveness in simultaneously removing organics (COD) and nutrients (PO_4^{3-} and $NO_3^- + NH_4^+$). Additionally, it provides a thorough characterization of the solids and biogas generated during Fe^0-aided anaerobic digestion of domestic wastewater, informing on their quantity and quality, which is crucial for practical waste management applications. Furthermore, the study evaluates the effectiveness of various models, particularly the Logistic, modified Gompertz, and Richard models, to describe the kinetic profiles of CH_4 production during Fe^0-aided anaerobic digestion of domestic sewage, offering valuable insights for future research and practical applications in this field.

1.3   Rationale of the Study

The rationale for this study is grounded in the necessity for further treatment of wastewater effluents generated from anaerobic wastewater treatment systems, primarily to diminish the concentration of residual pollutants, including organic compounds and nutrients. Removing nutrients through anaerobic secondary systems is a notably intricate process compared to dealing with organic pollutants (Metcalf *et al.,* 2014; Riffat, 2012). Furthermore, gaseous impurities such as hydrogen sulphide (H_2S) and ammonia (NH_3) can impede the efficiency of anaerobic digestion.

The study has significant implications for advancing the use of anaerobic digesters as a comprehensive solution for removing organic compounds and nutrients and reducing gaseous impurities such as H_2S and NH_3. This approach increases the percentage volume of methane in biogas, which can be harnessed for energy recovery and enhances the nutrient content in sludge, making it suitable for land application. Additionally, the research identifies the most appropriate model for predicting CH_4 production in Fe^0-supported anaerobic digestion of domestic sewage, which can help streamline resource utilization in future research endeavors.

1.4   Research Objectives

1.4.1   General Objective

To assess the impact of integrating Zero Valent Iron into anaerobic digestion to enhance performance and recover resources.

1.4.2   Specific Objectives

The study aimed to achieve the following specific objectives:

(i)   To investigate the ZVI optimum dosages during the anaerobic digestion of domestic sewage for simultaneous removal of ammonium, nitrate, phosphorus, and COD.

(ii)   To assess the effects of ZVI during anaerobic digestion of domestic sewage on biogas production, focusing on quality and quantity.

(iii)   To assess the quantity and composition of sludge resulting from using ZVI during the anaerobic digestion.

1.5   Research Questions

The study intended to answer the following questions:

(i)   What is the optimum dose of ZVI in anaerobic digestion for simultaneous removal of ammonium, nitrate, phosphorus, and COD?

(ii)   What are the effects of integrating ZVI in anaerobic digestion regarding biogas production and composition?

(iii)   What is the quantity and quality of sludge produced in an anaerobic digester integrated with ZVI?

1.6   Significance of the Study

The significance of this study spans environmental, economic, and scientific dimensions. Enhancing anaerobic wastewater treatment systems supports Sustainable Development Goals (SDGs) 6 and 14, which focus on clean water, sanitation, and marine resource conservation. Improved domestic sewage treatment reduces pollutant loads in natural water bodies,

mitigating eutrophication and aligning with Tanzania's Development Vision 2025. This study demonstrates the potential of zero-valent iron (Fe^0) to enhance anaerobic digestion processes, ensuring better effluent quality and compliance with stringent environmental regulations.

Integrating Fe^0 into anaerobic digesters economically offers a cost-effective alternative to traditional tertiary treatment methods, which require significant space and funding. This integration enhances treatment within existing infrastructure, reducing the need for additional treatment stages. Improved biogas production and quality through Fe^0 addition increases energy recovery potential, lowering operational costs and providing a renewable energy source, contributing to energy sustainability and reducing reliance on fossil fuels.

Scientifically, the study addresses critical research gaps in anaerobic digestion, particularly using Fe^0 materials. By systematically investigating the effects of different types and dosages of Fe^0 on pollutant removal, biogas production, and sludge characteristics, the research provides comprehensive insights into the mechanisms and efficiencies of Fe^0-supported systems. Additionally, by evaluating various kinetic models for predicting methane yield from Fe^0-aided anaerobic digestion, the study offers valuable data for optimizing and scaling up these systems, which contributes to the broader scientific understanding and development of sustainable wastewater treatment technologies, ultimately saving time and resources in future research and applications.

1.7 Delineation of the Study

This study explores and assesses zero-valent iron (Fe^0) use in enhancing anaerobic digestion processes, specifically for domestic sewage treatment. The research addresses unique environmental and infrastructural challenges within the context of Tanzania and is aligned with the country's Development Vision 2025. The findings and implications are particularly relevant to similar global contexts where resource limitations and regulatory compliance drive the need for innovative and cost-effective wastewater treatment solutions.

The study targets parameters with significant environmental impact and regulatory importance, focusing on the simultaneous removal of organic pollutants (COD) and nutrients (ammonium, nitrate, and phosphorus) from domestic sewage. It does not extend to other potential pollutants or types of wastewaters, such as industrial effluents, which may require different treatment approaches.

The investigation is limited to specific types of Fe^0 materials, namely scrap iron (SI) and steel wool (SW), chosen for their availability, cost-effectiveness, and prior demonstrated effectiveness in similar studies. Various dosages of these Fe^0 materials are systematically assessed to determine optimal pollutant removal and biogas production conditions. Other types of Fe^0 materials or combinations with other additives are not considered within the scope of this research.

Experimental methods are employed to evaluate the performance of Fe^0-aided anaerobic digestion systems. This includes controlled laboratory-scale experiments to measure pollutant removal efficiencies, biogas production rates, and sludge characteristics. The study also utilizes kinetic modeling to predict methane yields, focusing on specific models such as the Logistic, modified Gompertz, and Richard models. Field-scale validations or long-term operational studies are beyond the scope of this research.

The study was conducted over two months, which allows for a thorough assessment of the short-term effects of Fe^0 addition on anaerobic digestion processes. Long-term impacts, potential degradation of Fe^0 materials over extended periods, and sustainability assessments beyond the study duration are not addressed. By clearly delineating these boundaries, the study ensures a focused and manageable research process, enabling detailed and reliable conclusions relevant to the specified context and conditions. This focused approach enhances the applicability and practicality of the findings for improving anaerobic wastewater treatment systems in similar environmental and infrastructural settings.

CHAPTER TWO

LITERATURE REVIEW

2.1   Anaerobic Digestion and Circular Economy

Anaerobic digestion (AD) of domestic wastewater epitomizes the circular economy principles by transforming waste into valuable resources, thereby minimizing environmental impact and promoting sustainability (Hussain *et al.,* 2020; Wainaina *et al.,* 2020). At its core, the circular economy aims to close the loop of product life cycles through greater resource efficiency, waste reduction, and the continual use of resources (Wainaina *et al.,* 2020; Subbarao *et al.,* 2023). The AD contributes to these goals by converting organic matter in wastewater into biogas and nutrient-rich digestate, which can be harnessed for productive uses. This process reduces the volume of organic waste, mitigates environmental issues, and produces renewable energy, thus reducing reliance on fossil fuels and lowering greenhouse gas emissions (Hussain *et al.,* 2020; Wainaina *et al.,* 2020; Subbarao *et al.,* 2023).

The AD pathway involves four sequential stages: hydrolysis, acidogenesis, acetogenesis, and Methanogenesis (Metcalf *et al.,* 2014; Henze *et al.,* 2008). In hydrolysis, complex organic molecules such as carbohydrates, proteins, and lipids in domestic wastewater are broken down into simpler compounds, including sugars, amino acids, and fatty acids, making the organic material more accessible for further microbial degradation (Metcalf *et al.,* 2014; Qasim & Zhu, 2017; Dionisi, 2017). During acidogenesis, fermentative bacteria convert these simpler compounds into volatile fatty acids (VFAs), alcohols, hydrogen, carbon dioxide, ammonia, and other by-products (Metcalf *et al.,* 2014; Riffat & Husnain, 2022). In the acetogenesis stage, acetogenic bacteria convert VFAs and alcohols into acetic acid, hydrogen, and carbon dioxide (Metcalf *et al.,* 2014; Riffat & Husnain, 2022). Finally, methanogenic archaea convert acetic acid, hydrogen, and carbon dioxide into methane and water during Methanogenesis (Metcalf *et al.,* 2014; Riffat & Husnain, 2022). This methane, or biogas, can be used for electricity generation and heating or upgraded to biomethane for vehicle fuel or natural gas grid injection. The integration of AD in wastewater treatment aligns with the circular economy by turning waste into a clean energy source and closing the loop on energy use (Hussain *et al.,* 2020; Wainaina *et al.,* 2020; Subbarao *et al.,* 2023).

In addition to energy production, the by-products of AD, particularly nutrient-rich digestate, can be utilized as a soil conditioner or fertilizer in agricultural applications, providing a

sustainable alternative to chemical fertilizers, reducing the environmental impact of fertilizer production and application, and returning valuable nutrients such as nitrogen and phosphorus to the soil, promoting soil health and fertility. This nutrient recycling is a crucial element of the circular economy, enhancing resource efficiency and sustainability. The AD also supports environmental conservation by improving the quality of treated wastewater before it is released into natural water bodies. It significantly reduces the organic load and pathogen levels, protecting aquatic ecosystems and public health (Hussain *et al.*, 2020; Wainaina *et al.*, 2020; Subbarao *et al.*, 2023).

Advancements in AD technology further enhance its alignment with the circular economy and environmental conservation. Innovations such as co-digestion, which combines domestic wastewater with other organic wastes like food waste or agricultural residues, increase biogas yield and overall process efficiency (Chow *et al.*, 2020; Mu *et al.*, 2020; Paranjpe *et al.*, 2023). Adding zero-valent iron (ZVI) in wastewater treatment is another notable advancement (Zhang *et al.*, 2020). The ZVI enhances the breakdown of complex organic compounds and improves biogas production by facilitating electron transfer processes (Xu *et al.*, 2017; Zhang *et al.*, 2020).

2.2   Contribution of Fe^0 in Enhancing the Anaerobic Digestion Pathway

2.2.1   Hydrolysis

Hydrolysis, the initial phase of anaerobic digestion, is crucial for converting particulate organic matter like carbohydrates, proteins, and lipids into simpler compounds such as amino acids, fatty acids, and monosaccharides. This process enhances microbial accessibility by reducing the size of large organic molecules, facilitating their transport across microbial cell membranes (Dionisi, 2017; Ekama & Wentzel, 2008; Riffat, 2012). The hydrolysis process is represented by Equation (1) (Dionisi, 2017).

The Fe^0 ability to generate reactive species, such as Fe^{2+} and H_2 (Equations (4), (5) & (6)), is instrumental in enhancing hydrolysis. These reactive species act as co-catalysts for hydrolytic enzymes, facilitating the breakdown of complex organic compounds, as seen in the hydrolysis of chlorinated solvents. The ZVI transforms pollutants like protein, cellulose, trichloroethene (TCE), and perchloroethene (PCE) into simpler intermediates, making them more susceptible to subsequent microbial degradation (Bhanot *et al.*, 2020; Feng *et al.*, 2014; Sharma *et al.*, 2023; Xu *et al.*, 2017; Zhang *et al.*, 2020).

$$\text{High molecular eight sustances} + \text{Water} \xrightarrow{\text{hydrolysis}} \text{Low molecular weight substrates} \quad (1)$$

Various studies have reported on the contribution of Fe^0 material to enhance the hydrolysis stage of anaerobic digestion processes applied to diverse waste types (Zhang *et al.*, 2020). For instance, the Fe^0 materials have been reported to improve hydrolysis in the anaerobic digestion of dairy wastewater (Shi *et al.,* 2022), pre-concentrated domestic wastewater (Zang *et al.*, 2020), and waste-activated sludge (Feng *et al.,* 2014; Luo *et al.,* 2014; Yu *et al.,* 2016).

According to Antwi *et al.* (2020), Fe^0 promotes Firmicutes and Bacteroidetes, known as hydrolytic bacteria that significantly enhance hydrolysis processes. These bacterial species actively break down complex organic compounds into simpler forms through hydrolytic activities. Firmicutes include various cellulolytic bacteria that contribute to the breakdown of cellulose, while Bacteroidetes are known for their ability to degrade complex organic polymers.

The ZVI serves as a versatile agent, reducing toxic compounds like Cr^{6+} to less harmful Cr^{3+} (Fang *et al.,* 2021; Wu *et al.,* 2009). Similarly, it mitigates the inhibitory effects of non-dissociated H_2S on acetogens, methanogens, and sulphate-reducing bacteria (SRB) by regulating pH (Equation (4)) and inducing iron sulphide precipitation (Equations (6) & (8)). This dual mechanism enhances sulphate reduction capacity and alleviates inhibitory effects on hydrolytic processes, especially in challenging environmental conditions (Liu *et al.,* 2015).

According to Feng *et al.* (2014), Fe^0 significantly enhanced hydrolysis performance in anaerobic digestion by elevating the specific activities of crucial enzymes, including protease, cellulase, AK, PTA, BK, and PTB (expressed as units of enzyme activity per milligram of VSS). The study revealed significant improvements in average enzyme activities with the addition of Fe^0 materials. The ratio of enzyme activity in the system dosed with 20 g/L of Fe^0 compared to the control system was 1.9 for protease, 1.9 for cellulase, 1.8 for AK, 1.8 for PTA, 1.6 for BK, and 1.6 for BPT. Similar results were reported by Shi *et al.* (2022), who found that zero-valent iron (ZVI) enhanced the activity of enzymes such as protease, pyruvate oxidoreductase, and AK, leading to improved hydrolysis. Fe^0 can play a role as a core factor of enzymic activities (pyruvate-ferredoxin oxidoreductase) containing Fe-S clusters and facilitates fermentation in the hydrolysis stage (Boontian, 2015a). These findings demonstrate and confirm the positive impact of Fe^0 on enhancing the specific activities of these enzymes and, consequently, improving hydrolysis efficiency in anaerobic digestion.

The introduction of Fe^0 at concentrations ranging from 1 to 20 g/L exhibited a notable augmentation in the production and selectivity of medium-chain fatty acids (MCFAs) (Wang *et al.,* 2020). At a Fe^0 concentration of 20 g/L, the peak production of MCFAs reached 15.4 g COD/L, showing a substantial increase and a selectivity of 71.7% compared to scenarios without ZVI. Additionally, ZVI played a significant role in enhancing the degradation of WAS, leading to an increase from 0.61 to 0.96 g COD/g VS. The microbial community analysis highlighted an increase in relevant anaerobic species associated with hydrolysis, acidification, and chain elongation, attributable to the presence of Fe^0. Improving anaerobic processes, encompassing solubilization, hydrolysis, and acidification, yielded more substrates (short-chain fatty acids) for MCFAs production.

2.2.2   Acidogenesis

The Fe^0 materials play a beneficial role in enhancing the acidogenesis stage of anaerobic digestion processes applied to diverse waste types (Shi *et al.,* 2022; Zhang *et al.,* 2020). For example, the Fe^0 materials have been reported to enhance the acidogenesis stage in the anaerobic digestion of food wastes (Yuan *et al.,* 2020), swine manure (Yang *et al.,* 2019), artificial wastewater with fixed COD (Liu *et al.,* 2012), dairy wastewater (Shi *et al.,* 2022), and azo dye wastewater (Liu *et al.,* 2012).

The introduction of Fe^0 materials addresses acidification challenges in anaerobic systems by facilitating a transformation in non-acetic VFAs, converting them into acetic fatty acids. This alteration is crucial as it is pivotal in optimizing the performance of the methanogenesis stage, contributing to a more effective and efficient anaerobic digestion process (Kong *et al.*, 2018). Wang *et al.* (2020) noted that the incorporation of Fe^0 materials significantly improved the processes of solubilization, hydrolysis, and acidogenesis in WAS. This enhancement increased the production of crucial substrates, particularly short-chain fatty acids (SCFAs), essential in synthesizing medium-chain fatty acids (MCFAs). Feng *et al.* (2014) observed that introducing Fe^0 in the anaerobic digestion of WAS increased VFA production by 37.3%, leading to a greater acetate yield than propionate in the generated VFAs.

Similarly, Yang *et al.* (2018) reported that incorporating Fe^0 into swine manure appeared to hasten the acidification process, enhancing the production of VFAs and refining the fermentation dynamics. This included reducing the system's oxidation-reduction potential (ORP) level, ranging between -181.7 and -250.0 mV, which favored ethanol-type and butyric-

type fermentation over propionic-type fermentation. Similarly, according to Liu *et al.* (2023), the use of iron filings, iron powder, and nanoscale iron in the anaerobic digestion of corn stalks not only increased the concentrations of VFAs but also tended to facilitate the conversion of propionic acid into acetic acid.

2.2.3 Acetogenesis

Numerous research studies have consistently shown that Fe^0 materials enhance the acetogenesis stage of anaerobic digestion processes applied to diverse substrate types (Kong *et al.,* 2018; Meng *et al.,* 2013; Zhang *et al.,* 2020). As a case in point, the Fe^0 materials have been reported to enhance the acetogenesis stage in the anaerobic digestion of municipal solid wastes (Kong *et al.,* 2018), synthetic medium (Ma *et al.,* 2019), and propionate (Meng *et al.,* 2013).

According to Kong *et al.* (2018), the inclusion of Fe^0 materials is linked to an improved acetogenesis, influencing a transition from butyric-type to propionic-type fermentation and implying a role for Fe^0 in the conversion of non-acetic VFAs into acetic VFAs. Additionally, it has been reported that propionic fermentation occurs at oxidation-reduction potential (ORP) greater than -278 mV (Meng *et al.,* 2013; Ren *et al.,* 2007). In lower ORP, propionic shifts to acetic fermentation, favoring methane production (Fig. 1). The addition of ZVI in the acidogenic reactor simultaneously dropped the accumulation of propionate from 416 to 225 mg/L and raised acetate production from 222 to 408 mg/L. These results were linked to the inherent capacity of ZVI to lower ORP (Liu *et al.,* 2012; Meng *et al.,* 2013).

2.2.4 Methanogenesis

Methanogenesis is the final stage where intermediates like acetic acid, H_2, and CO_2 are converted into methane by methanogens. Carbon dioxide-reducing methanogens use CO_2 and H_2 to produce methane (Equation (3)), while aceticlastic methanogens cleave acetate to produce methane and CO_2 (Equation (2)). About 78% of methane in anaerobic digestion comes from acetate cleavage, with the remaining 22% from CO_2 and H_2. Effective methanogenesis removes H_2 to form acetate and methane (Equation (3)). If methanogenesis is slowed, butyrate and propionate may accumulate, increasing VFA levels and lowering pH, which can hinder waste stabilization (Henze *et al.,* 2008; Metcalf *et al.,* 2014).

Multiple research studies have consistently demonstrated that Fe^0 materials enhance the hydrolysis stage of anaerobic digestion processes applied to diverse wastewater types (Niu *et al.,* 2023; Zhang *et al.,* 2020; Zhong *et al.,* 2022). The Fe^0 materials have been reported to enhance the methanogenesis stage in the anaerobic digestion of sludge (Chen *et al.,* 2020; Lee *et al.,* 2023; Niu *et al.,* 2021; Wang *et al.,* 2018; Zhang *et al.,* 2015; Zhao *et al.,* 2018; Zhou *et al.*, 2020), food waste leachate (Antwi *et al.,* 2020), sulfate-rich wastewater (Paepatung *et al.,* 2020), pharmaceutical industries wastewater (Dai *et al.,* 2022), palm oil mill wastewater (Domrongpokkaphan *et al.,* 2021), swine manure (Meng *et al.,* 2020) and glucose-substrate (Zhong *et al.,* 2022).

The Fe^0 materials have been found to exhibit a dual influence by concurrently augmenting both the syntrophic acetate oxidation (SAO), hydrogenotrophic methanogenesis (HM), and acetoclastic methanogenesis (AM) pathways (Niu *et al.,* 2023). The Fe^0 materials have been reported to support cellular replication, enhance crucial enzyme activity for methane production, and act as mediators by facilitating direct interspecies electron transfer between fermentative bacteria and methanogens (Zhong *et al.,* 2022). Similarly, findings from a separate study conducted by Paepatung *et al.* (2020) document that introducing Fe^0 in the anaerobic treatment of wastewater with elevated sulfate concentrations resulted in a notable enhancement of both the maximum methane yield and methane content. In this context, the experimental group, with the inclusion of Fe^0, exhibited a significant increase to 0.25 L CH_4/g COD added day and 53% methane content, in stark contrast to the control system, which recorded values of 0.07 L CH4/g COD added day and 27% methane content. The findings from the same study (Paepatung *et al.*, 2020) further revealed that Fe^0 played a role in establishing favourable pH levels for methanogenesis and mitigated the toxicity linked to sulphides by precipitating FeS. This process subsequently heightened the competitive advantage of methanogens over sulfate-reducing bacteria (SRB). The findings highlight the significant contribution of Fe^0 in facilitating both the production and concentration of methane within treatment processes for wastewater rich in sulfate.

Moreover, the H_2 that is normally released during the corrosion of ZVI acts as an electron donor to different H_2-respiring microbes such as methanogens (Equation (3)) and denitrifying bacteria (Equation (7)) (Ou *et al.,* 2016).

2.3 Impact of Fe⁰ Materials Size and Dosages in Anaerobic Digestion

The size of Fe^0 material is an essential factor influencing the efficiency of anaerobic digestion, shaping its reactivity and role in microbial transformations. Smaller Fe^0 particles, with their larger surface area, foster superior microbial attachment and interaction, enhancing anaerobic digestion performance. This expanded surface area facilitates reduction reactions, aiding in removing inhibitory substances, thereby contributing to a more efficient digestion process (Dong *et al.,* 2019; He *et al.,* 2022; Ye *et al.,* 2021).

However, using nano and micro-sized Fe^0 particles introduces challenges, including increased aggregation, potential reactor or pipe clogging, and elevated pH levels. These issues arise as the high surface area promotes particle agglomeration, reducing reactivity and limiting their effectiveness. Furthermore, small Fe^0 particles are prone to rapid oxidation, diminishing their longevity and sustained impact on anaerobic digestion. Additionally, nano and micro-sized Fe^0 particles can accelerate H_2 generation, causing problems like inefficient utilization and potential escape from the system. Rapid H_2 generation may create high-pressure zones, risking system disruption (He *et al.,* 2022; Ye *et al.,* 2021).

Conversely, larger Fe^0 particles, while offering reduced surface area, exhibit slower reaction rates, mitigating issues associated with rapid H_2 generation and microbial inhibition. This controlled release of reactive species ensures steady microbial activity without overwhelming the system, minimizes particle aggregation, and reduces the risk of clogging. Larger ZVI particles also exhibit increased resistance to rapid oxidation, ensuring prolonged effectiveness in facilitating microbial transformations. Consequently, optimizing ZVI material size is crucial for maximizing its potential, balancing reactivity, and enhancing anaerobic digestion efficiency while mitigating inhibitory compound impacts in organic waste treatment systems (Hu *et al.,* 2020; Ye *et al.,* 2021).

Varying dosages of Fe^0 materials in anaerobic digestion systems critically influence overall performance and efficiency. These dosages, indicative of the applied amount, intricately shape interactions among Fe^0, microbial communities, and organic matter within the anaerobic environment. Higher Fe^0 dosages improve microbial-mediated activities, augmenting the reactive surface area and enhancing organic compound degradation and methane production. Conversely, lower dosages may decelerate reaction rates, impacting overall efficiency (He *et al.,* 2022; Xu *et al.,* 2019; Ye *et al.,* 2021). The Fe^0 dosages crucially affect the fate of inhibitory

substances; adequate amounts facilitate removal, improving stability, while excess dosages may release reactive iron species, particularly ferrous ions (Fe^{2+}) and H_2O_2, potentially harming the microbial community. The Fenton-like reaction induced by excess Fe^0 results in the rapid generation of ferrous ions, known for their toxicity to microorganisms, disrupting microbial activity and overall system performance (He *et al.,* 2022; Konadu-Amoah *et al.,* 2022b; Xu *et al.,* 2017; Ye *et al.*, 2021).

Additionally, excessive use of ZVI can lead to the production of H_2 peroxide through the catalysis of water decomposition, which, while contributing to the Fenton reaction and organic pollutant degradation, can become detrimental at high concentrations, acting as an oxidative stressor and negatively impact anaerobic microbial consortia and hindering metabolic processes. Dosages also influence H_2 production; higher dosages improve energy recovery benefits, but excess production must be avoided. Reactor or pipe clogging may arise from excessive use of ZVI, necessitating careful optimization based on waste stream characteristics, microbial community, and desired outcomes. Research-driven experiments and monitoring studies are imperative to determine optimal ZVI dosages for enhanced performance, stability, and efficiency in anaerobic digestion systems (He *et al.,* 2022; Konadu-Amoah *et al.*, 2022b; Ye *et al.,* 2021).

Zhong *et al.* (2022) investigated the effects of varying Fe^0 particle diameters (0.1 μm to 250 μm) on glucose substrate anaerobic digestion. Findings indicated that: (a) 2 g/L of 48 μm ZVI optimized methane production by 84.12% compared to the control; (b) 0.1 μm ZVI at 0.5 g/L increased methane production by 37.32%; (c) 4 μm ZVI enhanced the abundance of Bacteroidota, Proteobacteria, and Methanosaeta archaea; (d) Fe^0 particles (4–48 μm) promoted cell replication, enzyme activity, and facilitated direct interspecies electron transfer, reducing cell lysis from the nano effect.

2.4   Influence of Various Fe^0 Material Types on Anaerobic Digestion

The impact of various zero-valent iron (ZVI) materials on anaerobic digestion is multifaceted, with each type influencing different aspects of the process. Iron scraps or shavings, being larger, provide a robust surface area and lower reactivity than nano or microparticles. A sustained and slower release of reactive iron species often characterizes their impact. This can have implications on long-term stability in anaerobic digestion systems, contributing to a gradual and controlled enhancement of microbial activity (Xu *et al.,* 2017).

17

Due to their size, nano-sized Fe^0 particles can offer increased surface area and enhanced reactivity compared to bigger-sized particles (micro-scale Fe^0, iron scraps, iron filings, or steel wool). This elevated reactivity can lead to more rapid microbial transformations, potentially improving the overall efficiency of organic compound degradation and methane production in anaerobic digestion (Liu *et al.,* 2023; You *et al.,* 2017).

Micro-sized particles of ZVI, falling between the larger iron scraps and the nanoparticles, provide a balanced impact. They offer a moderately increased surface area and reactivity, contributing to microbial transformations without the extremes associated with nano-sized particles. This balance can lead to sustained improvement in anaerobic digestion performance without the potential drawbacks of excessive reactivity (Yang *et al.,* 2013).

Dosage optimization is another critical aspect influenced by the type of ZVI material. Each type may require specific considerations for optimal performance. For example, nano-sized particles may necessitate lower dosages due to their higher reactivity, while larger particles may require higher dosages to achieve similar effects. Careful optimization is essential to balance the positive impacts of ZVI with potential drawbacks, such as excessive H_2 production or unintended release of reactive iron species (Xu *et al.,* 2017; Ye *et al.,* 2021).

Therefore, the impact types of ZVI materials in anaerobic digestion encompass a spectrum of characteristics, including reactivity, surface area, inhibition mitigation, dosage optimization, and considerations related to material size and structure. A nuanced understanding of these impacts is essential for tailoring the application of ZVI to specific anaerobic digestion systems optimizing performance, stability, and efficiency.

2.5 Effects of Fe^0 on Pollutant Characteristics within Waste Streams

The effects of zero-valent iron (ZVI) materials on anaerobic digestion are intricately tied to the characteristics of pollutants present in different waste streams (Xu *et al.,* 2017; Ye *et al.*, 2021). The ZVI materials demonstrate effective mitigation for waste streams containing heavy metals. The reactivity of ZVI facilitates the precipitation and removal of heavy metals, preventing their inhibitory effects on microbial activity during anaerobic digestion. This contributes to enhanced stability and performance in treating metal-laden wastes (Li *et al.*, 2023; Xu *et al.*, 2017; Ye *et al.*, 2021).

In the case of waste streams with high concentrations of sulphides, such as sewage sludge, ZVI materials play a crucial role in addressing inhibition issues. The reactivity of ZVI with sulphides results in the formation of less inhibitory species, mitigating the adverse impact on microbial communities. This is particularly beneficial for maintaining optimal conditions in anaerobic digestion systems (François *et al.,* 2023; Paepatung *et al.,* 2020; Xu *et al.,* 2017).

The ZVI materials contribute to the degradation of waste streams characterized by persistent organic pollutants. The enhanced reactivity of ZVI aids in breaking down complex organic compounds, thereby facilitating their conversion into biogas during anaerobic digestion (Xu *et al.,* 2017). This can be advantageous for treating organic-rich wastes, such as industrial effluents or landfill leachate (Dai *et al.,* 2022; Ertugay *et al.*, 2017; Martins *et al.*, 2012; Xu *et al.,* 2017).

The ZVI materials provide a comprehensive solution in waste streams with diverse inhibitory substances, including heavy metals and organic compounds (Li *et al.,* 2023; Xu *et al.,* 2017). Their versatility in addressing various pollutants makes ZVI valuable for promoting stable and efficient anaerobic digestion across different waste compositions.

The Fe^0 improves nitrogen removal in anaerobic digestion through a dual mechanism involving biotic and abiotic processes (Narayanasamydamodaran *et al.,* 2021; Till *et al.,* 1998; Xu *et al.*, 2017; You *et al.,* 2017). Biotically, Fe^0 is a substrate for denitrifying bacteria, fostering an environment conducive to microbial activities. The surface of Fe^0 particles acts as an electron donor, accelerating the denitrification process where nitrate is reduced to nitrogen gas (Equation (11)) (An *et al.,* 2022; Zhang *et al.,* 2023). Simultaneously, abiotically, Fe^0 induces chemical precipitation reactions, particularly with ammonium and phosphorous, resulting in the formation of less soluble compounds such as ferric ammonium phosphates (*FeNH$_4$(HPO$_4$)$_2$ and Fe$_3$NH$_4$H$_8$(PO$_4$)$_6$*) (Equation (12)) (Doussan *et al.,* 1998; Flores-Alsina *et al.,* 2016). This abiotic mechanism leads to the efficient removal of nitrogen from the liquid phase through the precipitation of nitrogen compounds. The synergistic effects of enhanced microbial activity and chemical reactions, facilitated by the increased surface area of Fe^0 particles, contribute to a comprehensive approach to nitrogen removal in anaerobic digestion systems, addressing soluble and particulate nitrogen forms in the waste stream (Curcio *et al.,* 2022; Liu & Wang, 2019; Narayanasamydamodaran *et al.,* 2021; Orbuleţ *et al.,* 2022; Till *et al.,* 1998; Xu *et al.,* 2017; You *et al.,* 2017).

The Fe^0 enhances phosphorus removal in anaerobic digestion through a combination of mechanisms, including forming vivianite and other iron-phosphorus compounds, adsorption, and coprecipitation facilitated by Fe^0 corrosion products (Konadu-Amoah *et al.*, 2023; Konadu-Amoah *et al.*, 2022b; Narayanasamydamodaran *et al.*, 2021). Biotically, Fe^0 promotes the growth of bacteria that rely on an adequate supply of phosphorus as a macronutrient to support their growth, metabolism, and overall biological activities (Xu *et al.*, 2017). Abiotically, as Fe^0 corrodes, ferrous ions are released. These ions react with phosphate ions, leading to the formation of iron-phosphorus compounds such as vivianite ($Fe_2(PO_4)_2$), ferric phosphate ($FePO_4$), Strengite ($FePO_4.2H_2O$) and other forms of iron-phosphorus compounds (Puyol *et al.*, 2018; Zhang *et al.*, 2021). Additionally, ZVI corrosion products create surfaces that adsorb phosphate, effectively removing it from the liquid phase. Coprecipitation occurs as iron corrosion products, including ferric hydroxides (Equation (9)) and other iron-phosphorus compounds (Equation (10)), precipitate along with phosphorus compounds (Konadu-Amoah *et al.*, 2023; Konadu-Amoah *et al.*, 2022a). Therefore, combined biotic and abiotic action of Fe^0 ensures a comprehensive and efficient approach to removing phosphorus in anaerobic digestion, addressing soluble and particulate phosphorus in wastewater.

The Fe^0 corrosion involves the reaction of iron with water or other compounds, releasing ferrous ions (Fe^{2+}) into the surrounding solution (Equation (4)). This process contributes to increased pH, primarily due to the alkalinity generated during ZVI corrosion. The reaction of ferrous ions with H_2O (Equation (4)) or H^+ (Equation (5)) produces hydroxide ions, enhancing the alkalinity of the solution, particularly in the immediate vicinity of ZVI particles. This pH shift can impact anaerobic digestion, as microbial communities involved in this process have specific optimal pH ranges for activity. Altered pH resulting from ZVI-related corrosion may influence the balance of microbial consortia and the efficiency of anaerobic digestion processes (Konadu-Amoah *et al.*, 2022a; Xu *et al.*, 2017; You *et al.*, 2017). Thus, carefully considering potential pH effects related to ZVI corrosion is crucial in designing and managing anaerobic digestion systems to ensure optimal microbial activity and overall system performance (Xu *et al.*, 2017; You *et al.*, 2017).

Furthermore, the effects of ZVI materials extend to reducing overall toxicity in waste streams. By mitigating the effects of inhibitory substances, ZVI enhances the adaptability of microbial communities in anaerobic digestion systems. This adaptability is crucial for maintaining robust and consistent performance, especially in the presence of pollutants (organic and inorganic)

that may otherwise impede microbial activity (Dai *et al.,* 2022; Meng *et al.,* 2020; Xu *et al.,* 2021).

Therefore, the effects of ZVI materials on anaerobic digestion are closely linked to the specific characteristics of pollutants in different waste streams. Whether addressing heavy metals, sulphides, organic pollutants, or a combination of inhibitory substances, ZVI materials demonstrate versatility in promoting efficient and stable anaerobic digestion across diverse waste compositions. The contaminants removal mechanisms through bio-ZVI technologies are summarized in Fig. 2.

$$CH_3COOH \rightarrow CH_4 + CO_2 \tag{2}$$

$$CO_2 + H_2 \rightarrow CH_4 + H_2O \tag{3}$$

$$Fe^0 + 2H_2O \rightarrow H_2 + Fe^{2+} + 2OH^- \tag{4}$$
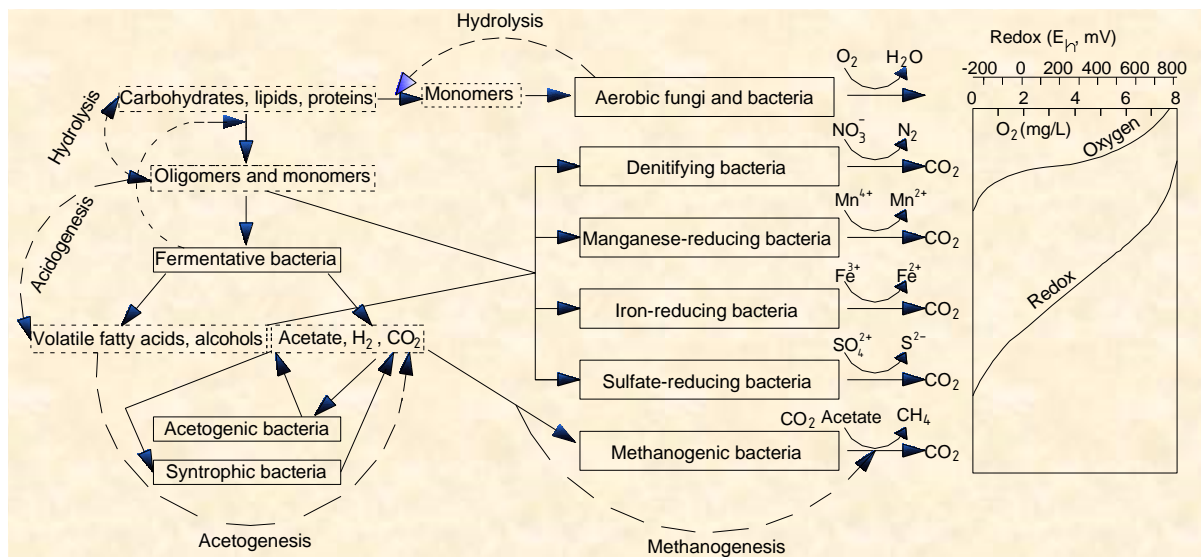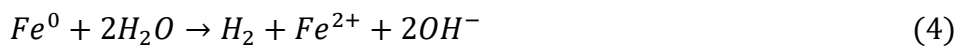
Figure 1: **Degradation of organic matter along an oxidation-reduction (redox) gradient, where organisms are denoted in solid boxes, and chemical processes are represented in dashed boxes**

The solid line curved arrows illustrate alternative acceptors for the oxidation of organic carbon. The desired oxidation-reduction state for each of these transformations approximately correspond to the oxidation-reduction curve depicted on the right.
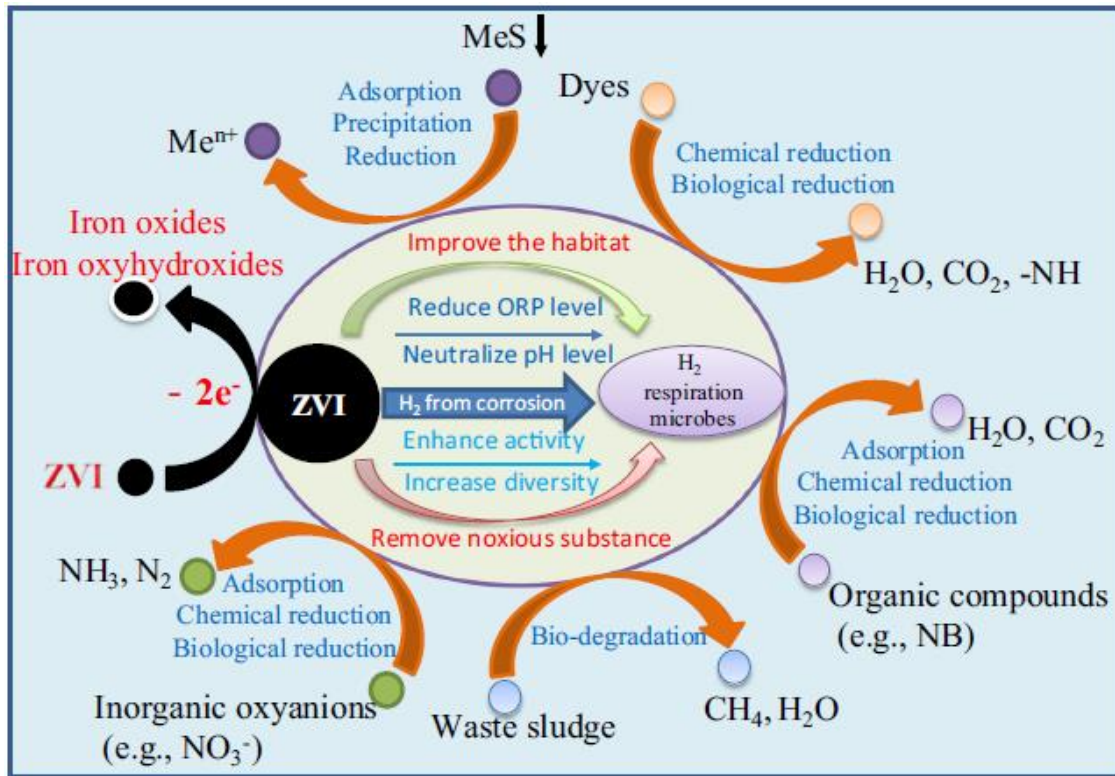
Figure 2: Mechanisms of the enhanced contaminant removal enabled by use of Fe^0 in wastewater treatment. Me^{n+}= metal; MeS↓ = precipitation of metal sulphide; NB = nitrobenzene (Xu *et al.,* 2017)

$$Fe^0 + 2H^+ \rightarrow Fe^{2+} + H_2 \tag{5}$$

$$8H^+ + 4Fe^0 + SO_4^{2-} \rightarrow S^{2-} + 4Fe^{2+} + 4H_2O \tag{6}$$

$$2NO_3^- + 5H_2 \rightarrow N_2 + 4H_2O + 2OH^- \tag{7}$$

$$Fe^{2+} + S^{2-} \rightarrow FeS \tag{8}$$

$$Fe^{3+} + Fe^{2+} + 2H_2O \rightarrow Fe^{II}, Fe^{III} \text{ and mixed oxyhydroxides} \tag{9}$$

$$1.6Fe^{3+} + H_2PO_4^- + 3.8OH^- \xrightarrow{pK = 67.2} Fe_{1.6}H_2PO_4(OH)_{3.8} \downarrow \tag{10}$$

$$Fe^0 + NO_3^- \rightarrow Fe^{2+}/Fe^{3+}/\text{iron oxides} + N_2/NO_2^-/NH_4^+ \tag{11}$$

$$4Fe^0 + NO_3^- + 7H_2O \rightarrow 4Fe^{2+} + NH_4^+ + 10OH^- \tag{12}$$
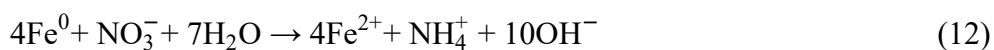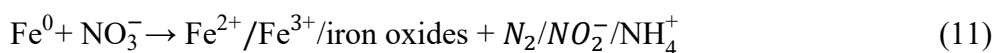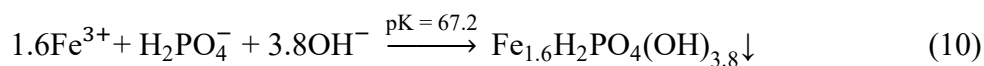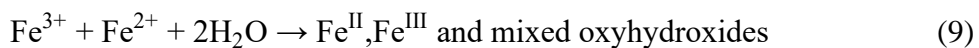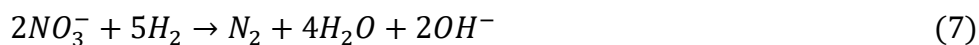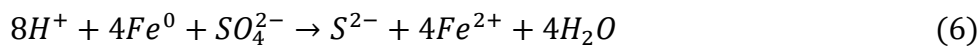
2.6   Characteristics of Domestic Sewage Sludge

2.6.1   Composition

The residues generated through primary, secondary, and advanced processes in wastewater treatment are commonly referred to as sewage sludge. Typically, this substance contains solids

ranging from 0.25% to 12% by weight in a liquid or semisolid state. It is categorized into primary, secondary, and sludge, resulting from advanced treatment processes. Primary sludge comprises settleable solids in untreated wastewater, while secondary sludge comprises biological solids and additional settleable components (Metcalf *et al.,* 2014; Riffat & Husnain, 2022).

While often considered waste, the sludge contains valuable nutrients, including nitrogen, phosphorus, and potassium. Furthermore, when properly treated and stabilized, sludge has the potential to serve as a resource for soil improvement and fertility enhancement. Besides, untreated sludge may harbor pathogenic microorganisms, including bacteria, viruses, and parasites. Ensuring the reduction of pathogen levels through proper treatment is imperative to meet health and safety standards for sludge management. Additionally, trace amounts of heavy metals, such as lead, cadmium, and mercury, may be present in domestic wastewater sludge due to inputs from household activities (Jamali *et al.,* 2007; Metcalf *et al.,* 2014; Riffat & Husnain, 2022).

Several household activities contribute to the presence of heavy metals in domestic wastewater. Common sources include the use of household cleaning products with heavy metal ingredients. These painting and renovation activities release metals from paints and construction materials, gardening practices involving the use of pesticides containing metals, corrosion of metal plumbing and fixtures, improper disposal of electronic waste and batteries, personal care products containing heavy metals, utensils, and cookware made from certain metals, vehicle maintenance activities, improper disposal of medications, and the use of fertilizers containing heavy metals in gardening or landscaping. These activities collectively introduce heavy metals such as copper, zinc, lead, mercury, and cadmium into domestic wastewater, posing environmental and water quality concerns (Kalinowska *et al.,* 2020).

2.6.2 Settleability

(i) Significance of Sludge Settleability in Wastewater Treatment

Assessing the settleability of sludge is essential in wastewater treatment processes (Qasim & Zhu, 2017). The capacity of sludge particles to settle not only guarantees the clarity of treated water by meeting stringent effluent quality standards but is also pivotal in averting the discharge of turbid or cloudy water, thereby mitigating potential environmental pollution and safeguarding aquatic ecosystems (Metcalf *et al.,* 2014; Qasim & Zhu, 2017; Riffat & Husnain,

2022). Moreover, the influence of sludge settleability extends to downstream treatment processes, where proficient settling facilitates enhanced dewatering, reducing sludge water content. This streamlined settleability not only eases the handling, transportation, and disposal of sludge but also substantially contributes to the overall operational efficiency of wastewater treatment plants (Qasim & Zhu, 2017; Riffat & Husnain, 2022). Furthermore, the systematic assessment of settleability proves indispensable for optimizing treatment facility design and operation. By comprehending the settling characteristics of sludge, operators can strategically adjust process parameters, such as detention time and flocculation conditions, to enhance the settleability. This proactive approach is instrumental in averting operational challenges, like sludge carryover in the effluent, thereby preventing regulatory non-compliance and potential environmental repercussions. Settleability assessments offer valuable insights into the intricate biological and chemical factors influencing sedimentation. Detecting changes in settleability allows for identifying variations in the influent wastewater composition or potential issues within the biological treatment stages (Metcalf *et al.,* 2014; Qasim & Zhu, 2017; Riffat & Husnain, 2022).

(ii)   Settling column

The settling column is a fundamental tool in wastewater treatment, playing a crucial role in evaluating the settleability of solids. Its primary purpose is to offer essential insights into critical parameters, including overflow rates, solids removal efficiency, and settling times. The apparatus is designed with a circular cross-section column featuring strategically positioned sampling ports at various depths. A column measuring 3 meters in height with a diameter of 150 mm and equipped with 5 to 6 sampling ports is well-suited for this purpose. This design enables the systematic collection of samples throughout the settling process, providing a detailed and dynamic perspective on solids' behavior in wastewater. The strategic placement of sampling ports at different depths is instrumental in collecting samples representing various layers within the settling column. This spatial distribution of sampling ports is crucial for comprehensively understanding how settling characteristics vary at different levels, offering a holistic view of the overall settleability of the solids (Metcalf *et al.,* 2014; Piro *et al.,* 2011; Riffat & Husnain, 2022).

Settling column analysis involves a systematic analysis of the influent and effluent samples collected at various depths within the settling column. A representative sample of the wastewater or sludge is introduced into the settling column to initiate the determination

process. Sampling ports, strategically positioned at different depths, facilitate the collection of samples at regular intervals during the settling period. The TSS concentration in both the influent and effluent samples is then analyzed using appropriate laboratory methods. The influent TSS concentration represents the initial suspended solids content introduced into the settling column, while the effluent TSS concentration reflects the residual suspended solids content after settling has occurred (Piro *et al.,* 2011).

The TSS removal efficiency is another critical parameter determined through the settling column analysis. This efficiency is calculated by comparing the influent (initial concentration, C_0) and effluent (concentration at any time, C_{ti}) (Equation (13)). The ability to collect samples at various depths allows for a nuanced analysis of how efficiently solids are removed across different layers of the settling column. Identifying variations in removal efficiency helps pinpoint potential issues and fine-tune operational parameters for improved performance (Metcalf *et al.,* 2014; Piro *et al.*, 2011; Riffat & Husnain, 2022).

Equation (3) is employed to calculate the percentage removal of Total Suspended Solids (TSS), and these calculated values are depicted as data points. Subsequently, these data points are graphically represented against both time and depth, leading to the creation of isoremoval curves, as illustrated in Fig. 3. The settling velocity, also known as the overflow rate, and the overall efficiency of TSS removal obtained from particle settling analysis for each reactor are calculated using the curves depicted in Figure 2.3, along with the application of Equations (14) and (15) (Metcalf *et al.,* 2014; Piro *et al.,* 2011; Qasim & Zhu, 2017; Riffat & Husnain, 2022).

The overflow rate (settling velocity), calculated using Equation (14), reflects the hydraulic loading on the settling tank (Equation (3)). By observing the behavior of the settling solids under different overflow rates, operators can gain insights into the system's capacity and identify optimal conditions for efficient settling. This information is important in the design and operational adjustments of settling tanks within the wastewater treatment plant (Metcalf *et al.,* 2014; Piro *et al.,* 2011).
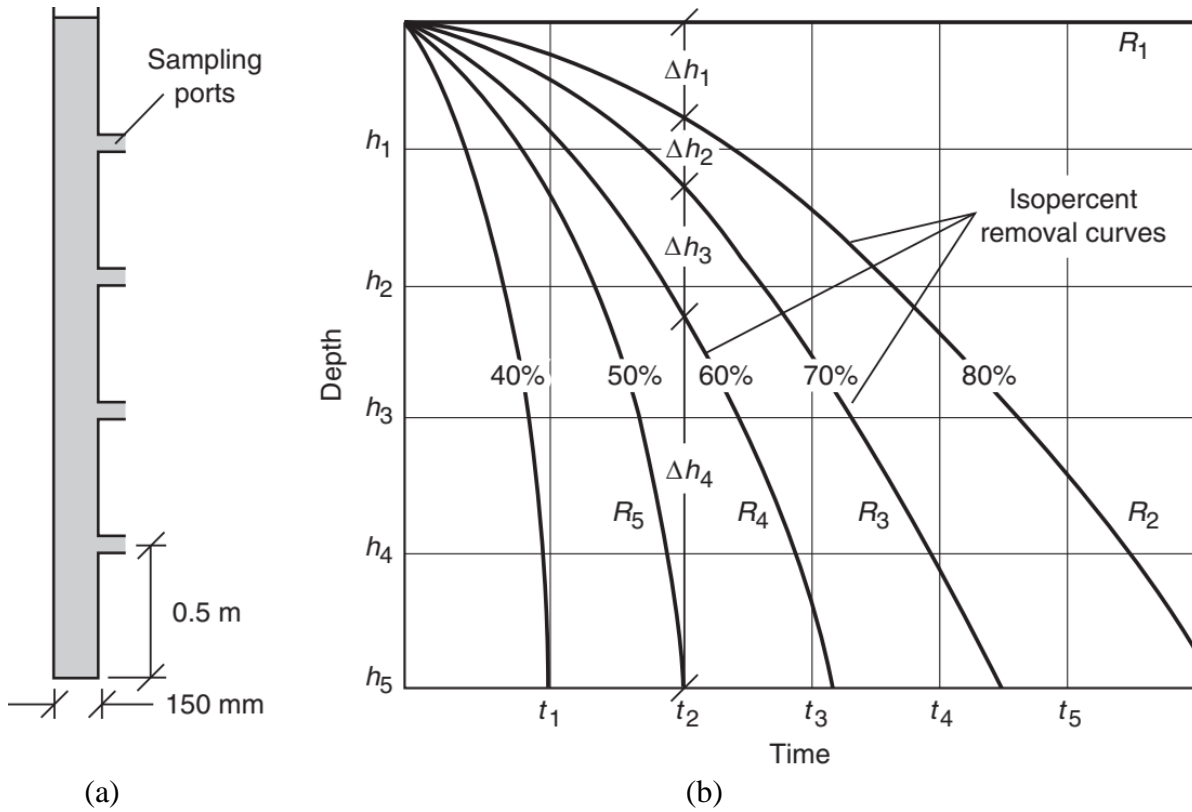
Figure 3: **Illustrative diagram detailing the settling column analysis of flocculent solids: (a) Settling column setup, (b) Isoremoval curves illustrating settling column analysis (Metcalf *et al.,* 2014)**

$$\eta = \left(\frac{C_0 - C_{ti}}{C_0}\right) \times 100 \tag{13}$$

Where; η = TSS removal efficiency (%), C_0 = Initial TSS concentration (mg/L), and C_{ti} = TSS concentration observed at time t for i^{th} port (mg/L).

$$V_s = \frac{H}{t_s} \tag{14}$$

Where; V_s = Settling velocity (m/min), H = side water depth that is equal to or less than settling column height (m), and t_s = time required to achieve a particular percentage removal of particles in the settling column analysis (min).

$$R_T = \frac{\Delta h_1}{H}\left(\frac{100 + R_1}{2}\right) + \frac{\Delta h_2}{H}\left(\frac{R_1 + R_2}{2}\right) + \ldots + \frac{\Delta h_n}{H}\left(\frac{R_n + R_{n+1}}{2}\right) \tag{15}$$

26

Where; R_T = Overall TSS removal, (%), $\Delta h_1, \Delta h_2, \ldots, \Delta h_n$ = vertical distance between two consecutive curves of equal percent removal, (m), $R_1, R_2, \ldots\ldots\ldots, R_n$ = consecutive isoremoval curves, (%).

(iii) Sludge Volume Index

The Sludge Volume Index (SVI) measures sludge classification based on its settling characteristics in wastewater treatment. This parameter provides valuable information about the settling behavior of activated sludge, aiding in the assessment and optimization of the treatment process. The Sludge Volume Index (SVI) is determined through a settleability test. The procedure involves placing a mixed-liquor sample into a cylindrical container with a volume between 1 to 2 liters. After a specific duration of 30 minutes, the settled volume (Vs) is accurately measured, and concurrently, the concentration of Mixed Liquor Suspended Solids (MLSS) within the sampled mixture is recorded. The SVI is then calculated using Equation (16) (Metcalf *et al.*, 2014; Torfs *et al.,* 2016).

$$SVI = \frac{V_s}{MLSS} \qquad\qquad (16)$$

Here, SVI is expressed in milliliters per gram (mL/g), *Vs* is the settled volume in milliliters, and MLSS is the mixed liquor suspended solids concentration in grams per liter. The resulting SVI value is a crucial indicator of the sludge's settleability.

Interpreting SVI values involves classifying sludge into different categories. A low SVI (typically below 100 mL/g) indicates good settling sludge, suggesting that the sludge settles rapidly and forms a dense, compacted blanket in the clarifier. This is desirable for effective solid-liquid separation. Conversely, a high SVI (above 150 mL/g) implies poor settling sludge, where the particles settle slowly or incompletely, leading to a less efficient clarification process. SVI values between 100 and 150 mL/g suggest moderate settling characteristics, prompting further investigation and potential process adjustments (Metcalf *et al.,* 2014; Torfs *et al.,* 2016).

The SVI is a tool for day-to-day process control in wastewater treatment plants. Regular monitoring allows operators to make timely adjustments to the treatment process, optimizing conditions for effective settling. Troubleshooting is another critical application of SVI; elevated values may indicate issues such as filamentous bulking or problems with biomass

settling. Identifying these issues early enables operators to implement targeted solutions, preventing adverse impacts on effluent quality (Metcalf *et al.,* 2014).

Furthermore, SVI serves as a design parameter in the planning and design of wastewater treatment facilities, particularly in the sizing and configuration of secondary clarifiers. The data obtained from SVI tests are instrumental in determining the appropriate dimensions of settling tanks, ensuring optimal settling conditions and efficient removal of suspended solids (Metcalf *et al.,* 214).

2.7 Modelling of Methane Production

2.7.1 Microbial Growth A Basis for Methane Modeling

Figure 4 exhibits various common cumulative methane production curves, as discussed by Koch *et al.* (2019), Labatut *et al.* (2011), and Ware and Power (2017). These studies emphasize the importance of these curves in assisting the identification of crucial biodegradability characteristics in the substrate and addressing any inhibition issues that may arise. The analysis of these curves can be substantially improved by employing mathematical models to understand the kinetics of methane production. This modeling approach provides an enhanced understanding of how the substrate behaves throughout the anaerobic digestion, offering more profound insights into its dynamics and behavior (Koch *et al.,* 2019; Labatut *et al.,* 2011; Ware & Power, 2017). The application of growth curves stands as a crucial analytical tool in various studies, elucidating the progression of a variable throughout a specific time frame until it nears its saturation point. In the context of bacterial growth, these curves exhibit a distinct pattern. Initially, the specific growth rate commences at zero.

Subsequently, it accelerates to attain a maximum growth rate (μ_m) within a defined timeframe known as the lag phase (λ), as illustrated in Fig. 5 (Koch *et al.*, 2019; Labatut *et al.*, 2011; Ware & Power, 2017). Furthermore, these growth curves encompass a concluding phase wherein the growth rate diminishes, eventually reaching zero. This signifies the point of saturation or the maximum asymptote (A). The occurrence of indefinite growth beyond the initial moments is implausible, as it contradicts logical and physical principles. As a result, a representative curve for a growth process typically takes on a sigmoidal form, as demonstrated in Fig. 2. This curve conventionally features a lag phase immediately following t = 0, succeeded by an exponential phase, and ultimately transitioning to a stationary phase (Huang, 2013; Koch *et al.,* 2019; Labatut *et al.*, 2011; Ware & Power, 2017; Zwietering *et al.,* 1990).

Microbial growth and methane production kinetics are closely intertwined processes within anaerobic digestion systems, where microorganisms play a pivotal role in converting organic matter into methane. Understanding the relationship between microbial growth and methane production kinetics is crucial for optimizing biogas generation. The lag phase initiates microbial growth, representing a period of adaptation and preparation for active metabolism. During this phase, microorganisms acclimate to the substrate and environmental conditions. The temporal dynamics observed in the lag phase provide essential insights into the initiation of microbial activity, influencing subsequent methane production kinetics (Dionisi, 2017; Metcalf *et al.,* 2014; Qasim & Zhu, 2017; Riffat & Husnain, 2022).

Methane production kinetics escalate as microbial growth progresses into the exponential phase, characterized by rapid cell division and metabolic activity. The specific growth rate (μ), a key parameter in microbial growth models, mirrors the efficiency of methane production during this phase. The faster the microorganisms multiply, the more effectively they utilize organic substrates, increasing methane production (Metcalf *et al.,* 2014; Qasim & Zhu, 2017; Riffat & Husnain, 2022; Ware & Power, 2017).

The transition to the stationary phase in microbial growth corresponds to a decrease in growth rates, mirroring the gradual decline in methane production rates observed in anaerobic digestion.
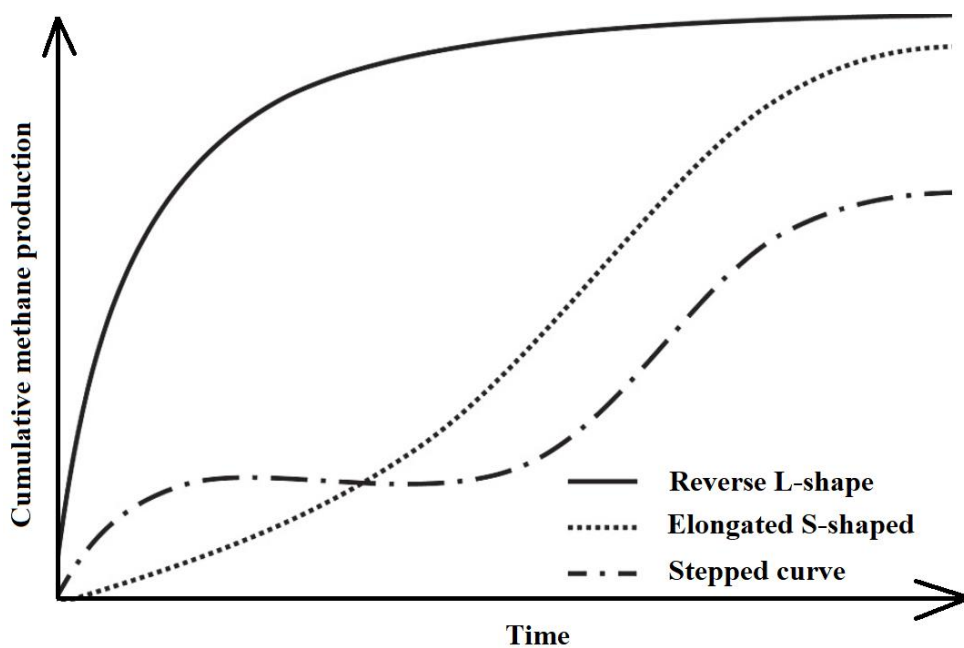
Figure 4:   **Illustrative Cumulative Methane Production Curves (Koch *et al.,* 2019; Labatut *et al.,* 2011; Ware & Power, 2017)**
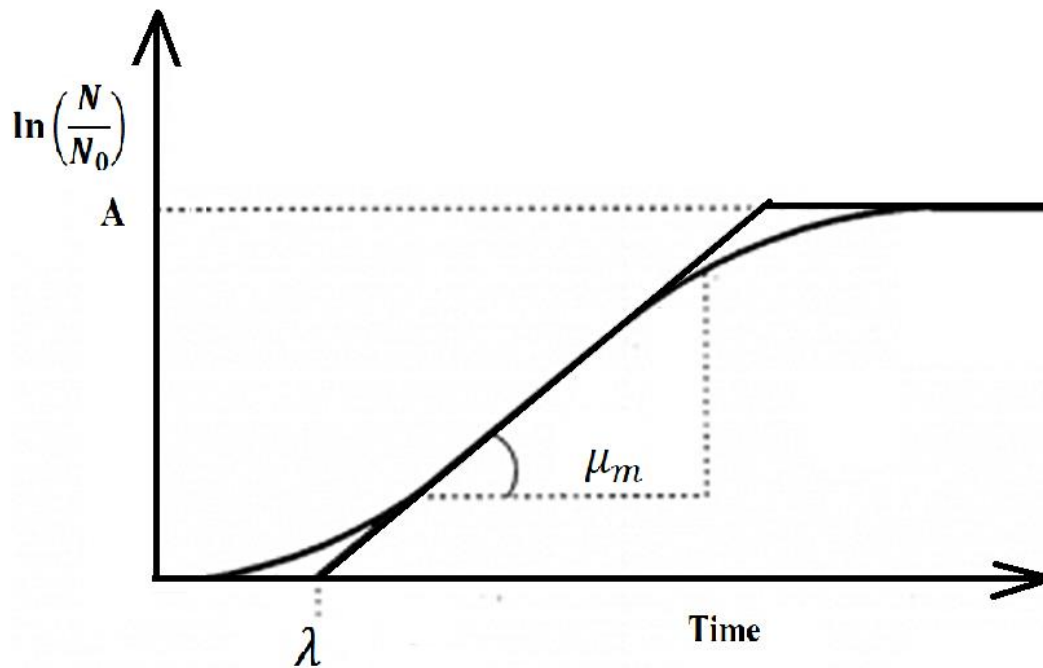
Figure 5: **Typical Bacterial Growth Curve (Huang, 2013; Ware & Power, 2017; Zwietering *et al.,* 1990)**

Factors such as nutrient depletion, the accumulation of inhibitory substances, and the stabilization of microbial populations influence the growth plateau and the reduction in methane production. The specific growth rate approaches zero during this phase, impacting the overall methane production kinetics (Metcalf *et al.,* 2014; Qasim & Zhu, 2017; Riffat & Husnain, 2022; Ware & Power, 2017; Zwietering *et al.,* 1990).

Parameters derived from microbial growth models, including lag time and specific growth rate, are crucial for constructing kinetic models for methane production. These models integrate complex equations that consider various factors influencing microbial activity, substrate utilization, and environmental conditions. Lag time provides insights into the duration before significant methane production begins, while the specific growth rate quantifies the efficiency of methane-producing microorganisms (Koch *et al.,* 2019; Ware & Power, 2017).

Therefore, microbial growth phases, from lag to exponential to stationary, directly influence the efficiency and dynamics of methane production. The relationship between these processes is essential for developing accurate models, optimizing conditions, and ensuring the sustainable generation of methane in biogas production.

2.7.2 Kinematic Models for Methane Production

Several criteria are crucial when selecting models to predict methane yield in the anaerobic digestion of wastewater (Donoso-Bravo *et al.,* 2011). Accuracy is paramount, as the model must reliably reflect empirical data and experimental results (Donoso-Bravo *et al.,* 2011; Metcalf & Eddy, 2014). The model's complexity should align with the data available and the specific needs of the process, balancing between detailed models, which use intricate biochemical kinetics, and simpler empirical models (Metcalf & Eddy, 2014). Data requirements, scalability, and flexibility ensure that the model can adapt to different wastewater types and operational conditions. Validation with real-world data, ease of use, computational efficiency, and integration with existing systems is critical for practical application (Metcalf & Eddy, 2014). Additionally, incorporating sensitivity and uncertainty analyses helps assess the impact of parameter variations on methane yield predictions, enhancing the model's robustness (Barahmand & Samarakoon, 2022; Barahmand *et al.,* 2023).

Various models have been employed to assess the kinetics of methane (CH_4) production, as documented in multiple studies (Mohamed *et al.,* 2018; Pererva *et al.,* 2020; Ware & Power, 2017). The models include the modified Richard (Equation (17)), Gompertz (Equation (18)), First Order (Equation (19)), and Logistic (Equation (20)). However, the modified Gompertz, Logistic, and Richard models are considered among the most suitable for predicting CH_4 generation (Bakraoui *et al.,* 2019). These models predict cumulative CH_4 yield, estimate CH_4 generation potential, determine the daily maximum CH_4 generation, and establish the lag phase required to initiate CH_4 production (Zhao *et al.,* 2018). Using diverse models provides a comprehensive framework for understanding and predicting the complex kinetics associated with methane production in different contexts and environmental conditions.

The selection of models for predicting methane production kinetics in anaerobic digestion is based on their ability to fit best the experimental data obtained from an anaerobic digestion system. The most suitable model demonstrates the closest alignment with the observed data, exhibiting minimal differences between predicted and observed values. The best-performing model achieves the highest correlation coefficient (R^2), indicating its superior accuracy compared to other models that show less precise fits. The selection process thoroughly compares cumulative methane production over digestion time for each model against the experimental results, ensuring that the chosen models accurately capture the methane

production dynamics under the studied conditions and provide reliable predictions and insights into the anaerobic digestion process (Bakraoui *et al.,* 2019).

$$y = A. \left\{ 1 + v. \exp(1+v). \exp\left[\frac{\mu_m}{A}.(1+v).\left(1+\frac{1}{v}\right).(\lambda - t) \right] \right\}^{\left(\frac{1}{v}\right)} \tag{17}$$

$$y = A. \exp\left[-\exp\left(\frac{\mu_m.e}{A}.(\lambda - t) + 1 \right) \right] \tag{18}$$

$$y = A \times [1 - \exp(-k_0 \times t)] \tag{19}$$

$$y = \frac{A}{\left[1 + \exp\left(\frac{4\mu_m}{A}.(\lambda - t) + 2 \right) \right]} \tag{20}$$

Where: y = cumulative specific CH_4 production (mLCH$_4$/gVS); A = maximum specific CH_4 production potential (mLCH$_4$/gVS); μ_m = specific rate of CH_4 production (mL/gVS/d); e = exp(1) = 2.7182; λ = phase delay time (days); t = incubation time (days); and v = shape coefficient of the curve.

This study seeks to identify the most suitable model for predicting methane (CH_4) production in Fe^0-supported anaerobic digestion of domestic sewage. By comparing various models with experimental data, the study aims to pinpoint the model that most accurately captures the kinetics of methane production in this specific setting. Selecting the best-fitting model is essential as it enables researchers to optimize resource utilization by concentrating on the most effective predictive tool. This focused approach can significantly enhance the efficiency of future research by providing a reliable framework for refining the anaerobic digestion process, boosting methane yield, and potentially lowering the costs associated with experimental trials and resource management. The accuracy and dependability of the chosen model will be essential in advancing both the understanding and practical application of Fe^0-supported anaerobic digestion for treating domestic sewage.

CHAPTER THREE

MATERIALS AND METHODS

3.1   Effects of Zero-Valent Iron on Pollutants Removal

The experiments in this section aimed to compare different types and dosages of Fe^0 for the simultaneous removal of organics (COD) and nutrients (PO_4^{3-} and $NO_3^- + NH_4^+$) from domestic sewage. Anaerobic batch reactors were operated at $37 \pm 0.5°C$ for 76 days. Samples from the Fe^0-supported anaerobic batch reactors and a control reactor (without Fe^0) were analyzed to assess their effectiveness in pollutant removal, particularly COD, PO_4^{3-} and $NO_3^- + NH_4^+$. The comparison criteria included (a) variations in pollutant removal performance among reactors with different Fe^0 dosages (ranging from 0 to 30 g/L) and (b) differences between reactors dosed with different types of Fe^0 materials (SI or SW).

3.1.1   Sludge and Wastewater

Sludge used as the inoculum was obtained from the operational septic tank used for treating domestic wastewater from the students' hostel at the Nelson Mandela African Institution of Science and Technology (NM-AIST). The sludge was collected using a long-handled scoop, and it was obtained from the lower section of the septic tank while carefully avoiding the scum layer. Subsequently, the sludge was transferred into a prepared plastic container before being dispatched to the laboratory for analysis. The characteristics of sludge are detailed in Table 1. On the other hand, the wastewater used in this study was collected from beneath the scum layer at the inlet zone of the septic tank to minimize the presence of floating objects, oil, and grease. The specific characteristics of this wastewater sample are also presented in Table 1.

Table 1: **Essential quality of inoculum sludge and tested domestic wastewater**

Parameters	M (n =3)	SD (n = 3)
I – Quality of Inoculum sludge		
pH	6.80	0.02
Chemical oxygen demand, COD (gCOD/L)	3.425	0.006
Total solids, TS (gTS/L)	12.85	0.07
Total volatile solids, TVS (gVS/L)	7.71	0.06
Volatile Suspended solids, VSS (gVSS/L)	5.25	0.08
Total phosphorus, TP (mg P/L)	165	3.1
Total Kjeldahl Nitrogen, TKN (mg/L)	885	5.5
II – Quality of tested domestic wastewater		
Potential of hydrogen, pH	7.50	0.01
Temperature, T (^{o}C)	22	0.1
Chemical oxygen demand, COD (mgCOD/L)	408	4.5
Orthophosphate, PO_4^{3-} (mg PO_4^{3-}/L)	17.8	0.9
Nitrate, NO_3^- (mg NO_3^-/L)	19.8	0.5
Ammonium, NH_4^+ (mg NH_4^+/L)	53.1	2.0

"M" stands for mean, and "SD" for standard deviation.

3.1.2 Fe^0 Materials Sources and Composition

Table 2 shows the elemental composition, and Plate 1 presents the size specifications for the Fe^0 materials utilized in this study. Both iron scraps and steel wool were used as Fe^0 materials. The steel wool was identified by the commercial product code FGSK003. These materials were chosen for the experiment based on their ready availability, affordability, and proven reactivity in previous experiments (Hu *et al.,* 2019; Lufingo *et al.,* 2019).

Table 2: Elemental composition of tested Fe^0 materials, LOD stands for the lowest

Name	Elemental composition (%)							
	Fe	Cu	Ni	Cr	Mn	Sn	Nb	Mo
Steel wool (SW)	99.25	0.09	0.09	0.04	0.50	< LOD	< LOD	< LOD
Iron scraps (SI)	98.68	0.33	0.15	0.27	0.40	0.07	0.01	0.02

The Iron scrap materials were the leftovers produced by the Mbeya University of Science and Technology (MUST) lathing machines. Steel Wool (Africa) Limited crafts the commercial steel wool product. It is noteworthy that neither of these materials was shielded from air oxidation. The steel wool materials used contained 99.25% iron, whereas the iron scraps materials displayed a composition of 98.68%, as presented in Table 2. The elemental composition of the Fe^0 materials was analyzed with the Bruker S1 TITAN 800 XRF spectrometer (Bruker, Billerica, MA, USA). The steel wool material was sliced into 25 mm segments, whereas the Iron scraps varied in size, falling within the 4 mm to 20 mm range, as depicted in Plate 1.
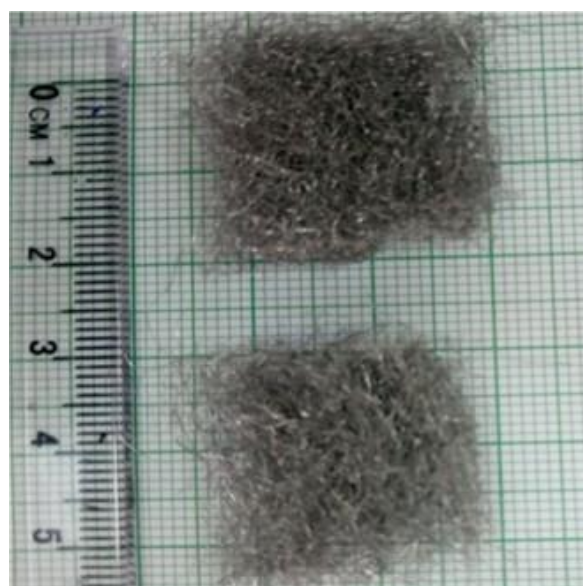
(a) (b)

Plate 1: Size specification of Fe^0 materials tested: (a) Iron scraps, (b) Steel wool

3.1.3 Experimental Procedure

(i) The Fe^0 reactivity

A dissolution experiment was conducted using 0.1 g of each material (SW or SI) within 50 mL of 2 mM 1,10 Phenanthroline over 120 hours under undisturbed conditions. The materials were weighed and immersed in plastic bottles containing 50 mL of 1,10 Phenanthroline. No pre-treatment procedures were applied to the materials before testing. The experiments were carried out in triplicate and safeguarded from direct sunlight (Lufingo *et al.,* 2019). The results of total iron concentrations presented are the average values.

(ii) Contaminants removal

The laboratory-scale experimental setup designed to optimize the dosages of zero-valent iron (ZVI) in anaerobic digestion for organics and nutrient removal is presented in Fig. 6 and Plate 2. The contaminants removal study examined nine distinct reactors, as described in Table 3. These reactors were constructed using PVC pipes with a nominal diameter of 110 mm, and each possessed a total capacity of 3500 mL. Except for two reactors, namely System VIII and System IX, which received a combination of 3000 mL of distilled water and Fe^0 materials, the remaining reactors (Systems I to VII) were supplied with 3000 mL of domestic sewage, 300 mL of inoculum, and Fe^0 materials.

Table 3: **Identities of reactors used in tested reactors. Each system contains 3000 mL of the medium (DS or DW)**

System	Medium	Fe^0 material	Fe^0 dosage (g/L)	Fe^0 to Inoculum ratio (g Fe^0/gTS)
I	DS	none	0	0.00
II	DS	SI	1	0.08
III	DS	SI	4	0.31
IV	DS	SI	10	0.78
V	DS	SI	15	1.17
VI	DS	SI	30	2.33
VII	DS	SW	10	0.78
VIII	DW	SI	10	-
IX	DW	SW	10	-

"DS" stands for Domestic Sewage, "DW" Distilled Water, "SI" for Iron Scrap, "SW" for steel wool, and TS for total solid. The Fe^0 materials dosages measurement accuracy was 0.1 g Fe^0/L.

$$Fe^0 \text{ to inoculum ratio } (g\ Fe^0\ /g\ TS) = \frac{Fe^0 \text{ dosage } \left(\frac{g}{L}\right)}{TS \text{ of the inoculum sludge } \left(\frac{g}{L}\right)} \quad (21)$$

Where Fe^0 dosage = 0 -30 g/L for SI or SW (Table 3.3), and TS of the sludge = 12.85 g/L (Table 1).

All the reactors operated in parallel, in a water bath under quiescent conditions, following a batch mode approach, and maintained a mesophilic temperature of $37 \pm 0.5°C$. Systems II to VI were anaerobic reactors that received varying quantities of SI materials, as specified in Table 3, to examine the influence of different SI material dosages on pollutant removal and to determine the optimal dosage. Additionally, the study assessed the effects of SI and SW materials on pollutant removal using Systems IV and VII. Although Systems IV and VII were supplied with the same domestic sewage and Fe^0 materials dosage, they utilized different Fe^0 materials, as detailed in Table 3.

The study also investigated the behavior of Fe^0 materials (SI or SW) in domestic sewage within Systems IV, VII, VIII, and IX, with distilled water serving as a comparative medium. As mentioned earlier, each system (IV, VII, VIII, and IX) received a dose of 10 g/L of Fe^0 materials.
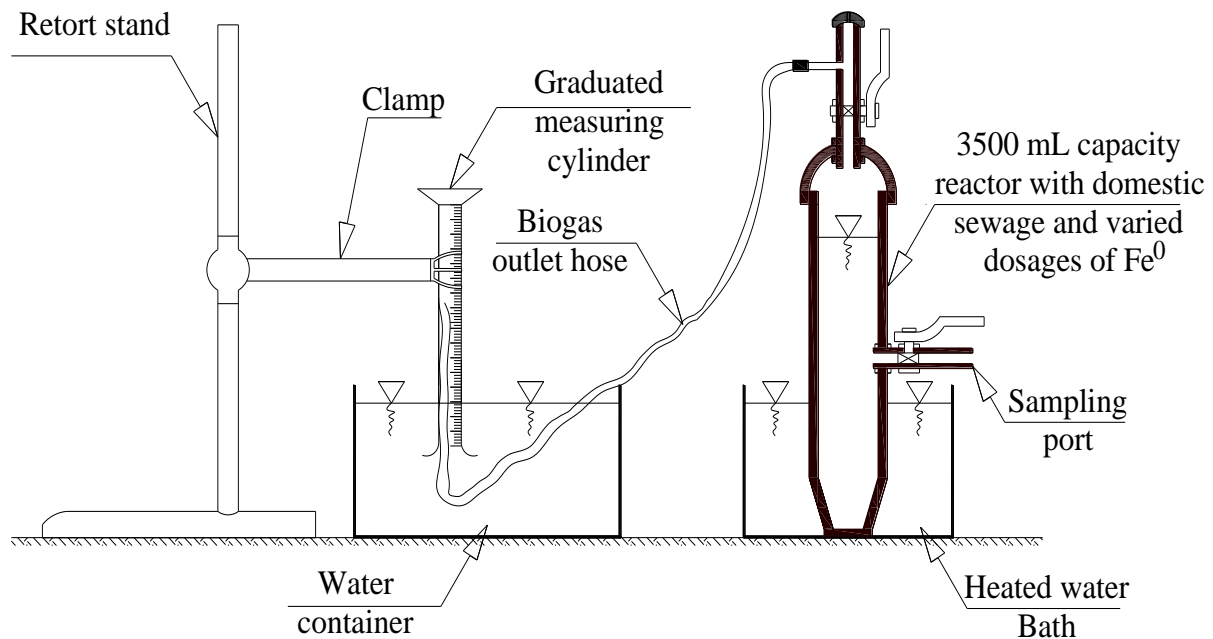
Figure 6: **Schematic diagram of the laboratory-scale experimental setup designed to optimize the dosages of zero-valent iron in anaerobic digestion**

Furthermore, System I was designated as a control group, excluding the addition of any Fe^0 materials, and served as a control point for Systems II to VII, which treated domestic sewage (Table 3). The laboratory-scale experimental setup designed to optimize the dosages of zero-valent iron (ZVI) in anaerobic digestion for organics and nutrient removal is presented in Fig. 6 and Plate 2. Samples from the reactors (Systems I to IX) were collected via sampling ports regulated by ball valves approximately every second to third day of operation.

The ZVI optimization procedures employed in this study are grounded in methodologies from previous research, extensively documented in the literature. Key references include the studies by Lufingo *et al.* (2019), Antwi *et al.* (2017), Kong *et al.* (2016), Wu *et al.* (2015), and Zhao *et al.* (2016). These foundational works provided the framework and specific techniques that guided the development of the optimization process.

Plate 2: **A photograph depicting a laboratory-scale experimental setup designed to optimize zero-valent iron (ZVI) dosages in anaerobic digestion**

To evaluate the effectiveness of pollutant removal, the samples underwent analysis for chemical oxygen demand (COD), nitrate (NO_3^-), orthophosphate (PO_4^{3-}), and ammonium (NH_4^+). Additionally, the analysis included the assessment of Total Iron (Total -Fe) and pH for monitoring purposes. For Systems VIII and IX, only pH and Total-Fe were examined to compare the impact of the medium on material dissolution and pH fluctuations. Analyzing COD, NH_4^+, NO_3^-, PO_4^{3-}, and Total-Fe adhered to the standard methods recommended by APHA for wastewater analysis.

3.1.4 Analytical Methods

During the reactivity study involving Fe^0 materials, iron concentrations were determined using a DR2800 spectrophotometer, a product of HACH Company in Berlin, Germany. The analysis took place at a wavelength of 510 nm and employed a 5 cm cuvette. The testing procedures for this assessment were adopted from the methodologies documented in Lufingo *et al.* (2019) and Hu *et al.* (2019). The methods employed, along with their respective quantification limits for the analyzed parameters, are as follows: the Low Range (LR) reactor digestion method for COD, with a quantification range of 3 - 150 mgCOD/L; the Nessler reagent method for NH_4^+, covering a range of 0.02 – 2.5 mg NH_4^+/L; the High Range (HR) Cadmium reduction method for NO_3^-, with a range of 0.3 – 30 mgNO_3^-/L; the PhosVer 3 method for PO_4^{3-}, with a quantification range of 0.02 – 2.5 mgPO_4^3/L; the FerroVer method for Total iron, spanning from 0.002 – 3.00 mgFe/L; and the Nessler method for Total Kjeldahl Nitrogen (TKN), with a quantification range of 1 - 150 mgTKN/L. It is worth noting that while the pH was measured using the Orion Star A214 pH meter, all other monitored parameters were analyzed utilizing the DR2800 spectrophotometer manufactured by HACH Company, headquartered in Berlin, Germany.

The analyses were conducted using the standard methods the American Public Health Association (APHA) recommended for examining water and wastewater. Detailed in the APHA's 2017 publication, these methods provided comprehensive guidelines and protocols for assessing the characteristics of wastewater samples.

3.1.5 Statistical Analysis

The statistical analysis of various datasets and graphs was accomplished using the Microsoft Excel program. The software was utilized to calculate means, standard deviations, correlation coefficients and assess significance. The software facilitated the calculation of statistical

significance tests for observations where n >10, employing a two-tailed student t-test with n − 2 degrees of freedom and a confidence interval of p = 0.01. These tests assessed whether significant differences in pollutant removal existed between (a) systems with Fe^0 materials and the control system without Fe^0 materials and (b) systems using IS Fe^0 materials and SW Fe^0 materials.

The Pearson correlation coefficient (R^2) was employed to assess the strength and direction of the linear relationship between observed total iron and residual pollutant concentrations (COD, PO_4^{3-}, and $NO_3^-+NH_4^+$) in the tested Fe^0-supported anaerobic digestion systems. The evaluation criteria used were as follows: (a) R^2 values > 0.8 or < -0.8 indicated high positive or high negative correlation, (b) R^2 values ranging from 0.6 to 0.8 or -0.6 to -0.8 suggested good positive or negative correlation, (c) R^2 values between 0.4 to 0.6 or -0.4 to -0.6 indicated moderate positive or negative correlation, (d) R^2 values from 0.2 to 0.4 or -0.2 to -0.4 reflected low positive or negative correlation, and (e) R^2 values between 0.2 and -2 were indicative of no significant correlation (Günther *et al.,* 2012). In this study, the Design-Expert Pro Version 13 software was pivotal in optimizing the dosages of metallic iron (Fe^0) materials. The primary objective of this optimization process was to identify the ideal dosage, measured in mg/L, for Fe^0 materials that effectively minimize the observed concentrations of pollutants (COD, PO_4^{3}, and $NO_3^-+NH_4^+$) within the context of Fe^0-supported anaerobic digestion of domestic sewage.

The Design-Expert software was applied to generate desirability indices, used to rank the performance of the anaerobic digestion systems under examination. These indices were computed based on multiple responses, factors, and objectives. Specifically, the responses encompassed the observed concentrations of COD, PO_4^{3-}, and $NO_3^-+NH_4^+$; the factors included time and Fe^0 material dosages; and the overarching goal was the minimization of pollutant concentrations (COD, PO_4^{3-}, and $NO_3^-+NH_4^+$). The desirability indices ranged from zero outside the defined limits to one when the goal was achieved (Akteke-Ozturk *et al.,* 2018; Aly *et al.,* 2012).

3.1.6 Determination of Pollutants Removal Efficiency

The pollutants (COD, $PO_4^{3-},$ and $NO_3^- + NH_4^+$) removal efficiency achieved in each reactor was calculated using the formula in Equation (22).

$$\eta = \frac{C_0 - C_t}{C_0}$$
(22)

Where: η = pollutants removal efficiency (%), C_{0} = Initial pollutants concentration (mg/L), and C_t = pollutants concentration observed at any time (mg/L).

3.2 Effects of Zero-Valent Iron on Sludge and Methane Production

This section involved experimentation with three bench-scale batch reactors. Biogas and sludge samples from the Fe^0-aided anaerobic batch reactors (10 g/L IS or 10 g/L SW) were compared with those from the control reactor (without Fe^0). This comparison evaluated the reactors' significance in enriching (a) sludge with organics, nutrients, and toxic elements and (b) biogas with CH_4 or other gaseous impurities like H_2S, CO_2, and NH_3. The basis for comparison included two main aspects. First, the differences in the concentrations of organics, nutrients, and toxic elements in the sludge between anaerobic reactors with Fe^0 materials (10 g/L IS or 10 g/L SW) and the control (0 g Fe^0/L). Second, the variations in the concentrations of CH_4, H_2S, CO_2, and NH_3 between the reactors dosed with Fe^0 (10 g/L IS or 10 g/L SW) and the control (0 g Fe_0/L). The 10 g Fe^0/L dosage was chosen based on lab-scale optimization studies, the first experiment in this study, employing the same Fe^0 materials for organics and nutrient removal from domestic wastewater. It is important to note that optimal dosages of less than 30 g Fe^0/L of various types of Fe^0 materials with different waste streams have been reported in the literature (Antwi *et al.,* 2017; Kong *et al.,* 2016; Wu *et al.,* 2015; Zhao *et al.,* 2016).

3.2.1 Inoculum Sludge and Wastewater

Table 4 shows findings related to the characteristics of the tested inoculum sludge and domestic wastewater collected from the septic tank, as detailed in Section 3.1.1, and adhering to the sampling procedures outlined in the same section.

Table 4: **Essential quality of inoculum sludge and tested domestic wastewater**

Parameters	M (n =3)	SD (n = 3)
I – Quality of Dry Inoculum sludge		
Potential of hydrogen, pH (1:2.5)	6.83	0.02
Chemical oxygen demand, COD (gCOD/L)	3.945	0.004
Total solids, TS (gTS/L)	14.75	0.04
Total volatile solids, TVS (gVS/L)	7.98	0.1
Volatile Suspended solids, VSS (gVSS/L)	5.57	0.2
Total Organic Carbon, TOC (%)	27.1	1.1
Total Kjeldahl Nitrogen – TN (%)	0.81	0.03
Sulfur, S (mg/kg)	0.51	0.03
Extractable Phosphorus – P (mg/kg)	135.7	3.4
Potassium, K (%)	0.02	0.003
Magnesium, Mg (%)	7.2	0.4
Calcium, Ca (%)	4.83	0.3
Iron, Fe (%)	0.11	0.03
Manganese, Mn (mg/kg)	285.2	4.9
Copper, Cu (mg/kg)	9.9	0.7
Zinc, Zn (mg/kg)	306.2	6.2
Chromium, Cr (mg/kg)	23.7	1.3
Nickel, Ni (mg/kg)	5.8	0.6
Lead, Pb (mg/kg)	0.34	0.04
II – Quality of tested domestic wastewater		
Potential of hydrogen, pH	7.51	0.03
Temperature, T (^{o}C)	22	0.1
Chemical oxygen demand, COD (gCOD/L)	428	3.6
Orthophosphate, PO_4^{3-} (mg PO_4^{3-}/L)	28.6	0.6
Nitrate, NO_3^- (mg NO_3^- /L)	24.8	0.9
Ammonium, NH_4^+ (mg NH_4^+/L)	55.5	1.5
Sulfate, SO_4^{2-} (mg SO_4^{2-}/L)	41.4	1.2

"M" stands for mean, and "SD" for standard deviation.

3.2.2 Experimental Procedure

An experiment was conducted to anaerobically digest domestic sewage (DS) dosed with Fe^0 materials in a controlled environment to obtain and characterize the resulting biogas and sludge. The experimental setup consisted of bench-scale plastic anaerobic reactors, each with a 60-liter capacity (Fig. 7(a) & Plate 3). The first reactor (Reactor I) was a control (Table 5). Except for the control reactor, which received 50 liters of DS and 3 liters of inoculum only, each of the other two reactors (Reactors II and III) was supplied with 50 liters of DS, 3 liters of inoculum, and 10 g/L of Fe^0 materials (Table 5). The COD/VS (Wastewater/Inoculum) ratio for the wastewater and inoculum mixture was 5.4%. Reactor II was fed with SI, while Reactor III was fed with SW materials (Table 5) to compare the impact of different Fe^0 materials on biogas production and sludge characteristics. The same inoculum and domestic sewage were used in each tested reactor. The 10 g/L dosage of Fe^0 material was selected based on the findings of a lab-scale study with the same materials, which established this dose as optimal for organics and nutrient removal. All the anaerobic reactors were operated simultaneously for 53 days under quiescent conditions, batch mode, at a room temperature of 24 ± 3°C, and an initial pH of 7.3. Biogas monitoring was carried out throughout the 53 days of reactor operation, as the biogas generated after that was too minimal to measure.

Table 5: **Identities of reactors used in the bench-scale study**

Reactor	Medium	Fe^0 material	Fe^0 dosage (g/L)	Fe^0 to inoculum ratio (g Fe^0/g TS)
I	DS	none	0	0.0
II	DS	SI	10	0.7
III	DS	SW	10	0.7

"DS" stands for Domestic Sewage, "SI" for Iron Scraps, "SW" for steel wool, and TS for total solid. The Fe^0 materials dosages measurement accuracy was 0.1 g Fe^0/L.

Fe^0 to inoculum ratio (g Fe^0/g TS) ratio was calculated using Equation (21).

Where; TS of the sludge =14.75 g/L (Table 4), and Fe^0 dosage = 10 g/L for SI or SW (Table 5).

Treated domestic sewage (DS) samples measuring 50 mL were collected from each reactor twice a week to analyze Chemical Oxygen Demand (COD) and pH. Biogas samples from the airbag were collected and analyzed daily for the initial two weeks of reactor operation. Subsequent sampling and analysis were conducted after accumulating at least 300 mL of biogas from the reactor with the slowest biogas release rate. The analysis of the generated biogas aimed at determining both its volume and composition.

After the 53-day experiment, a portion of the sludge sample from each bench-scale reactor was extracted through the sludge sampling port (Fig. 7(a)) and subjected to analysis for Total Solids (TS), Total Suspended Solids (TSS), Volatile Suspended Solids (VSS), and settleable solids. Additionally, another portion of the sludge samples was air-dried away from direct sunlight and then subjected to analysis for a range of parameters, including macro-nutrients (such Ca, K, Mg, N, P, and S), micro-nutrients (including Cu, Fe, Mn, and Zn), organic carbon, pH, and toxic elements (Cr, Ni, and Pb). All experiments were conducted in triplicates.

3.2.3   Experimental Procedure for Sludge Settling

The settling assessment of solids resulting from the 53-day anaerobic digestion of domestic sewage (DS) in each bench-scale reactor (Fig. 7(a) & Plate 3(a)) was conducted using a settling column, shown in Fig. 7(b) and Plate 3(b). The primary objective of this analysis was to determine the settling velocities of solids and the overall Total Suspended Solids (TSS) removal efficiencies at 90 and 120 minutes of settling time. These measurements were made on samples collected from the ports located at different depths within the 3-meter-tall settling column (Fig. 7(b) and Plate 3(b)) for comparison.

The settling column was constructed using a class C uPVC pipe with a nominal outside diameter of 160 mm. The column's height was 3 meters, with an effective water depth of 2.5 meters. Sampling ports were strategically placed at equal intervals of 500 mm from the top, as illustrated in Fig. 7(b). To ensure uniform suspension of particles, the contents from each reactor were manually stirred before promptly taking a sample to measure the initial TSS concentration. Subsequently, the contents were poured into the settling column from the top.
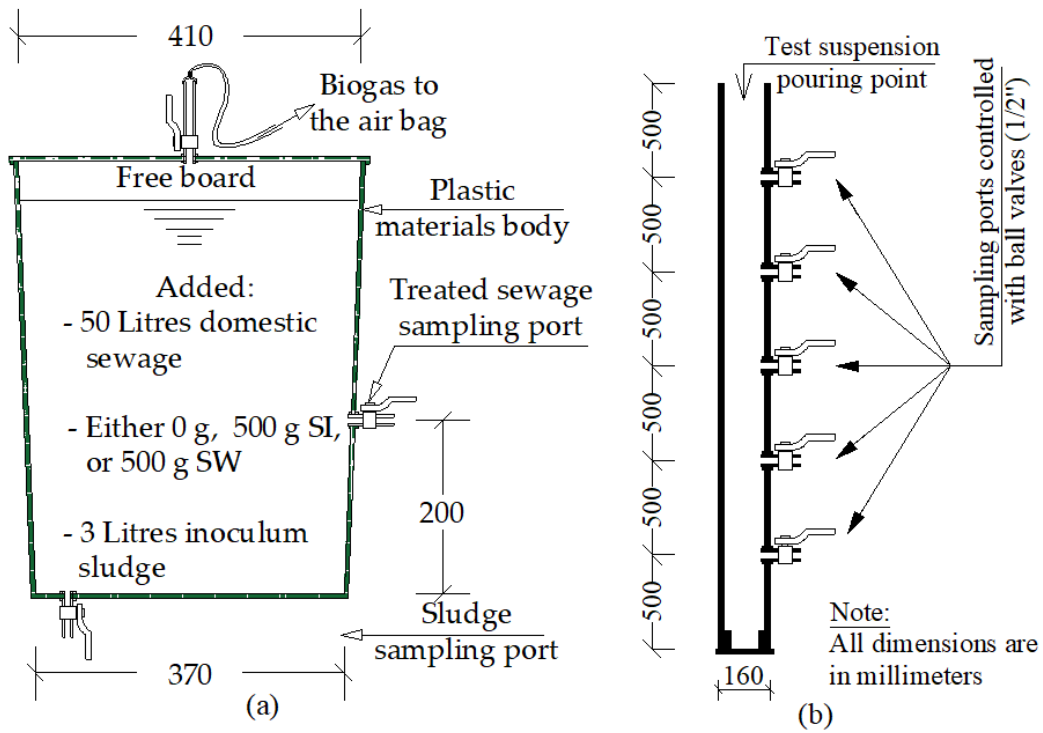
Figure 7: Schematic diagram of the experimental setup: (a) Anaerobic digester (b) Settling column

Plate 3: A photograph depicting a bench-scale experimental setup: (a) Anaerobic reactors (b) Settling column

The stirring process involved inverting the capped container five times, each inversion lasting approximately 10 seconds. Each settling column test utilized 3 liters of sludge, and samples

45

were simultaneously collected from all ports of the settling column every 10 minutes over 150 minutes. These collected samples were then analyzed for TSS in triplicate.

The method used for the column settling analysis adhered to established procedures documented in various scientific literature (Davis, 2010; Gray, 2004; Qasim & Zhu, 2017; Riffat & Husnain, 2013; Tchobanoglous *et al.,* 2014; Weiner *et al.,* 2003)

3.2.4 Analytical Methods

The methods employed for the analysis of various parameters were as follows: aqua regia for K, Mg, Ca, Na, S, Fe, Mn, Cu, Zn, Cr, Ni, and Pb; Olsen method for P; Kjeldahl method for TN; Walkley-Black method for organic carbon; Low Range reactor digestion for COD; Nessler reagent for NH_4^+; High Range (HR) Cadmium reduction for NO_3^-; and PhosVer 3 method for PO_4^{3-}.

The pH of the sludge was measured in a 1:2.5 sludge-to-water ratio using an Accsen benchtop pH meter by Lasec SA (Pty) Ltd. In contrast, the pH of domestic sewage (DS) was measured using an Orion Star A214 pH meter. The K, Mg, Ca, and Na were measured using a Flame photometer (Model 2655-00) manufactured by Cole-Parmer Company in Chicago, USA. On the other hand, Fe, Mn, Cu, Zn, Cr, Ni, S, and Pb were measured using the Thermo Scientific iCE 3000 series atomic absorption spectrometer designed in the UK; P was determined using the Spectronic 200E UV-VIS spectrometer by Thermo Fisher Scientific in China. TKN was analyzed with the Kjeldahl distillation unit manufactured by Jinan Biobase Biotech Co. Ltd in China. Parameters such as COD, NH_4^+, NO_3^-, and PO_4^{3-} were measured using a spectrophotometer (DR2800), a product of HACH Company. The generated biogas volume was measured using the syringe method, while composition analysis was conducted with a biogas analyzer (Geotech Biogas 5000 analyzers).

3.2.5 Statistical Data Analysis

The statistical analysis of the collected data was carried out using Microsoft Excel 2019. This software was utilized to perform statistical significance tests for observations when the sample size (n) was less than 30. The analysis involved employing a two-tailed student t-test with degrees of freedom equal to n–2 and a confidence interval of $p = 0.05$. These t-tests were conducted to assess whether significant differences existed in the concentrations of observed nutrients and organic matter in the produced sludge, as well as in the quantity and quality of

biogas, between (a) the control reactor and the reactors with Fe^0 materials, and (b) the reactor with Iron Scraps (SI) materials and the one with Steel Wool (SW) materials.

3.2.6 Determination of Overall TSS Removal Efficiency

The AUTOCAD software was exclusively employed for creating the percent removal and isoremoval curves, while the Excel application was used for generating all other graphs and conducting various calculations. The percent Total Suspended Solids (TSS) removal values were determined using Equation (13) and represented as data points within circular markers, plotted against both time and depth, as shown in Figs. 18 and 19(c). The settling velocity (overflow rate) and the overall TSS removal efficiency obtained in the particle settling analysis for each reactor were calculated using the curves illustrated in Fig. 16, in conjunction with the Equations (15) and (16).

3.2.7 Simulation of Kinematic Models for Methane Production

Kinematic models predict the cumulative CH_4 yield, estimate CH_4 generation potential, determine the daily maximum CH_4 generation, and establish the lag phase required to start CH_4 production (Zhao *et al.,* 2018). During the study, methane yield data were gathered over 53 days through 15 distinct reactor runs. The dataset was divided into two subsets to ensure a robust evaluation of the models: 70% of the data, corresponding to 10 runs, were allocated for model calibration, while the remaining 30%, or 5 runs, were used for model validation.

The primary objective of the calibration phase was to apply kinematic models to predict various aspects of methane production. These models aimed to forecast cumulative methane yield, estimate methane generation potential, determine the daily maximum methane production rate, and identify the lag phase required to initiate methane production. For this purpose, three kinematic models were utilized: the modified Richard model (Equation (17)), the Gompertz model (Equation (18)), and the Logistic model (Equation (20)). These models were selected based on their proven efficacy in predicting methane production, as supported by previous research (Bakraoui *et al.,* 2019).

In the model validation phase, regression analysis was performed using Excel's Data Analysis Toolpak, focusing on achieving a 95% confidence interval. This analysis involved comparing the predicted methane production values with the actual observed data to assess the accuracy and reliability of each model. The models' performance was evaluated using the correlation

47

coefficient, R^2, which quantifies the degree of correlation between observed and predicted values. A higher R^2 value signifies a better fit of the model to the data. Furthermore, a fitting error of 10% or less between observed and predicted biogas yields is considered favorable, as established by various studies (Kafle *et al.,* 2013; Raposo *et al.,* 2009; Ugwu & Enweremadu, 2019). This threshold provided a practical standard for evaluating the models' predictive performance in the study.

4.1   The Fe^0 Reactivity

Figure 8 presents the observed iron concentration results from SW and SI materials dissolution by 2 mM 1, 10 Phenanthroline. The results indicate that the observed iron concentrations increase with time and continuously increase even after 120 hours of experimental operation. However, a linear increase was observed within 24 hours of the experimental procedure. Similar observations were reported elsewhere (Lufingo *et al.,* 2019). The results indicate a higher iron concentration (7.11 mg-Fe/L) was attained with SW materials than that (3.7 mg-Fe/L) with SI materials within 120 hours of experiment operation. Based on the procedures for specifying the Fe^0 materials' reactivity as adopted from Lufingo *et al.* (2019), the following results were obtained: (a) the identified linear (R^2=0.9786 for SI and R^2=0.9612 for SW) timeframe was between 2nd to 10th hour (Fig. 8) (b) the rate of dissolution *(K_{phen})* for SI and SW materials were 4.41 µg/h and 5.05 µg/h respectively (c) amount of FeCPs (mg/L) on Fe^0 materials or the fraction thereof that is dissolved by 1, 10 Phenanthroline (b) for SI and SW were 5.23 µg and 91.36 µg respectively. Therefore, SW materials have a higher dissolution rate and are more reactive than SI materials.

Figure 8 illustrates the outcomes of iron concentration observed due to the dissolution of SW and SI materials by 2 mM 1,10 Phenanthroline. The data reveals a continual increase in iron concentrations over time, persisting beyond 120 hours of experimental operation. Notably, a linear increase is evident within the initial 24 hours of the experiment, a trend consistent with findings reported elsewhere (Lufingo *et al.,* 2019). The results further highlight that SW materials achieved a higher iron concentration (7.11 mg-Fe/L) than SI materials (3.7 mg-Fe/L) within the 120 hours experimental timeframe.

The trend in total iron concentration during the dissolution of ZVI can be described in three stages: Initially, the concentration of iron increases slowly as ZVI starts dissolving and releasing Fe^{2+} ions. The dissolution process becomes more pronounced in the middle stage, showing a linear increase due to a consistent oxidation rate. Finally, the linear increase continues, though it may slightly plateau as the ZVI surface becomes less reactive or the complexation process approaches its limit (Hu *et al.,* 2019; Rui *et al.,* 2019; Lufingo *et al.,* 2019).

In line with the methodologies for determining the reactivity of Fe^0 materials, as outlined by Lufingo *et al.* (2019) the following key findings emerged: (a) a discernible linear timeframe ($R^2 = 0.9786$ for SI and $R^2 = 0.9612$ for SW) spanning from the 2nd to the 10th hour (Fig. 8); (b) dissolution rates (K_{phen}) for SI and SW materials were 4.41 µg/h and 5.05 µg/h, respectively; (c) the quantity of FeCPs (mg/L) on Fe^0 materials, or their dissolved fraction by 1,10 Phenanthroline, indicated values of 5.23 µg for SI and 91.36 µg for SW. Consequently, SW materials exhibit a higher dissolution rate and greater reactivity than SI materials.

The results suggest that SW materials are likely to demonstrate the superiority of pollutant removal mechanisms over SI materials, primarily due to the reactivity of Fe^0 materials. However, highly reactive Fe^0 materials, such as nano-scaled Fe^0, have been linked to impeding the microbial degradation of pollutants (He *et al.*, 2022; Ye *et al.*, 2021). Conversely, less reactive Fe^0 materials, like micro-scaled Fe^0, demonstrate extended effectiveness in anaerobic digestion, gradually releasing H_2 that supports microbial respiration (Summer *et al.*, 2020).
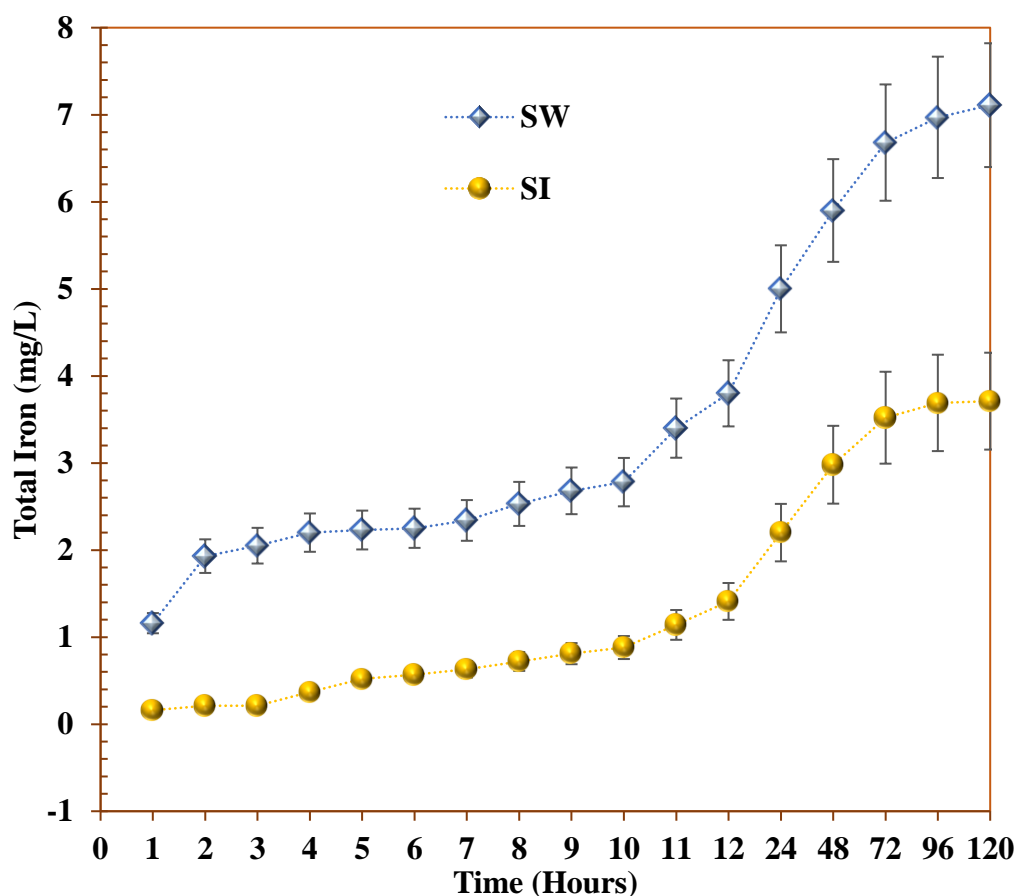
Figure 8: Comparison of iron dissolution by 2 mM 1, 10 Phenanthroline from SI and SW materials for 120 hours. Experimental conditions: Mass of each Fe^0 = 0.1 g, Volume of working solution, V = 50 mL, room temperature, T = 37 ± 0.5 ^{O}C

The variation in reactivity among various Fe^0 materials could be attributed to the surface area and the elemental composition, which involves the alloying of iron with other metals (Li *et al.,* 2019; Li *et al.,* 2016; Lufingo *et al.,* 2019). This study has identified varying percentages of heavy metals in the Fe^0 materials (Table 2). Despite heavy metals being recognized for their inhibitory and toxic effects on specific biochemical reactions in anaerobic digestion systems (Abdel-Shafy & Mansour, 2014; Alrawashdeh *et al.,* 2020; Mudhoo & Kumar, 2013), the application of Fe^0 material has been found to decrease the concentrations of heavy metals in anaerobic digestion systems supported by Fe^0 (Chen *et al.,* 2008; Fu *et al.,* 2013).

4.2   Effect of Fe^0 Materials Dosage on Pollutant Removal

4.2.1   Chemical Oxygen Demand

Figure 9(a) presents the chemical oxygen demand (COD) removal efficiencies from varying SI materials dosages. The findings indicate that systems II to VI, treated with Fe^0 materials, achieved a steady state more rapidly between the 35th and 39th days than system I (the control system), which reached a steady state two weeks later on the 53rd day of operation. Additionally, the COD removal efficiencies varied, with the lowest (68.9%) and highest (87.7%) efficiencies observed in systems I and IV, respectively (Fig. 11).

Statistical analysis reveals a significant difference in COD removal between System I (M = 42.3%, SD = 28.1%) and System IV (M = 63.2%, SD = 32.0%), t (31) = -10.4, p < 0.01, two-tailed. Furthermore, considering the maximum pollutant removal efficiencies (Fig. 11) and the average observed COD concentrations (Table 6), a ranking of COD removal performance is established, with the order from best to least performing system (among those dosed with SI materials) as follows: IV > V > VI > III > II > I. This ranking underscores the trend of improved COD removal efficiency with increasing SI material dosages from 0 to 10 g/L and decreasing efficiency for SI dosages above 10 mg/L (15 and 30 g/L).

The enhancement of anaerobic digestion performance with the addition of Fe^0 materials has been documented in various studies (Xu *et al.,* 2017). Zero-valent iron (ZVI) enhances anaerobic digestion by acting as electron donors and catalysts, accelerating the breakdown of organic compounds and boosting the production of metabolites crucial for methanogenesis (Antwi *et al.,* 2020; Xu *et al.,* 2017). It also reduces inhibitory compounds like hydrogen sulphide and heavy metals, improves microbial activity, and increases methane production, leading to ZVI-dosed reactors reaching a steady state faster, resulting in a more stable and

efficient digestion process (Xu *et al.,* 2017; Dong *et al.,* 2019; He *et al.,* 2022; Zhong *et al.,* 2022). Numerous studies have documented these benefits, showing that Fe^0 materials facilitate fermentation, expedite hydrolysis and fermentation, enhance methanogenesis, and stimulate microbial growth (Antwi *et al.,* 2017; Antwi *et al.,* 2020; Meng *et al.,* 2013; Wei *et al.,* 2018; Wu *et al.,* 2015; Zhang *et al.,* 2011).

Conversely, the observed decline in pollutant removal efficiency at higher dosages (15 and 30 g/L) of Fe^0 materials (Fig. 9(a)) may be attributed to adverse effects from higher SI dosages, as reported elsewhere (Antwi *et al.,* 2017; Wu *et al.,* 2015). Antwi *et al.* (2017) noted that the impact of Fe^0 dosing on biomethanation and the distribution of microbial communities in Fe^0-supported anaerobic digestion (AD): (a) optimal enhancement of microbial community population at a 10 g/L dosage of Fe^0 and (b) significant depopulation of microbes at a higher dose (20 g/L) of Fe^0 materials. Wu *et al.* (2015) state that higher Fe^0 dosages negatively impact microbial activities in anaerobic digestion by encapsulating and damaging cell structures. In this study, detrimental effects became apparent at 15 and 30 g/L dosages of Fe^0 materials, exhibiting a distinct departure from observations in other research endeavors. Similar adverse effects were reported even in the 50 g/L dosage of Fe^0 powder implemented in swine wastewater treatment, as evidenced in the study by Wu *et al.* (2015).

Konadu-Amoah *et al.* (2022a), noted that adding Fe^0 materials to polluted water results in the generation of iron corrosion products (FeCPs) that mediate contaminant removal. Nevertheless, excessive precipitation of FeCPs (Equation (9)) due to higher Fe^0 materials doses may entangle, adsorb, or inactivate some microorganisms responsible for the digestion of pollutants (Konadu-Amoah *et al.,* 2022a; Noubactep, 2011; You *et al.,* 2005)**.** Although an increased mass loading of Fe^0 materials is desirable to produce sufficient H_2 for microbial respiration (Equation (4)) (Deng *et al.,* 2020; Summer *et al.,* 2020; Zhang *et al.,* 2011), it is essential to avoid excessively large doses to prevent counterproductivity, as evidenced in this study (Fig. 10(a) & Table 6) and in other studies (Domrongpokkaphan *et al.,* 2021; Wu *et al.,* 2015).

Therefore, case-specific optimization studies for Fe^0 materials dosage are imperative, as the effects of these materials on the anaerobic digestion of wastes may significantly vary depending on the nature of the treated wastes and the type and dosage of Fe^0 materials employed.

4.2.2 Orthophosphate PO_4^{3-}

Figure 9(b) shows the removal efficiencies of PO_4^{3-} resulting from varied dosages of SI materials. The impact of these diverse dosages on orthophosphate removal in the reactors was evaluated by assessing the removal efficiencies. The ranking of reactor performances, determined by both the maximum PO_4^{3-} removal efficiencies (Fig. 11) and the average observed PO_4^{3-} concentrations (Table 6), reveals a descending order from the best to the least performing system among those dosed with SI materials: IV > V > VI > III > II > I. Within this context, the recorded PO_4^{3-} removal efficiencies ranged from the lowest at 7.3% in the 0 g/L reactor to the highest at 98.3% in the 10 g/L reactor (Fig. 11). Importantly, the statistical analysis shows a significant difference in PO_4^{3-} removal between System I (M = 7.9%, SD = 16.6%) and System IV (M = 74.5%, SD = 35.2%), t (31) = -20.1, p < 0.01, two-tailed.

Figure 9(b) provides the trend of orthophosphate removal observed in the reactors, revealing an initial upswing in orthophosphate concentration during the initial eight days of the start-up phase. This rise is potentially attributed to the partitioning of soluble phosphorus between the solid (originating from the seed sludge and domestic sewage) and liquid phases, influenced by alterations in pH and temperature. The decline in pH and the increase in temperature contribute to the dissolution of bound phosphorus. Over this period, noteworthy changes include (a) a rapid increase in reactor contents' temperatures from 24°C to a constant operational temperature of 37 ± 0.5°C within 22 minutes in a water bath, (b) a drop in pH across all reactors (Fig. 10(b)), (c) the highest increase in PO_4^{3-} concentration from 17.8 to 26.1 mg/L (Fig. 9(b)), and the most significant pH decrease from 7.5 to 7.1 observed in System I (Fig. 10(b)), and (d) a negative correlation between observed PO_4^{3-} concentration in System I and pH with a correlation coefficient, R^2 = -0.99. This observed trend is in line with the results from the previous studies associating elevated soluble phosphate concentrations in anaerobic digestion with hydrolysis of bound phosphorus and dissolution under low pH conditions (Latif *et al.,* 2015; Mehta & Batstone, 2013).
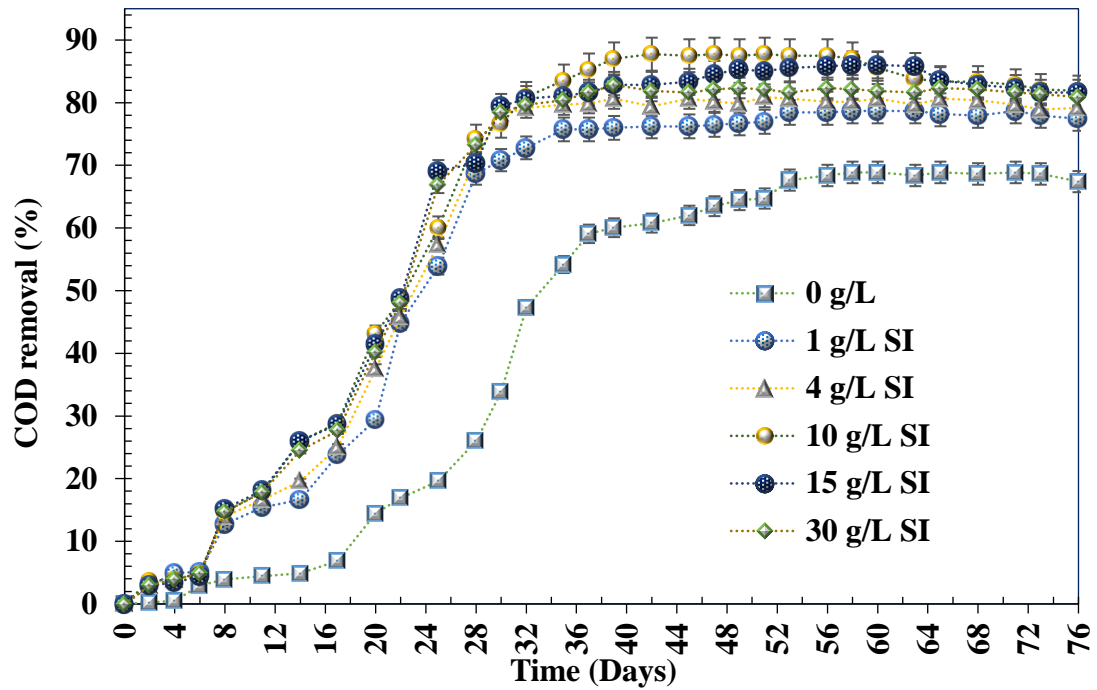
(a)
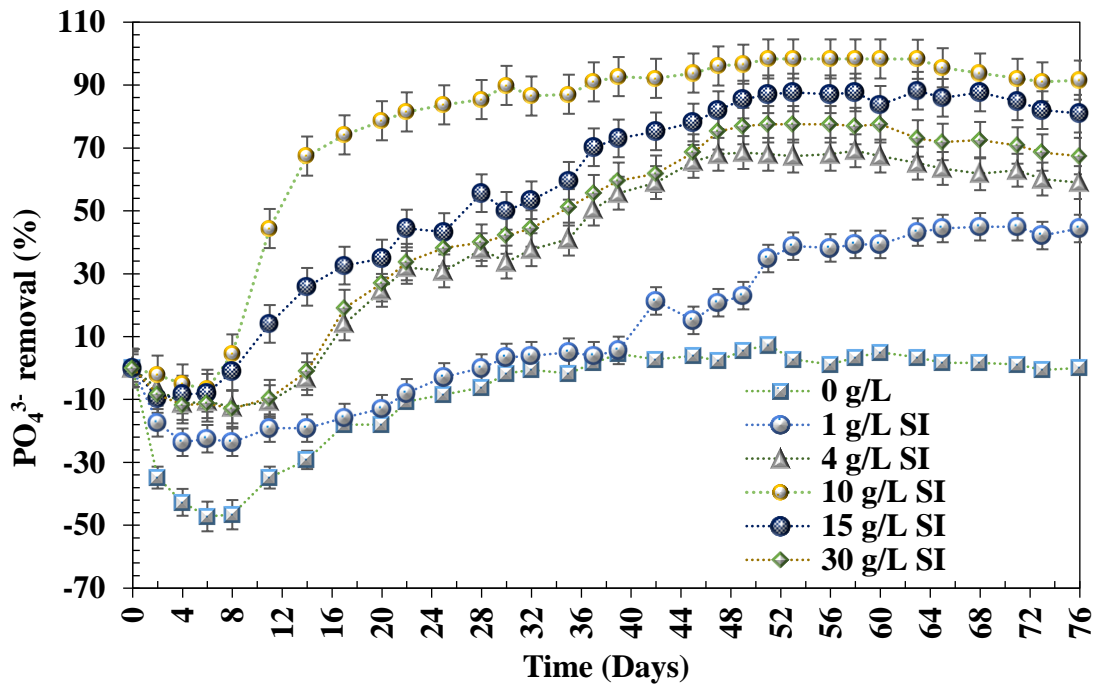
(b)

Figure 9: Comparison of the effects of varying SI materials dosages in pollutants removal efficiency for (a) COD and (b) PO_4^{3-}. SI materials' dosages were 0 g, 4g/L, 10 g/L, 15 g/L and 30 g/L; Systems' temperature, $T = 37 \pm 0.5\ {}^{O}C$
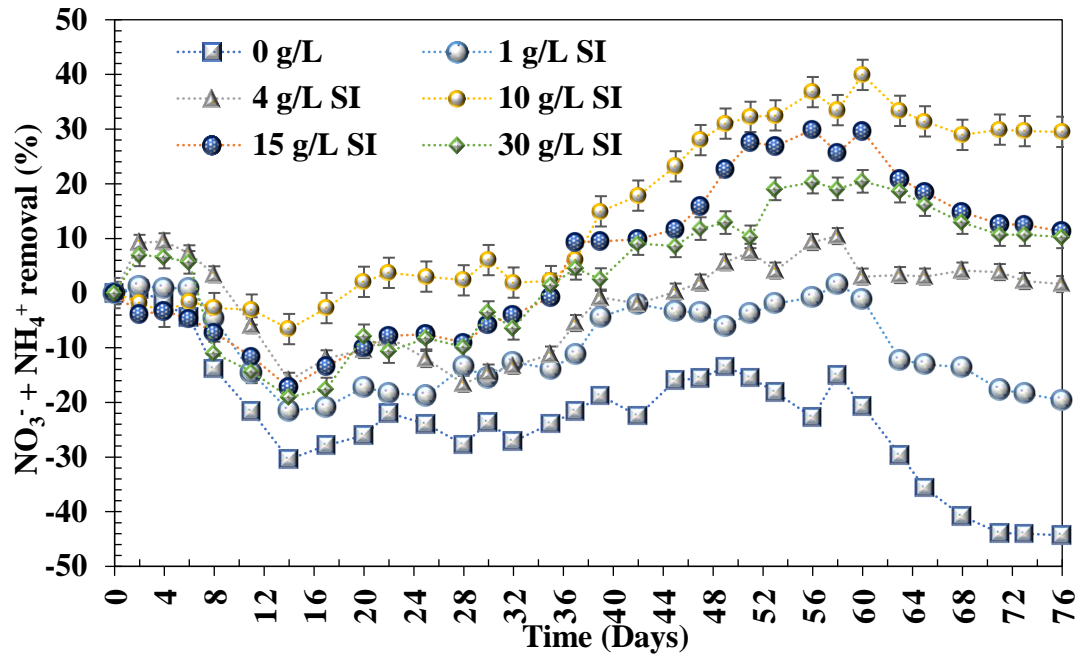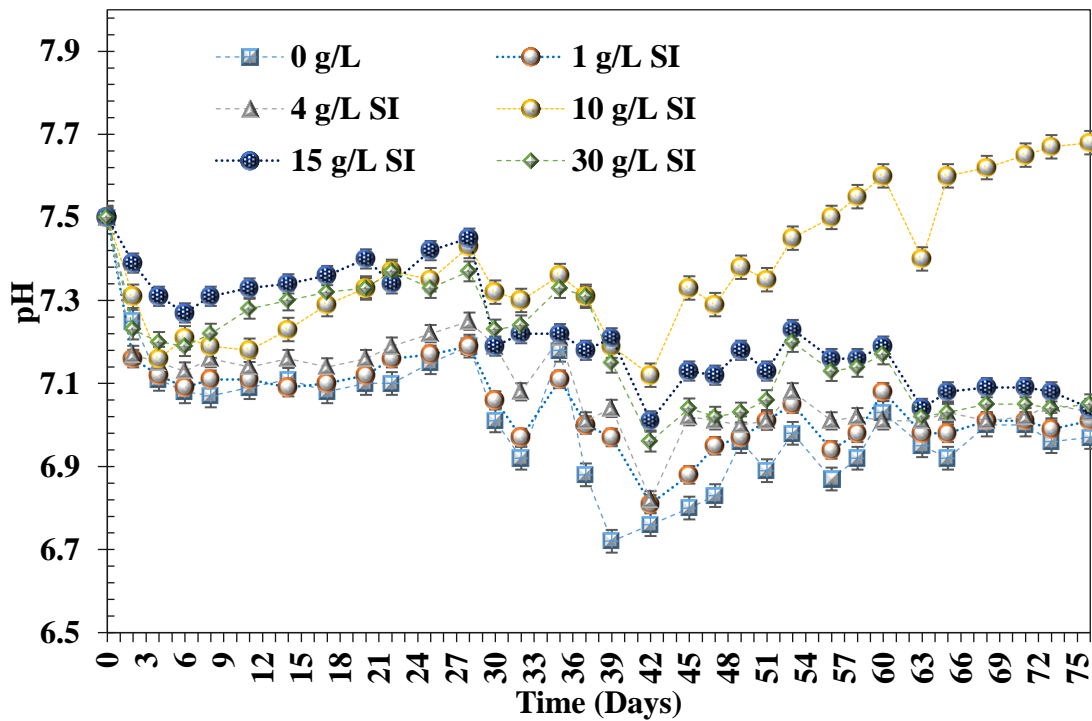
Figure 10: Comparison of the effects of varying SI materials dosages in pollutants removal efficiency for (a) NO_3^- + NH_4^+ and (b) pH variation. SI materials' dosages were 0 g, 4 g/L, 10 g/L, 15 g/L and 30 g/L; Systems' temperature, $T = 37 \pm 0.5\ ^{\circ}C$

The decline in PO_4^{3-} concentration observed from the second week of operation (Fig. 9(b)) for the control reactor is likely attributed to microbial removal through cell synthesis

(Tchobanoglous, 2014) and precipitation by cations (Ca^{2+} and Mg^{2+}, Al^{3+} and Fe^{2+}) that usually present in wastewaters or adsorption by suspended solids (Latif *et al.*, 2015; Lin *et al.*, 2015; Marti *et al.,* 2008). While not all cations were monitored in this study, the maximum total iron concentration of 1.09 mg/L was observed in the reactor without Fe^0 materials (Fig. 15(b)).

Results depicted in Fig. 11 underscore that the lowest (7.3%) and highest (98.3%) PO_4^{3-} removals were achieved in the control reactor (System I) and System IV, respectively. These results suggest that Fe^0 materials substantially improved the overall performance of the anaerobic system in PO_4^{3-} removal by more than 90%. Low PO_4^{3-} removal is commonplace in conventional anaerobic wastewater treatment, with full-scale anaerobic digestion plants reporting overall phosphorus removal of less than 10% (Schievano *et al.,* 2011). The enhanced PO_4^{3-} deduction observed in reactors dosed with SI materials (Fig. 11) is conceivably attributable to the improved precipitation and adsorption of phosphorus by the corrosion products of Fe^0 materials. The removal of phosphate by metallic iron can occur through adsorption by hydrous ferric, phosphate incorporation into the structure of hydrous oxide, and the formation of ferric phosphates, as generally described by Equation (10) (Akunna, 2018; Tchobanoglous, 2014).

On the contrary, anticipation existed that higher Fe^0 dosages, precisely 15 and 30 g Fe^0/L, would yield superior performance in PO_4^{3-} removal due to the proportional increase in active sites corresponding to the increased Fe^0 dosages, as suggested by a linear relationship (Sun *et al.,* 2016). However, the intricate nature of Fe^0-mediated biological pollutant removal systems introduces complexity, leading to nonlinear relationships, as reported in previous studies (Xu *et al.,* 2017). For example, in a fluidized Fe^0 bed reactor designed for nitrate removal, nitrate concentrations remained constant for Fe^0 dosages exceeding 10 g (Yin *et al*., 2012).

The relatively diminished performance of higher dosages of Fe^0 materials in this particular study could potentially be attributed to two main factors: (a) a reduced bioaccumulation of phosphorus due to a lower microbial population in systems with higher Fe^0 dosages (as described in Section 4.2.1), and (b) the rapid precipitation of FeCPs, forming a layer that expeditiously obstructs the mass transfer of the pollutant (PO_4^{3-}) between the Fe^0 materials at the bottom of the reactor and the pollutants in the solution (domestic sewage), as elucidated in Section 4.2.1. The inactivation by FeCPs in this study is possibly intensified by the batch mode operation of the reactors without mixing, aligning with previous findings (Sun *et al.,* 2016; Xu *et al.*, 2017).

4.2.3   Nitrate NO_3^- + Ammonium NH_4^+

Figure 10(a) provides the effects of varied dosages of SI materials on the removal of NO_3^- + NH_4^+. The results show a general increasing trend in NO_3^- + NH_4^+ concentration across all reactors during the initial two weeks of operation, succeeded by a continuous decrease over the subsequent six weeks, only to revert to an increasing trend for the final three weeks of operation. The order of NO_3^- + NH_4^+ removal performance among systems dosed with SI materials, from the most effective to the least, follows the order: IV > V > VI > III > II > I (Fig. 11 & Table 6). System I exhibited the lowest (0.7%), while System IV showcased the highest (39.9%) NO_3^- + NH_4^+ removal efficiencies (Fig. 11). Statistically, a significant difference in NO_3^- + NH_4^+ removal was observed between System I (M = -22.2%, SD = 11.9%) and System IV (M = 14.9%, SD = 15.7%), t (31) = -5.2, p < 0.01, two-tailed.

The study by Till *et al.* (1998) reported that abiotic reactors fed with steel wool entirely converted the added nitrate to ammonium (Equation (12)). In contrast, the biotic reactor provided with the same materials led to more denitrification (Equation (7)) than ammonium generation. These findings suggest that Fe^0 materials convert nitrogen to ammonium in reactors without microbes, while in the presence of microbes, the materials induce more denitrification than ammonium production. Therefore, based on these observations, the initial increase in NO_3^- + NH_4^+ concentration during the early stages of reactor operation was likely a result of a relatively lower denitrifying bacteria population, leading to a more significant portion of nitrogen being converted to ammonium.

Conversely, the observed decrease in NO_3^- + NH_4^+ concentration in the reactors may be linked to the accumulation of a denitrifying bacterial population that effectively denitrified most of the available nitrogen. The comparatively higher performance of Fe^0-material-dosed reactors compared to the control reactor can be associated with the proliferation of the microbial community, facilitated by enhanced hydrogen respiration due to the presence of Fe^0 materials (Deng *et al.,* 2020; Zhang *et al.,* 2011). Deng *et al.* (2020) further reported that Fe^0 materials enrich autotrophic denitrifiers. The observed reduction in NO_3^- + NH_4^+ removal efficiency at higher dosages (15 and 30 g/L) of Fe^0 materials as depicted in Fig. 10(a) can potentially be attributed to the inactivation and depopulation of nitrifiers, a phenomenon detailed in Section 4.2.1. Specifically, the inactivation and mortality of denitrifiers have been documented by Schädler *et al.* (2009). According to the report, FeCPs adsorb and form a layer on the surfaces of microbial cells, disrupting the diffusion of substrates and nutrients to the cells. This

interference ultimately leads to the stagnation and, ultimately, the death of the microbial population.
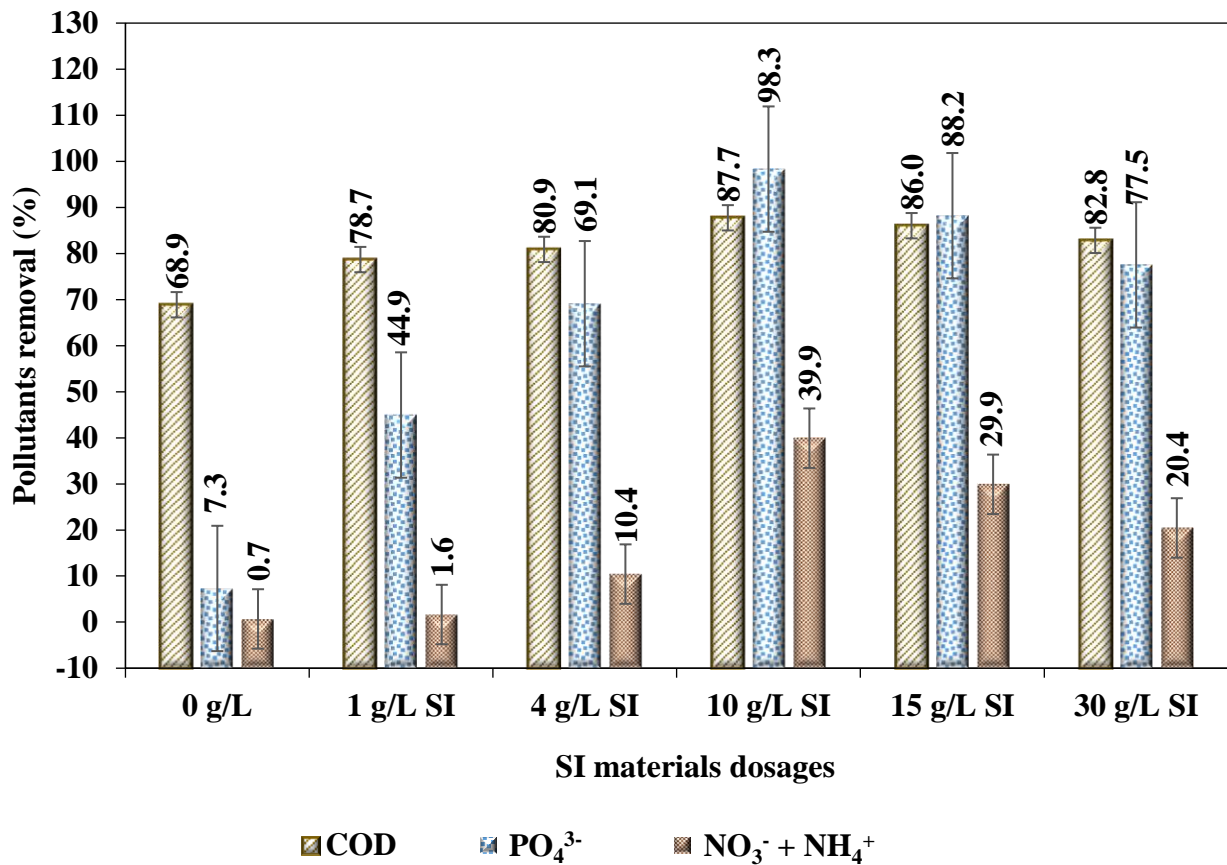
Figure 11: **Comparison of maximum pollutant removal efficiencies among systems. SI materials' dosages were 0 g, 4g/L, 10 g/L, 15 g/L and 30 g/L; Systems' temperature, T = 37 ± 0.5 ^OC**

The diminishing trend in $NO_3^- + NH_4^+$ removal, observed around the 45th day of operation depicted in Fig. 10(a), is likely a consequence of a higher cell death rate compared to production, attributed to substrate deficit (Riffat & Husnain, 2013; Tchobanoglous, 2014). Consequently, the elevation in nitrogen concentration within the system is presumed to result from the release of the decomposed dead cells. Additionally, it is inferred that the nitrate originating from the decomposition of deceased microbes is more likely to be converted into ammonium by Fe^0 than undergo denitrification, owing to the minimal number of microbes, as elucidated in previous studies (Till *et al.,* 1998).

Table 6: Residual pollutants concentration in the systems. Experiments were operated at "37 ± 0.5 " ^{O}C for 76 days. Avrg stands for average, and S.D for standard deviation

	COD (mg COD/L)		$NO_3^- + NH_4^+$ (mg $NO_3^- + NH_4^+$/L)		PO_4^{3-} (mg PO_4^{3-}/L)		Total - Fe (mg Fe/L)		pH	
System	**Avrg**	**S.D**	**Avrg**	**S.D**	**Avrg**	**S.D**	**Avrg**	**S.D**	**Avrg**	**S.D**
I	235	115	89.09	8.65	19.21	2.96	0.53	0.25	7.01	0.16
II	177	120	79.72	5.65	15.62	4.40	1.38	0.29	7.05	0.12
III	166	124	73.78	6.06	10.70	5.26	2.19	0.87	7.09	0.12
IV	150	130	62.01	11.43	4.53	6.26	3.99	1.62	7.38	0.15
V	153	128	68.28	10.39	7.83	6.03	3.18	1.70	7.22	0.13
VI	159	125	69.94	8.54	9.74	5.83	2.52	1.02	7.18	0.14

4.2.4 Effects of Types of Fe^0 Materials on Pollutants Removal

Figure 12 (a) compares the effects of different Fe^0 materials on COD removal. Generally, the Figure indicates that compared to the control (reactor without Fe^0 materials), both SI and SW materials improved the performance of the reactors to remove COD. However, statistically, there was no significant difference in the observed COD removal between System IV (M = 63.2%, SD = 32.0%) and System VII (M = 63.5%, SD = 31.9%), t (31) = -1.2, $p > 0.01$, two-tailed. Therefore, based on the statistical analysis, similar results are expected when either SI or SW materials are applied in Fe^0 - supported anaerobic digestion of domestic sewage for COD removal.

Results in Fig. 12 (b) show the effects of SI and SW materials on PO_4^{3-} removal. The results indicate that the PO_4^{3-} removal in all observations was lower in the control (System I) than in System IV or VII. Therefore, compared to the control, both SI and SW.
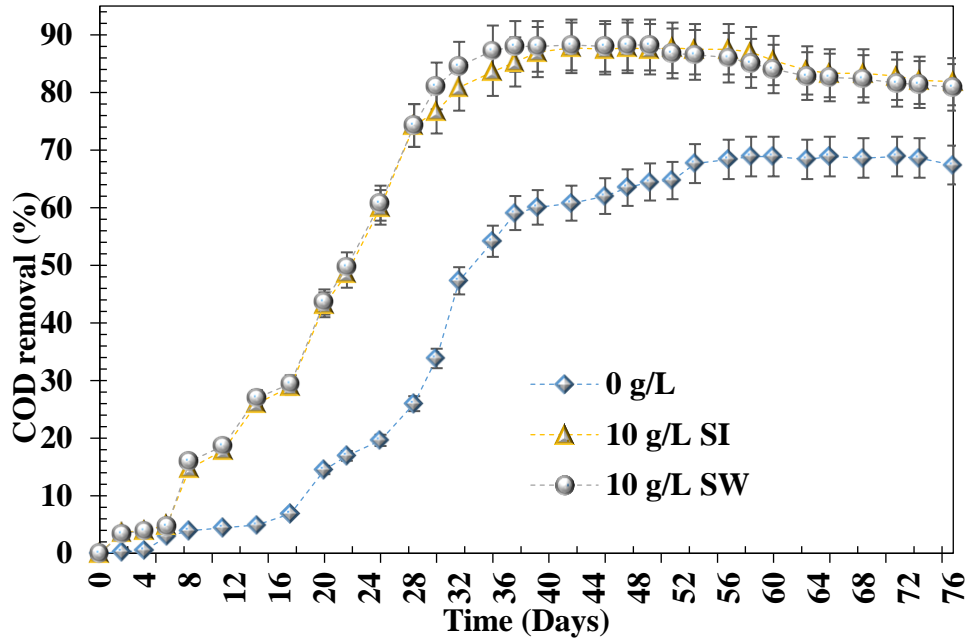
(a)
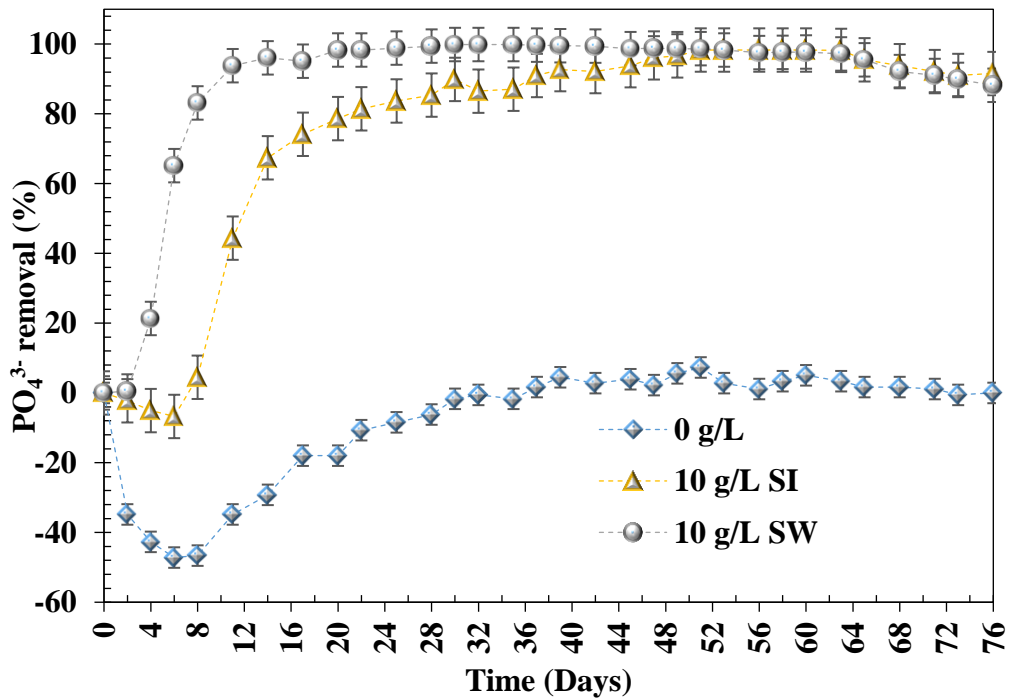
(b)

Figure 12: **Comparison between SI and SW materials' effect on pollutants removal: (a) COD and (b) PO$_4^{3-}$. Fe^0 materials' dosages were 0 g, 10 g/L SI, and 10 g/L SW; Systems' temperature, T= 37 ± 0.5 ^{O}C**
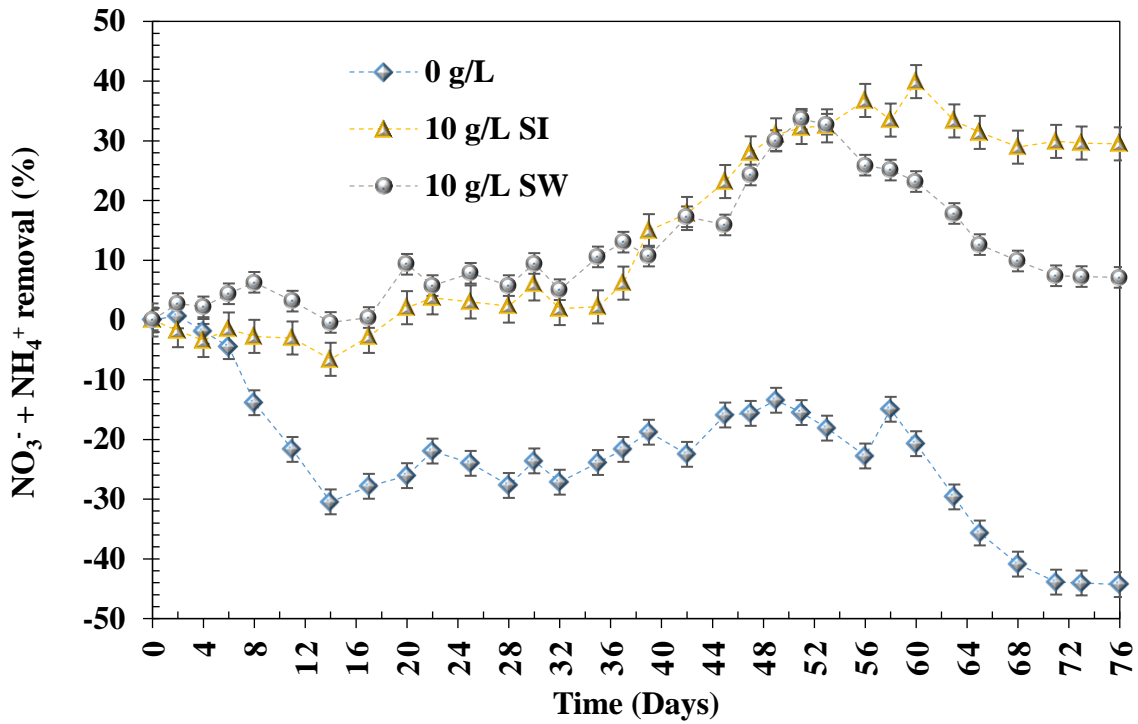
(a)
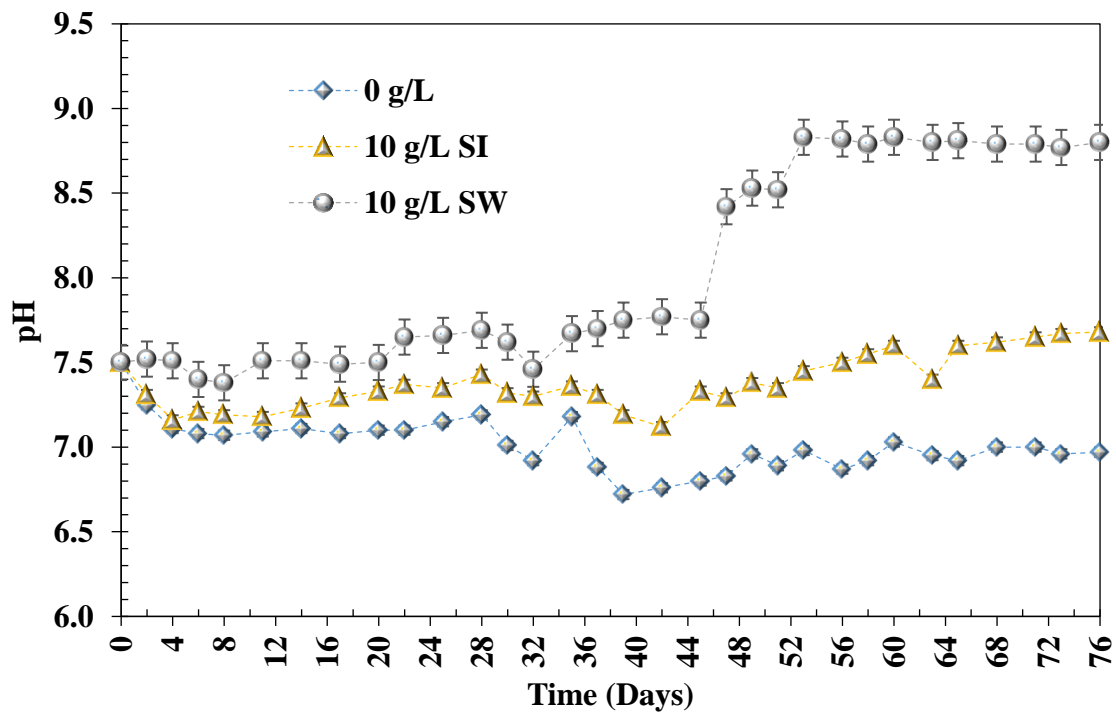
(b)

Figure 13: **Comparison between SI and SW materials' effect on pollutants removal: (a)**
NO_3^- + NH_4^+ and (b) pH variation. Fe^0 materials' dosages were 0 g, 10 g/L SI
and 10 g/L SW; Systems' temperature, T= 37 ± 0.5 ^{O}C

The SW materials improved the performance of the reactors in removing PO_4^{3-}. There was a statistically significant difference in PO_4^{3-} removal between System IV (M = 74.5%, SD = 35.2%) and System VII (M = 87.1%, SD = 27.1%), t (31) = -3.5, $p < 0.01$, two-tailed.

The statistics show that SW materials performed better than SI materials in Fe^0-supported anaerobic digestion of domestic sewage for PO_4^{3-} removal. The PO_4^{3-} removal is mainly due to enhanced precipitation and adsorption of phosphorus by the Fe^0 materials corrosion products. The results patterns were expected because the SW materials have a higher dissolution rate than iron scrap materials (Section 4.1). The higher reactivity of SW compared to SI materials results in more generation FeCPs that scavenge and remove more PO_4^{3-} (Section 4.2.2). It was expected that the remarkable raising of pH observed in system VII from around the 45th day of the operation of the reactor (Fig. 13 (b)) could significantly affect the removal of PO_4^{3-} because, at higher pH values, passivation of Fe^0 materials by FeCPs is high (Wang *et al.,* 2021). However, the expected pH-raising effects were probably not evident because the Fe^0 materials performance was already affected by passivation caused by aging, as reported elsewhere (Sleiman *et al.,* 2017).

Figure 12(a) shows the effects of various Fe^0 materials on COD removal. Overall, both SI and SW materials enhance the reactors' performance in COD removal compared to the control (reactor without Fe^0 material). However, statistically, there was no significant difference in COD removal between System IV (M = 63.2%, SD = 32.0%) and System VII (M = 63.5%, SD = 31.9%), t (31) = -1.2, p > 0.01, two-tailed. Hence, based on the statistical analysis, similar outcomes can be anticipated when either SI or SW materials are employed in Fe^0-supported anaerobic digestion of domestic sewage for COD removal.

Figure 12(b) shows the effects of SI and SW materials on PO_4^{3-} removal. The results reveal that PO_4^{3-} removal in all instances was lower in the control (System I) compared to System IV or VII. Consequently, compared to the control, both SI and SW materials enhance the reactors' performance in removing PO_4^{3-}. However, statistically, there was a significant difference in PO_4^3 removal between System IV (M = 74.5%, SD = 35.2%) and System VII (M = 87.1%, SD = 27.1%), t (31) = -3.5, p < 0.01, two-tailed. The statistics indicate that SW materials performed better than SI materials in Fe^0-supported anaerobic digestion of domestic sewage for PO_4^3 removal. This could be attributed to the fact that PO_4^{3-} removal is primarily facilitated by the enhanced precipitation and adsorption of phosphorus by the corrosion products of Fe^0

materials. The results align with expectations, considering the tested SW materials exhibit a higher dissolution rate than iron scraps materials (Section 4.1).

The heightened reactivity of SW compared to SI materials leads to generating more FeCPs, which scavenge and remove more PO_4^{3-} (Section 4.2.2). It was anticipated that the substantial increase in pH observed in System VII from around the 45th day of reactor operation (Fig. 13 (b)) could significantly improve the PO_4^{3-} removal, as higher pH values contribute to the passivation of Fe^0 materials by FeCPs (Wang *et al.,* 2021). However, the expected effects on pH were not evident, possibly because the performance of Fe^0 materials had already been affected by passivation due to aging, as reported elsewhere (Sleiman *et al.,* 2017)

Figure 13(a) presents the effects of SI and SW materials on removing nutrients in the form of $NO_3^- + NH_4^+$. The findings reveal that the minimum observed $NO_3^- + NH_4^+$ removal in all instances was consistently lower in the control system (System I) compared to Systems IV or VII. Consequently, both SI and SW materials enhanced the reactors' performance for $NO_3^- + NH_4^+$ removal compared to the control. However, from a statistical standpoint, there was no discernible difference in the observed removal of $NO_3^- + NH_4^+$ between the 10 g/L SI reactor (M = 14.9%, SD = 15.7%) and the 10 g/L SW reactor (M = 12.1%, SD = 9.8%), t (31) = 1.6, p > 0.01, two-tailed.

Despite the significant improvement in $NO_3^- + NH_4^+$ removal enhanced by Fe^0 (as discussed in Section 4.2.3), it is noteworthy that $NO_3^- + NH_4^+$ consistently exhibited the lowest removal efficiency among COD, $NO_3^- + NH_4^+$, and PO_4^{3-}, regardless of the type of Fe^0 material used (Figs. 12 & 13(a)). This lesser removal of the pollutant is plausible due to the conversion of some nitrate in the system to ammonium instead of undergoing denitrification (Section 4.2.3).

The relatively higher decline rate in removal efficiency of $NO_3^- + NH_4^+$ observed from the 45th day onwards for the 10 g/L SW system (Fig. 13(c)) may be attributed to the elevated death rate of microbes resulting from substrate deficit and a sudden increase in pH. It is recognized that the suitable pH range for anaerobic wastewater treatment is 6.5 to 7.8, and ammonia toxicity to methanogens begins above a pH of 8.5 (Akunna, 2018). Hence, it is conceivable that the decomposition of biomass from deceased microorganisms' releases nitrogen into the system.

The statistical analysis reveals negative associations between the concentrations of observed pollutants (COD, $NO_3^- + NH_4^+$, and PO_4^{3-}) and the total iron concentrations in Systems IV and VII. For System IV, the correlation coefficients between the observed pollutants and total iron

concentrations were as follows: $R^2 = -0.93$ for COD, $R^2 = -0.90$ for PO_4^{3-}, and $R^2 = -0.21$ for $NO_3^- + NH_4^+$. Meanwhile, for System VII, the correlation coefficients were $R^2 = -0.78$ for COD, $R^2 = -0.86$ for PO_4^{3-}, and $R^2 = -0.45$ for $NO_3^- + NH_4^+$. These results suggest that a higher dissolution of Fe^0 materials correlates with increased removal of pollutants (COD, $NO_3^- + NH_4^+$, and PO_4^{3-}).

Given this, it was anticipated that the tested SW materials, with a higher dissolution rate than iron scraps materials (Section 4.1), would perform significantly better in removing all analyzed pollutants (COD, $NO_3^- + NH_4^+$, and PO_4^{3-}). However, this expectation was not particularly the case for the COD and $NO_3^- + NH_4^+$. This discrepancy could be attributed to the fact that the removal of COD and $NO_3^- + NH_4^+$ primarily relies on microbial digestion, unlike PO_4^{3-} removal, which predominantly depends on enhanced precipitation and adsorption by the corrosion products of Fe^0.

Nevertheless, the correlation coefficient $R^2 = -0.21$ for $NO_3^- + NH_4^+$ suggests a low negative correlation between the observed $NO_3^- + NH_4^+$ and total iron concentrations (Section 2.4). Consequently, the removal of $NO_3^- + NH_4^+$ is not strongly influenced by an increase in the total iron concentration in the system. This may be because excessive iron concentrations could abiotically convert NO_3^- to NH_4^+ instead of facilitating the desired denitrification (Section 4.2.3).

The introduction of SW materials led to a domestic sewage pH elevation beyond the recommended range for anaerobic digestion. The optimum pH range for anaerobic wastewater treatment typically falls between 6.5 and 7.8, with values exceeding 8.5 considered unfavorable (Akunna, 2018). However, the observed pH changes in the studied systems were 7.5 to 6.7 in System I, 7.5 to 7.7 in System IV, and 7.5 to 8.8 in System VII (Fig. 13(b)). Consequently, these findings suggest two key observations: (a) Fe^0 materials can raise the pH of domestic sewage, and (b) SW materials are more prone than SI to causing the issue of elevated pH in Fe^0-supported anaerobic digestion of domestic sewage.

Various studies have reported varying pH increases from introducing Fe^0 materials (He *et al.,* 2022; Xu *et al.,* 2017; You *et al.,* 2017). For instance, Domrongpokkaphan *et al.* (2021) observed a pH range of 7 to 9 in the anaerobic treatment of palm oil mill effluent facilitated by Fe^0. In a separate study by Paepatung *et al.* (2020), a pH increase from 6.3 to 8.1 was noted in the anaerobic digestion of sulfate-rich wastewater dosed with iron scraps. The potential of Fe^0

materials to elevate pH in anaerobic digestion can be attributed to the release of hydroxyl ions during the anaerobic oxidation of the materials (Equation (4)). Similarly, as reported in the study by Till *et al.* (1998), steel wool Fe^0 materials with a smaller specific area did not significantly elevate the pH in the anaerobic digestion of synthetic wastewater, while Fe^0 powder with a relatively larger specific area increased the pH of the wastewater to above 10. This could explain why SW materials in this study caused a comparatively higher rise in the pH of domestic sewage than SI materials.

The observed increase in pH in System VII from around the 45th day of reactor operation (Fig. 13(b)) may be attributed to the depletion of volatile fatty acids, which served as a pH buffer (Charalambous & Vyrides, 2021). The pH effect was particularly significant in System VII, possibly due to the higher reactivity of SW compared to SI materials, leading to a more significant generation of hydroxyl ions (Equation (4)).

4.2.5 Optimization of Fe^0 Materials Dosage

The analysis was undertaken to determine the optimal dosage of the investigated Fe^0 materials, aiming to remove the pollutants (COD, $NO_3^- + NH_4^+$, and PO_4^{3-}) in the treated effluents. The concise overview of optimization constraints is detailed in Table 7. Furthermore, Table 8 comprehensively summarizes the optimal solutions derived from the objective function, focusing on the highest desirability index for each tested dosage of Fe^0 materials.

The performance ranking of systems, gauged by the simultaneous removal of pollutants (COD, $NO_3^- + NH_4^+$, and PO_4^{3-}), is presented in terms of desirability indices in Table 8. The order of treatment removal efficiency is as follows: IV > VII > V > VI > III > II > I. Strikingly, the optimal system (System IV) scored the highest desirability index of 0.985.

The remaining concentrations of COD, $NO_3^- + NH_4^+$, and PO_4^{3-} in the effluent from the optimum reactor were measured at 57.9 mg/L, 43.8 mg/L, and 0.5 mg/L, respectively, and these levels were achieved within a 60-day operational timeframe (Table 8).

Table 7: **Set of constraints for optimization of the objective function**

Name	Goal	Lower Limit	Upper Limit	Lower Weight	Upper Weight	Importance
A: Time	is in range	0 days	76 days	1	1	3
B: Fe^0 Dosage	is in range	0 g/L	30 g/L-S	1	1	3
COD	minimise	48 mg/L	408 mg/L	1	1	3
PO_4^{-3}	minimise	0.3 mg/L	26.2 mg/L	1	1	3
$NO_3^- + NH_4^+$	minimise	43.8 mg/L	105.2 mg/L	1	1	3

Table 8: **Ranking of systems performance based on desirability indices**

Time (days)	System	COD (mg COD/L)	PO_4^{3-} (mg PO_4^{3-}/L)	$NO_3^- + NH_4^+$ (mg NO_3^- + NH_4^+/L)	Desirability
60	IV	57.9	0.5	43.8	0.985
53	VII	54.5	0.3	54.6	0.932
53	V	56.7	3.6	50.8	0.907
51	VI	65.3	6.7	52.5	0.848
58	III	66.1	6.3	65.3	0.777
58	II	81.2	11.4	71.7	0.654
49	I	142.3	15.4	82.7	0.482

4.2.6 Behaviour of Fe^0 Materials in Domestic Sewage

Figure 14 intricately depicts a thorough comparison of the pH-elevating capabilities exhibited by distinct Fe^0 materials (SI and SW) in diverse media, encompassing both domestic sewage and distilled water. Notably, System IX demonstrated a considerably higher maximum pH value, reaching 9.4, in contrast to the value of 8.8 observed in System VIII (Fig. 14(a)). In a parallel vein, System VII exhibited a relatively higher maximum pH value of 8.8 compared to the recorded value of 7.5 in System IV (Fig. 14(b)).

Beyond these comparisons, it is noteworthy that the pH of distilled water in System IX swiftly reached its peak value of 9.4 within a mere six days of operation (Fig. 14(a)), while in System VII, the pH of domestic sewage took a more extended sixty-day operational period to attain its maximum value of 8.8 (Fig. 14(b)). Consequently, the findings confirm that: (a) SW materials showcase a superior potential for elevating the pH of both water and domestic sewage compared to SI materials, and (b) Fe^0 materials manifest a more rapid impact on raising the pH of distilled water as opposed to domestic sewage.

In wastewater treatment, the anaerobic digestion process progresses through the acidogenesis stage, characterized by generating volatile fatty acids, including butyrate, propionate, and valerate (Metcalf *et al.,* 2014). In light of this, a fraction of the hydroxide ions (OH-) released during the anaerobic oxidation of Fe^0 materials (Equation (4)) undergoes neutralization, thereby contributing to the regulation of the system's pH.

Results on the effect of SI and SW materials on the observed total iron concentration in the reactors fed with the same domestic sewage or distilled water are presented in Fig. 15. The results indicate that the maximum total iron concentrations in Systems IV, VII, VIII, and IX were 6.19 mg/L, 7.05 mg/L, 7.70 mg/L, and 10.80 mg/L, respectively. The results imply that SW material's dissolution is higher than SI materials in domestic sewage and distilled water. The observed total iron concentration dropped sharply from maximum to the lower minimum in distilled water (Fig. 15 (a)) compared to domestic sewage (Fig. 15 (b)). The phenomenon occurs because the passivation rate of metallic iron materials reduces in the presence of organic carbon (Deng *et al.,* 2020).

The organic carbon content in distilled water is negligible compared to domestic sewage. The higher decreasing rate of the total iron concentration observed in system VII compared to system IV from around the 45th day of the reactors' operation (Fig. 15(b)) was perhaps due to the higher passivation rate of SW materials caused by the rise in pH (Fig. 13(b)) in system VII compared to IV. The passivation rate of Fe^0 by FeCPs is higher in alkaline conditions (Wang *et al.,* 2021).
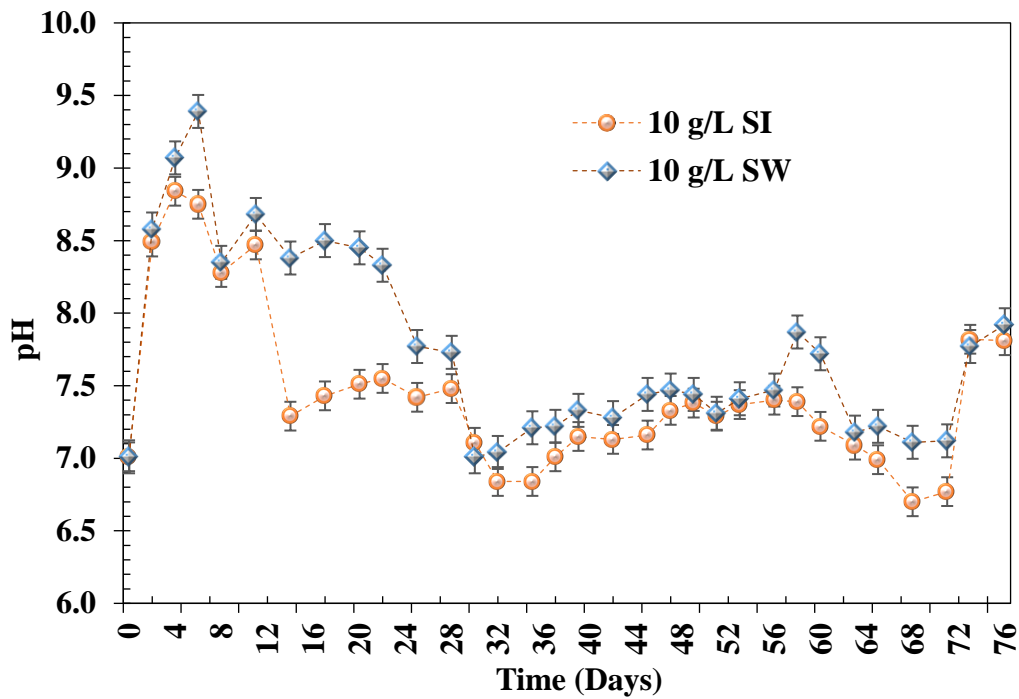
(a)
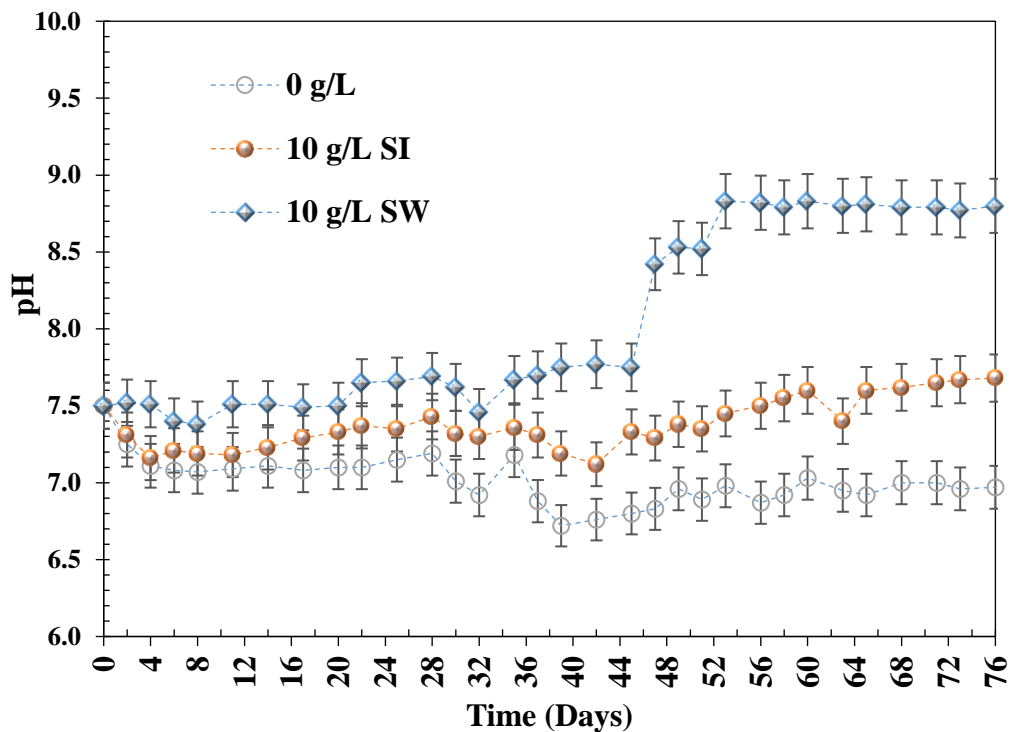
(b)

Figure 14: pH variations resulting from 10 g/L of Fe^0 materials (SW or SI) dosage in distilled water or domestic sewage: (a) Fe^0 materials in distilled water; (b) Fe^0 materials in domestic sewage. Systems' temperature, T = 37 ± 0.5 ^OC
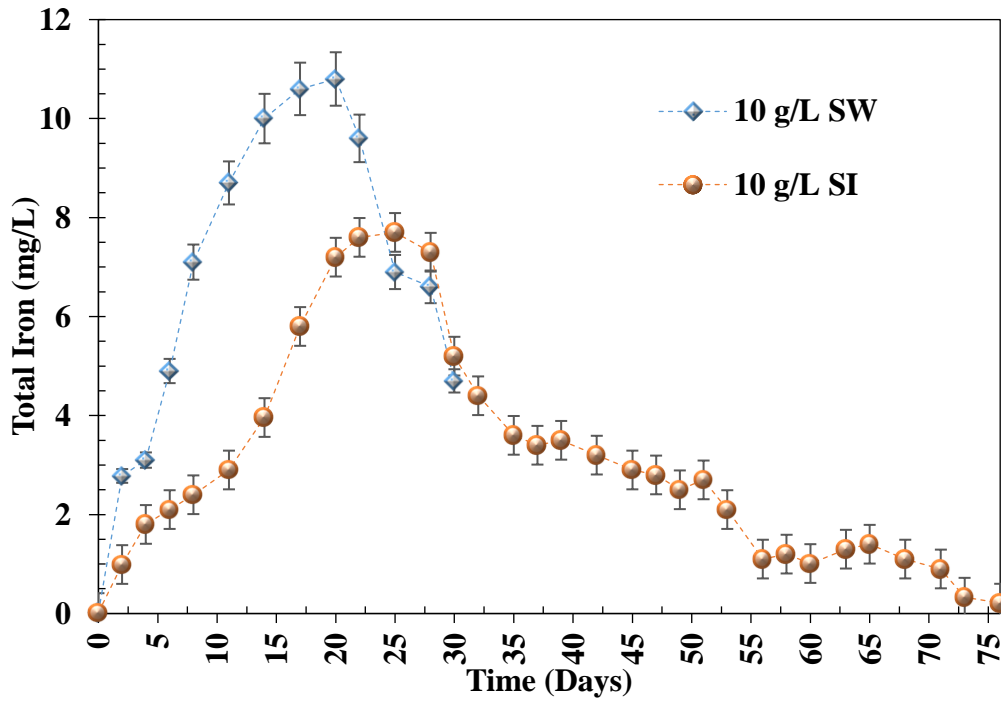
(a)
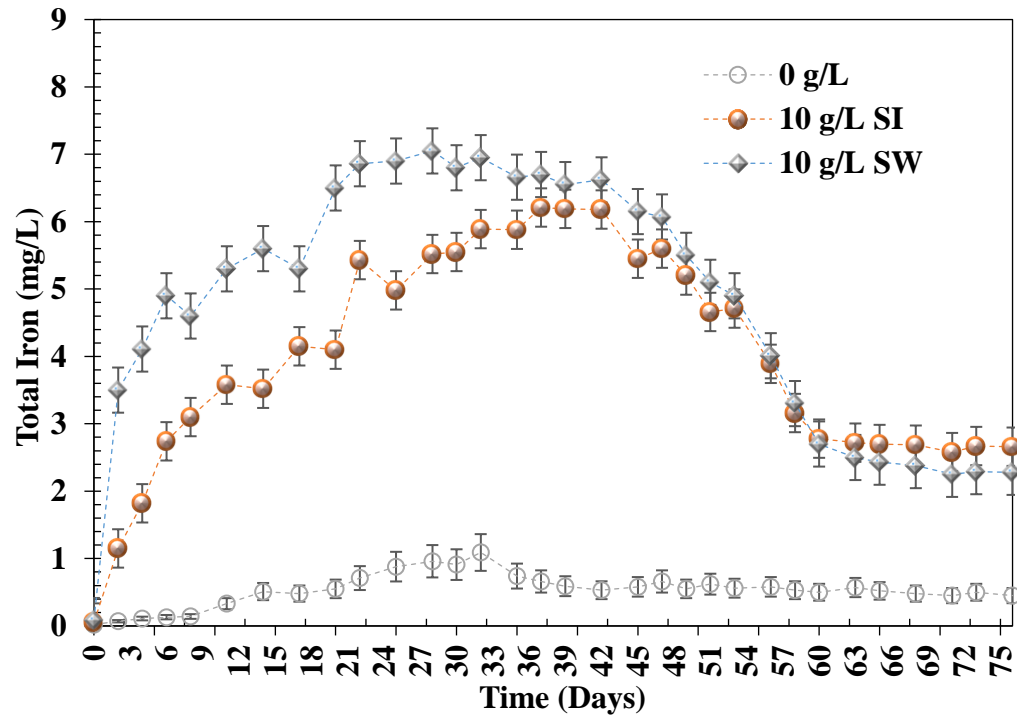
(b)

Figure 15: **Total iron concentration variations resulting from 10 g/L of Fe⁰ materials (SW or SI) dosage in distilled water or domestic sewage: (a) Fe⁰ materials in distilled water; (b) Fe⁰ materials in domestic sewage. Systems' temperature, T = 37 ± 0.5 °C**

4.3 Effects of Fe^0 Materials Types on Sludge Quantity and Quality

4.3.1 Physical Characteristics of Sludge

The results of solids analysis for the sludges produced from varying dosages of Fe^0 materials in anaerobic reactors are presented in Tables 9 and 10. Table 9 findings reveal that, compared to the control reactor, Fe^0 materials fed anaerobic reactors generated sludge with increased weight, volume, total suspended solids (TSS), and volatile suspended solids (VSS). For instance, the 10 g/L iron scrap (SI) reactor produced 275 mL/L of settled sludge, exceeding by more than 1.4 times the 190 mL/L produced in the control reactor. However, it is noteworthy that the control reactor produced sludge with a VSS to TSS ratio of 69%, the highest compared to 52% for the 10 g/L SI reactor and 45% for the 10 g/L steel wool (SW) reactor.

The large volume of sludge generated from Fe^0-aided anaerobic reactors, in contrast to the control system, can be attributed to three main factors: (a) the accumulation of passivated Fe^0 solids (Wu *et al.,* 2015), (b) increased biomass generation due to the proliferation of microbial populations enhanced by Fe^0 materials (Deng *et al.,* 2020; Zhang *et al.,* 2011), and (c) the contribution of solids from enhanced precipitation and adsorption of pollutants by Fe corrosion products (Lufingo *et al.*, 2019; Noubactep, 2010).

The data in Table 10 further indicates that the observed TSS concentrations at 60 min, 90 min, and 150 min settling times were 329 mg/L, 319 mg/L, and 310 mg/L for the 10 g/L SI reactor and 663 mg/L, 635 mg/L, and 555 mg/L for the 10 g/L SW reactor, respectively. These results suggest that relatively more solids will remain suspended (unsettled) in the 10 g/L SW reactor, resulting in lower collected sludge compared to the 10 g/L SI reactor. This discrepancy is likely due to the higher reactivity of steel wool (SW) materials (Section 4.1), causing more corrosion and the formation of a more concentrated range of finer particles with lower settling velocities than the particles from iron scrap (SI) materials.

On a different note, the overall solid removal efficiencies achieved at settling times of 60 min and 90 min were 93.07% and 94.13% for the control reactor, 92.31% and 93.30% for the 10 mg/L SI reactor, and 83.86 % and 85.22 % for the 10 mg/L SW reactor (Figs. 16 &17). The 90-minute and 120-minute settling times at a 2.5 m column depth correspond to settling velocities (overflow rates) of 40 m/day and 30 m/day.

The findings from this study strongly suggest the feasibility of removing over 80% of particles generated from Fe^0-aided anaerobic digestion of domestic sewage using sedimentation tanks (clarifiers) designed with an overflow rate of 40 m/d or less. These results also reveal that Fe^0-aided anaerobic digestion generates suspended solids with lower average settling velocities than anaerobic digesters without such materials. Beyond the typical biosolids generated from the anaerobic digestion of solids from domestic sewage, certain particles arise from precipitation and the adsorption of pollutants by the Fe^0 materials' corrosion products (FeCPs).

Table 9:   Comparison of the physical characteristics of sludges from different reactors

Sample parameters	Unit	Systems					
		0 g/L		10 g/L SI		10 g/L SW	
		M	SD	M	SD	M	SD
Sludge weight at 105 °C (TS)	kg/m^3	9.2	0.38	15.5	0.41	20.5	0.43
TSS	mg/L	8730	7.8	14550	8.1	19520	8.6
VSS	mg/L	6040	6.2	7550	7.1	8720	7.8
VSS/TSS	%	69	1.3	52	1.5	45	1.7
Sludge volume/Settleable solids (After 30 min settling time)	mL/L	190	2.4	275	2.2	200	2.3
Sludge volume index (SVI)	mL/gTSS	22	0.7	19	0.5	10	0.8

"TS" stands for total solids, "VSS" for volatile suspended solids, "TSS" for total suspended solids, "M" for mean, and "SD" for standard deviation.

Table 10:   TSS concentrations for domestic sewage from different reactors observed at a 2.5 m depth of the settling column

Reactor name	TSS_0 (mg/L)		TSS_{60} (mg/L)		TSS_{90} (mg/L)		TSS_{150} (mg/L)	
	M	SD	M	SD	M	SD	M	SD
0 g/L	2510	8.4	257	7.4	244	6.6	217	5.8
10 g/L SI	3433	10.1	329	9.8	319	9.1	310	8.7
10 g/L SW	3506	12.2	663	10.8	635	11	555	9.7

"M" stands for mean, "SD" for standard deviation, and "TSS_0'', "TSS_{60}'', and "TSS_{150}'' for total suspended solids concentrations at 0 min, 60 min, and 90 min settling times, respectively.
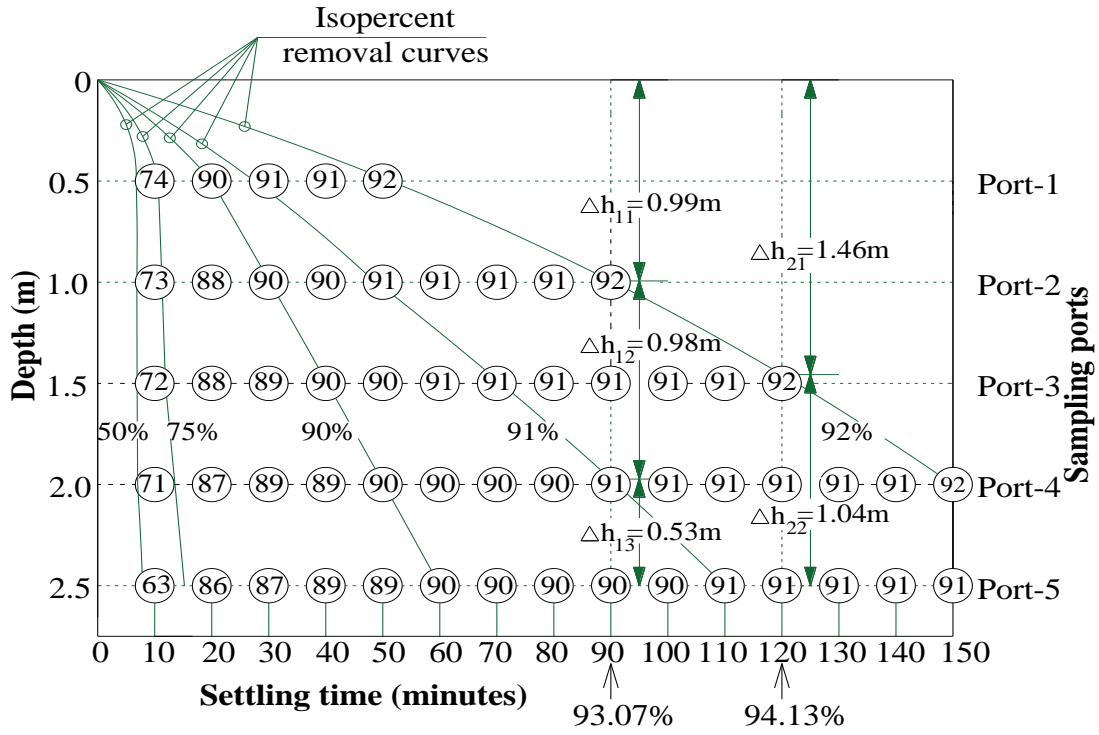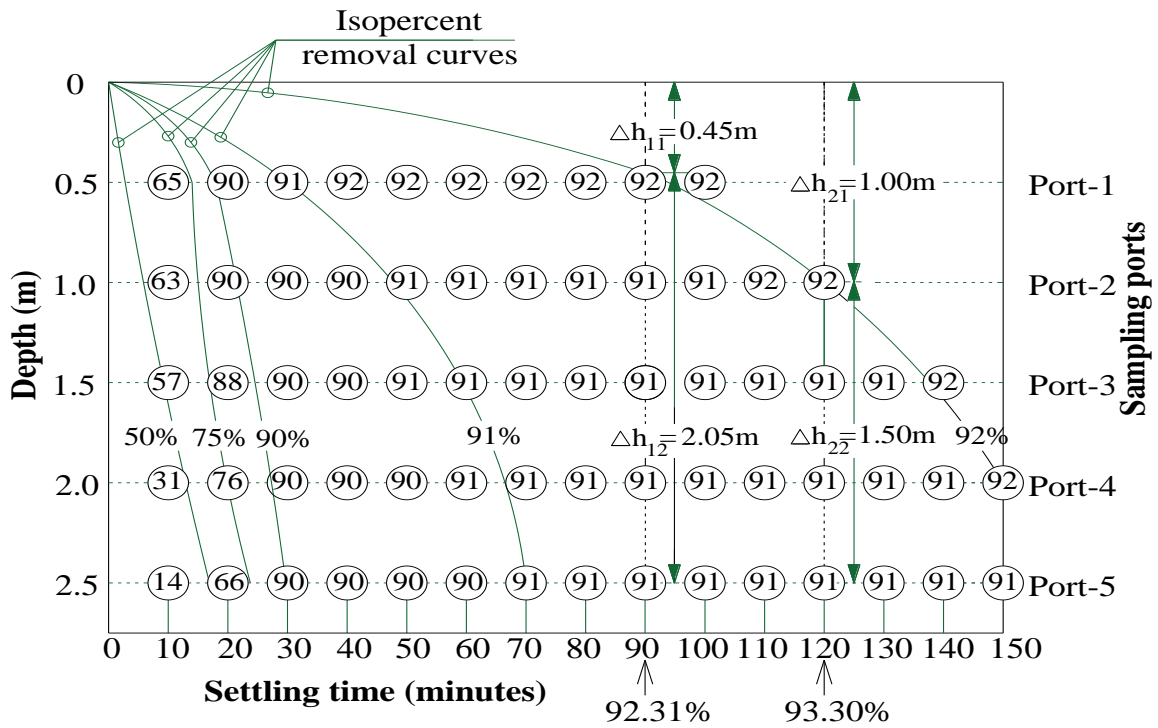
Figure 16: Percent removal and isoremoval curves for settling column analysis: (a) Reactor without Fe⁰ materials (b) Reactor dosed with 10 mg/L SI materials
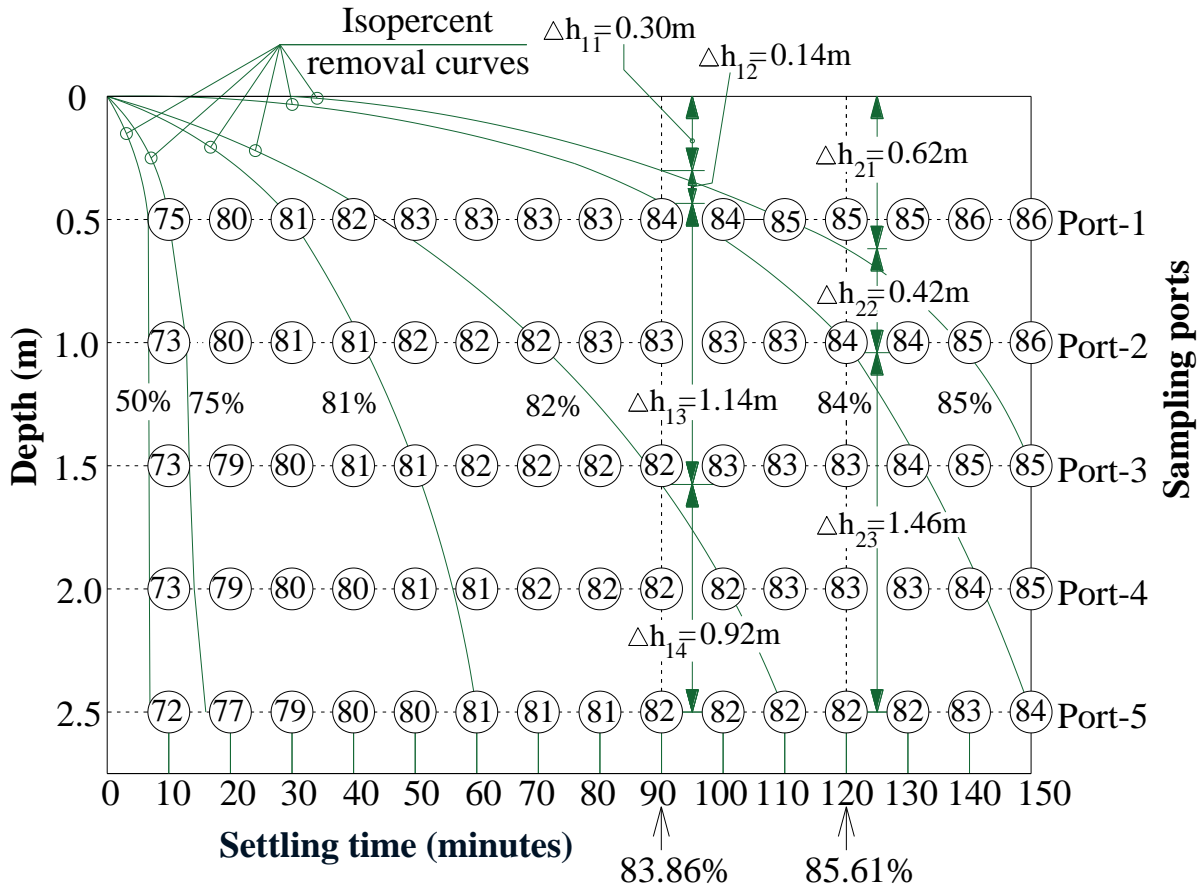
Figure 17: Percent removal and Isoremoval curves for settling column analysis: (c) Reactor dosed with 10 mg/L SW materials

The observed low settling velocity may be attributed to the varied nature and sizes of precipitates from Fe^0-aided anaerobic reactors. For instance, nitrogen may be removed as metal ammonium phosphates ($FeNH_4PO_4.H_2O$) (Booker *et al.,* 1999; Bridger *et al.,* 1962; Zhou *et al.,* 2018), phosphates as ferric phosphate precipitates ($Fe_{0.8} HPO_4(OH)_{1.4}$), and sulfur as iron sulphide (Fe_2S) (Lytras *et al.,* 2021b; Metcalf *et al.,* 2014; Puyol *et al.,* 2018; Ruan *et al.,* 2017; Su *et al.,* 2013b; Zhang *et al.,* 2011).

Although the average settling velocity of solids from reactors dosed with Fe^0 materials is noticeably lower than that of solids from the control reactor (Figs. 16 & 17), a substantial fraction of solids with relatively higher settling velocities was sufficient to form more sludge in the reactors dosed with Fe^0 materials compared to the control reactor (Table 9). Adding Fe^0 materials has been reported to enhance the size and settling rate of granules formed in municipal wastewater treatment (Eljamal *et al.,* 2020). Despite the observed lower settling velocities, it is essential to emphasize that the sludges from all reactors are consistently

73

categorized as well-settling, as their Sludge Volume Indices (SVIs) are below 100 (Table 9). This classification of sludge based on SVI has been documented in the literature (Cornwell, 2022; Filipe & Grady, 1998; Gray, 2004; Vesilind *et al.,* 2009; Weiner *et al.,* 2003).

4.3.2 Chemical Characteristics of Sludge

(i) Organic matters

The concentrations of organic matter in the three distinct types of tested sludges are presented in Table 11. The findings suggest that the sludge from reactors dosed with Fe^0 materials exhibited comparatively higher concentrations of nitrogen (N) and sulfur (S) but lower concentrations of organic carbon than the control reactor (Table 11). Statistical analysis of the tested sludges from the anaerobic reactors (I, II, and III) reveals that (a) there was a significant difference in the observed concentrations of organic matters (C, N, and S) and C/N ratio between reactor I and II or III, $p < 0.05$, two-tailed (Figs. 18, 19 & 20) (b) there was a significant difference in the observed concentrations of C and N, and C/N ratio between Reactor II and III, $p < 0.05$, two-tailed (Table 11) (c) there was no significant difference in the observed S concentrations between Reactor II and III, $p < 0.05$, two-tailed.

The comparatively reduced quantity of organic carbon in the sludges from reactors II and III (Table 11) is likely attributed to the more extensive conversion of organics into CO_2 and CH_4 (Abdelsalam *et al.,* 2017; Belay & Daniels, 1990; Lytras *et al.,* 2021a; Ma *et al.,* 2018). The removal of COD and the production of biogas are elevated in the anaerobic reactors aided by Fe^0 materials compared to the control (reactor without Fe^0 materials), as demonstrated in Section 4.2.1 and other studies (Charalambous & Vyrides, 2021; Dykstra & Pavlostathis, 2017; Konaté *et al.,* 2013; Liu, Wang, *et al.,* 2015; Paepatung *et al.,* 2020; Wei *et al.,* 2018; Wu *et al.,* 2015). Moreover, adding Fe^0 materials leads to the accumulation of passivated Fe^0 solids (Sleiman *et al.,* 2017; Wu *et al.,* 2015) that contribute to the increase in the inorganic solids in the Fe^0-aided anaerobic reactors compared to the reactor without Fe^0 (control).

Table 11: **Comparison of the observed parameters' in dry sludges from the test anaerobic digestion reactors**

Groups	Parameters	Reactor I		Reactor II		Reactor III	
		M	SD	M	SD	M	SD
Micronutrients and toxic elements in plants	Fe (%)	0.1	0.01	7.6	0.4	14.6	0.8
	Mn (mg/kg)	270.9	2.3	584.5	2.9	948.4	3.2
	Cu (mg/kg)	9.5	0.5	249.8	1.5	420	2.2
	Zn (mg/kg)	298.2	1.9	534.8	3.3	376	2.0
	Cr (mg/kg)	22.0	0.5	25.4	1.0	27.2	1.0
	Ni (mg/kg)	6.0	0.4	45.6	0.8	58.0	1.1
	Pb (mg/kg)	0.25	0.04	1.4	0.1	3.1	0.1
	Cd (mg/kg)	ND	-	ND	-	ND	-
Macronutrients	P (mg/kg)	129.2	3.6	280.4	4.3	364.2	4.9
	K (%)	0.02	0.003	0.07	0.002	0.08	0.003
	Mg (%)	6.29	0.53	0.2	0.02	0.51	0.03
	Ca (%)	4.67	0.25	3.5	0.17	1.33	0.06
	SAR	0.1	0.02	0.8	0.13	2.3	0.2
Organic matters	N (%)	0.78	0.03	1.78	0.07	1.48	0.06
	S (mg/kg)	0.42	0.05	0.94	0.07	0.82	0.06
	C (%)	27.1	1.3	15.8	0.9	6.6	0.8
	C/N	34	0.3	9	0.8	5	0.6
	pH (1:2.5)	6.16	0.01	6.57	0.02	6.96	0.02

"M" stands for mean and "SD" for a standard deviation for $n = 3$; ND for not detected.

On the other hand, a relatively higher amount of N in Fe^0 materials dosed reactors compared to the control reactor may be due to the precipitation of nitrogen as metal ammonium phosphates ($FeNH_4PO_4.H_2O$) (Booker *et al.,* 1999; Bridger *et al.,* 1962; Zhou *et al.,* 2018) and nitrogen released from the dead microbes. The Fe^0-aided AD is associated with the proliferation of microbial populations (Deng *et al.,* 2020; Zhang *et al.,* 2011). Furthermore, a higher amount of S in Fe^0 materials dosed reactors than the control may be due to the precipitation of iron-sulphide (FeS) due to Fe^0 materials dosage (Lytras *et al.,* 2021a; Puyol *et al.,* 2018; Ruan *et al.,* 2017; Su *et al.,* 2013a; Zhang *et al.,* 2011). Furthermore, the relatively higher concentration of organic matter (C, N, and S) in the sludges from reactor II compared

to that from reactor III is perceivably due to a higher accumulated amount of FeCPs in reactor III compared to reactor II. Because SW materials are more reactive than SI materials (Li *et al.*, 2016; Lufingo *et al.*, 2019; Till *et al.*, 1998), more FeCPs may have contributed to the increase in the percentage of inorganic solids in reactor III than II.

The mass C/N ratio of the sludges from the reactors was 34 for 0 g/L, 9 for 10 g/L SI, and 5 for 10 g/L SW (Table 1). The C/N ratio in the reactors dosed with Fe^0 materials was below the optimum range of 25 to 35 for the composting process (Alidadi *et al.*, 2007). The relatively higher N and lower C contents in the sludges from the systems dosed with Fe^0 materials resulted in lower C/N ratios than the control system (Table 11). Therefore, during AD of the sludge from Fe-aided anaerobic digestors, materials with more organic carbon, such as sawdust, rice husks, leaves, wood chips, and old compost, may be added to regulate the C/N ratio (Alidadi *et al.*, 2007). However, the results clearly show that the Fe^0-aided AD increased the concentration of N and S by more than 1.5 times that of the N and S in the control reactor (Figs. 18, 19 & 20). Therefore, the sludge from the Fe^0-aided anaerobic reactors can potentially increase soil organic matter for N and S if applied to land.

(ii) Macro-nutrients

The concentrations of macro-nutrients in the three different types of sludges tested are presented in Table 11. The results indicate relatively higher N, P, K, S, and SAR but lower mg and Ca concentrations in the sludge from the reactors dosed with Fe^0 materials than in the control reactor (Table 11). The sludges analysis results for the tested Fe^0-aided anaerobic reactors (0 g/L, 10 g/L SI, and 10 g/L SW) indicate that statistically: (a) there was a significant difference in the observed concentrations of macro-nutrients (N, P, K, Mg, Ca, and S) and SAR between reactor I and II, $p < 0.05$, two-tailed or reactor III, $p < 0.05$, two-tailed (Table 11) (b) there were significant differences in the observed concentrations of macro-nutrients (N, P, Mg, Ca, and S) and SAR between reactor II and III, $p < 0.05$, two-tailed (Figs. 18, 19 & 20) (c) there was no significant difference in the observed K concentrations between reactor II and III, $p > 0.05$, two-tailed (Table 11).

The elevated concentrations of N, P, K, and S in the sludge from reactors dosed with Fe^0 materials, as compared to the control reactor, can be attributed to several factors: (a) The formation of metal ammonium phosphates, such as $Fe_5(PO_4)_2(OH)_9$, and $FePO_4$, as reported in other studies (Bridger *et al.*, 1962; R.-h. Li *et al.*, 2018; Zhang *et al.*, 2019; Zhang *et al.*, 2022;

Zhang *et al.,* 2021); (b) The precipitation of S as Fe_2S, as reported elsewhere (Lytras *et al.,* 2021a; Mamais *et al.,* 1994; Puyol *et al.,* 2018; Ruan *et al.,* 2017; Zhang *et al.,* 2011) and (c) The potential precipitation of K as $FeKPO_4$, as informed by Lin *et al.* (2015). Despite the fact that the bonding of P with Fe in precipitation reduces the availability of P, as noted by Puyol *et al.* (2018), the results in Table 11 demonstrate that extractable P has more than doubled in reactors dosed with Fe materials compared to the control reactor (reactor without Fe^0 materials). Hence, it is conceivable that a more substantial phosphorus recovery could be achieved if the sludges underwent additional treatment with lime or other established phosphorus recovery methods (Almeelbi & Bezbaruah, 2014; Wang *et al.,* 2021).

Conversely, the relatively diminished concentrations of calcium (Ca) and magnesium (Mg) metals in the sludge from reactors treated with Fe^0 materials can be attributed to (b) the prevalence of iron in the reactors, making it the preferred cation for the precipitation of available anions and (b) The heightened affinity of iron to anions such as phosphorus, potentially resulting in reduced precipitation of compounds like calcium phosphate ($Ca_3(PO_4)_2$) and struvite ($MgNH_4PO_4$) (Flores-Alsina *et al.,* 2016).

(iii)   Micronutrients and toxic elements to plants

Table 11 provides findings on the measured concentrations of micronutrients (Fe, Mn, Cu, and Zn) and toxic elements (Cr, Ni, and Pb) in three distinct types of sludges. The concentrations of micronutrients in the sludge originating from the reactor without Fe^0 materials were lower than those in sludges from reactors dosed with Fe^0 materials. Consequently, it is apparent that anaerobic digestion of domestic sewage with the assistance of Fe^0 has the capacity to enhance the concentration of both micronutrients and toxic elements in the resulting sludge.

The results of the sludge analysis for the tested Fe^0-aided anaerobic reactors (0 g/L, 10 g/L SI, and 10 g/L SW) show statistically significant findings: (a) a significant difference in the observed concentrations of micronutrients (Fe, Mn, Cu, and Zn) and toxic elements (Cr, Ni, and Pb) between Reactor I and II, $p < 0.05$, two-tailed, or Reactor III, $p < 0.05$, two-tailed (Table 11); (b) a significant difference in the observed concentrations of micronutrients (Fe, Mn, Cu, and Zn) and toxic elements (Ni and Pb) between Reactor II and III, $p < 0.05$, two-tailed (Table 11); (c) no significant difference in the observed Cr concentrations between Reactor II and III, $p > 0.05$, two-tailed (Table 11).

The elevated concentrations of metals, including Mn, Cu, Zn, Cr, Ni, and Pb, in the sludge from reactors dosed with Fe^0 materials, as opposed to the control reactor, may be attributed to adsorption onto the surface of metallic iron materials or FeCPs (Wilkin & McNeil, 2003). Moreover, the increased reactivity of Fe^0 materials, leading to producing more FeCPs, could potentially explain the higher concentrations of micronutrients and toxic elements in reactor III compared to reactor II (Table 11).

However, the concentration of toxic elements in the sludges from the reactors (II and III) dosed with Fe^0 materials (Table 11) is far better than the European Directive 86/278/EEC proposed allowable concentrations of heavy metals in Wastewater sludge used in agriculture: 20 to 40 for Cd, 1000 to 1750 mg/kg for Cu, 300 to 400 mg/kg for Ni, 750 to 1200 mg/kg for Pb, 2500 to 4000 mg/kg for Zn, and Cr is not limited (Wiśniowska *et al.,* 2019a). Similarly, the concentrations are also far better than US EPA pollutant ceiling concentrations (85 mg/kg for Cd, 3000 mg/kg for Cr, 4300 mg/kg for Cu, 840 mg/kg for Pb, 420 mg/kg for Ni, and 7500 mg/kg for Zn) for the land application of Wastewater sludge (USEPA, 1994). Therefore, sludges from Fe^0-aided AD of DS contain heavy metals within acceptable concentrations for application in agricultural lands.

Nevertheless, the concentrations of toxic elements in the sludges from reactors II and III, dosed with Fe^0 materials (Table 11), are far better than the proposed allowable concentrations of heavy metals in wastewater sludge for agricultural use according to European Directive 86/278/EEC: 20 to 40 for Cd, 1000 to 1750 mg/kg for Cu, 300 to 400 mg/kg for Ni, 750 to 1200 mg/kg for Pb, 2500 to 4000 mg/kg for Zn, with no specified limit for Cr (Wiśniowska *et al.,* 2019a). Similarly, these concentrations are also far better than the pollutant ceiling concentrations set by the US EPA for the land application of wastewater sludge (85 mg/kg for Cd, 3000 mg/kg for Cr, 4300 mg/kg for Cu, 840 mg/kg for Pb, 420 mg/kg for Ni, and 7500 mg/kg for Zn) (USEPA, 1994). Therefore, the sludges resulting from Fe^0-aided anaerobic digestion of domestic sewage still contain heavy metals within acceptable concentrations for application in agricultural lands.

4.3.3 Effects of Fe^0 Materials Types on Biogas Quantity and Quality

Figures 18, 19, and 20 show the influence of different Fe^0 types on both the quantity and quality of the produced biogas. The outcomes indicate that, within the examined reactors, the highest CH_4 contents (Fig. 18(a)) and cumulative specific CH_4 yield (Fig. 20(a)) were attained as 79.8% and 684.3 mLCH4/gVS for 10 g/L SI, 78.9% and 609.8 mLCH4/gVS for 10 g/L SW, and 67.4% and 422.6 mLCH4/gVS for the control reactor. Based on the cumulative specific CH_4 yield (Fig. 20(a)), introducing 10 g/L SI augmented CH4 gas production by 38.3%, while including 10 g/L SW resulted in a 30.7% increase in gas production. Conversely, the highest observed concentrations of CO_2 (Fig. 18(b)), H_2S (Fig. 19(a)), and NH_3 (Fig. (b)) were 7.9%, 135 ppm, and 97 ppm for 0 g/L, 6.7%, 93 ppm, and 68 ppm for 10 g/L SI, and 7.0%, 70 ppm, and 62 ppm for 10 g/L SW.

Furthermore, the results depicted in Fig. 20(b) reveal specific CH_4 yields of 0.22 m^3/kgCOD for reactor I (0 g/L), 0.33 m^3/kgCOD for reactor II (10 g/L SI), and 0.31 m^3/kgCOD for reactor III (10 g/L SW). Generally, the findings suggest that: (a) reactors with Fe^0 materials (SI or SW) produced biogas with higher CH_4 (Fig. 18(a)) but lower CO_2 (Fig. 18(b)), H_2S (Fig. 19(a)), and NH_3 (Fig.19(b)) contents compared to the reactor without Fe^0 materials (control); (b) reactors with Fe^0 materials (SI or SW) generated a more significant amount of CH_4 (mL) compared to the reactor without Fe^0 materials (Fig. 20); (c) reactors with SI materials (10 g/L SI) produced biogas with higher CH4 (Fig. 18(a)), H_2S (Fig. 19(a)), and NH_3 (Fig.19(b)) but lower CO_2 (Fig. 18(b)) contents compared to the reactor with SW materials (10 g/L SW); (d) reactors with SI materials produced a more significant amount of CH_4 (mL) compared to the reactor with SW materials (Fig. 20).

Statistically, (a) a significant difference was observed in the CH_4 content between biogas produced in 0 g/L (M = 53.2%, SD = 15%) and 10 g/L SI (M = 63.4%, SD = 17.30%), t (14) = -11.4, $p < 0.05$, two-tailed, or 10 g/L SW (M = 62.3%, SD = 17.4%), t (14) = -10.3, $p < 0.05$, two-tailed. Conversely, there was no distinguishable difference in the observed CH_4 content in the biogas between 10 g/L SI (M = 63.4%, SD = 17.30%) and 10 g/L SW (M = 62.3%, SD = 17.4%), t (14) = -1.0, $p > 0.05$, two-tailed. (b) A significant difference was found in the observed CO_2 content between biogas produced in 0 g/L (M = 6.5%, SD = 1.7%) and 10 g/L SI (M = 5.5%, SD = 1.4%), t(14) = 8.9, $p < 0.05$, two-tailed, or 10 g/L SW (M = 5.6%, SD = 1.6%), t(14) = 18.9, $p < 0.05$, two-tailed.
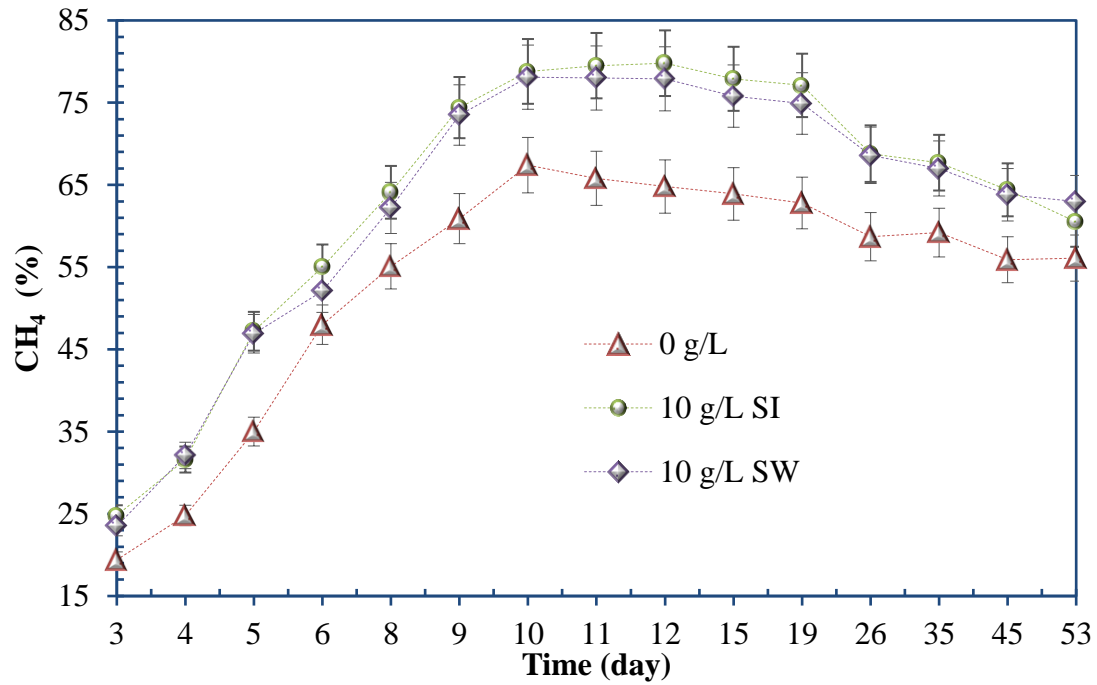
(a)
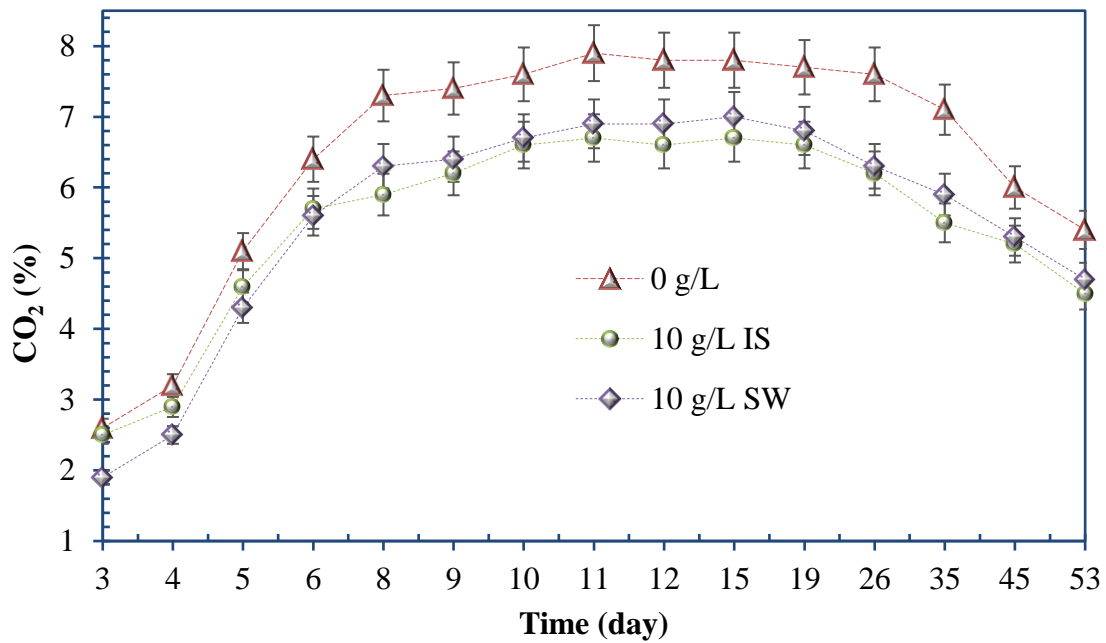
(b)

Figure 18: **Effects of Fe⁰ types on biogas production: (a) variations in CH₄ content; (b) variations in CO₂ concentration**

Effects of Fe^0 types on biogas production: (a) variations in CH_4 content; (b) variations in CO_2 concentration
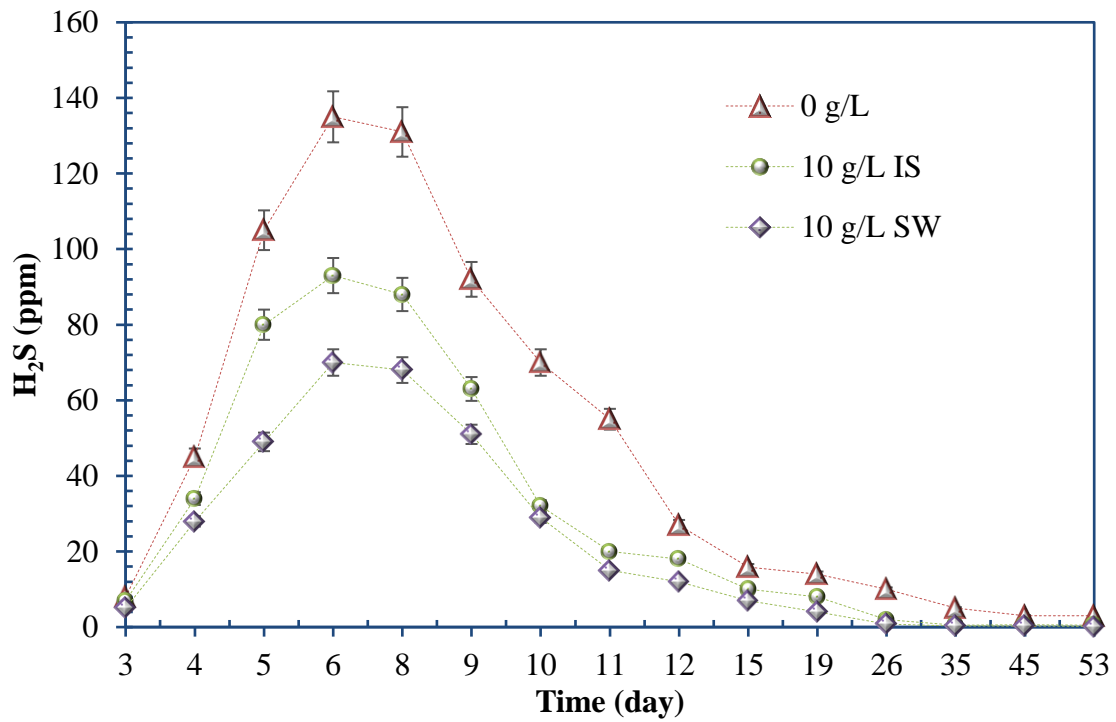
(a)
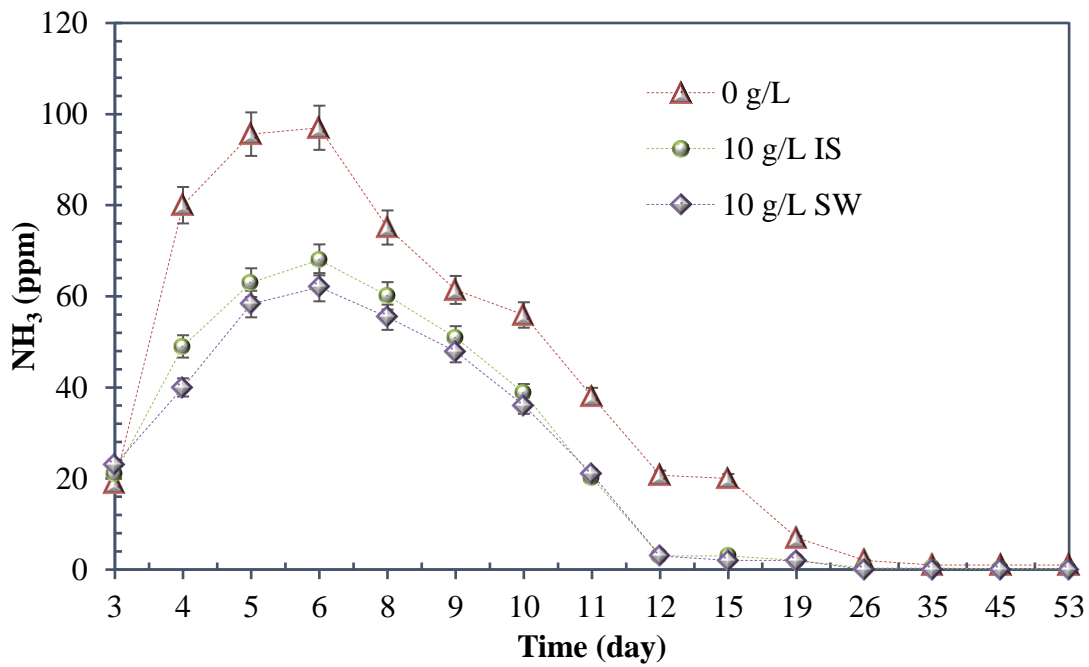
(b)

Figure 19: Effects of Fe^0 types on biogas production: (a) variations in H_2S content; (b) variation in NH_3 concentration
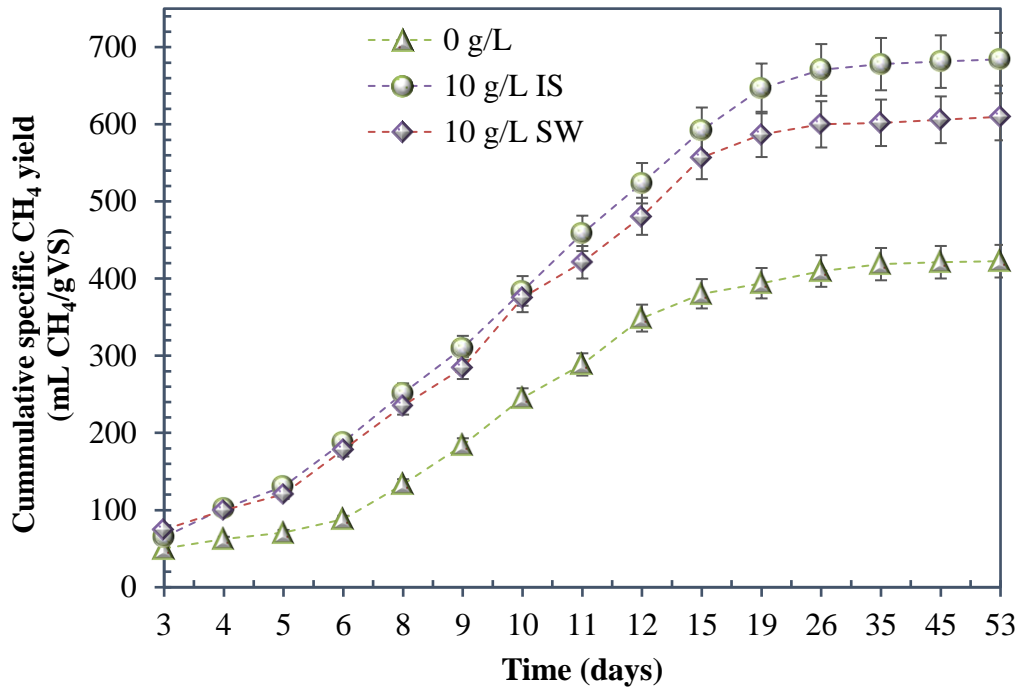
(a)
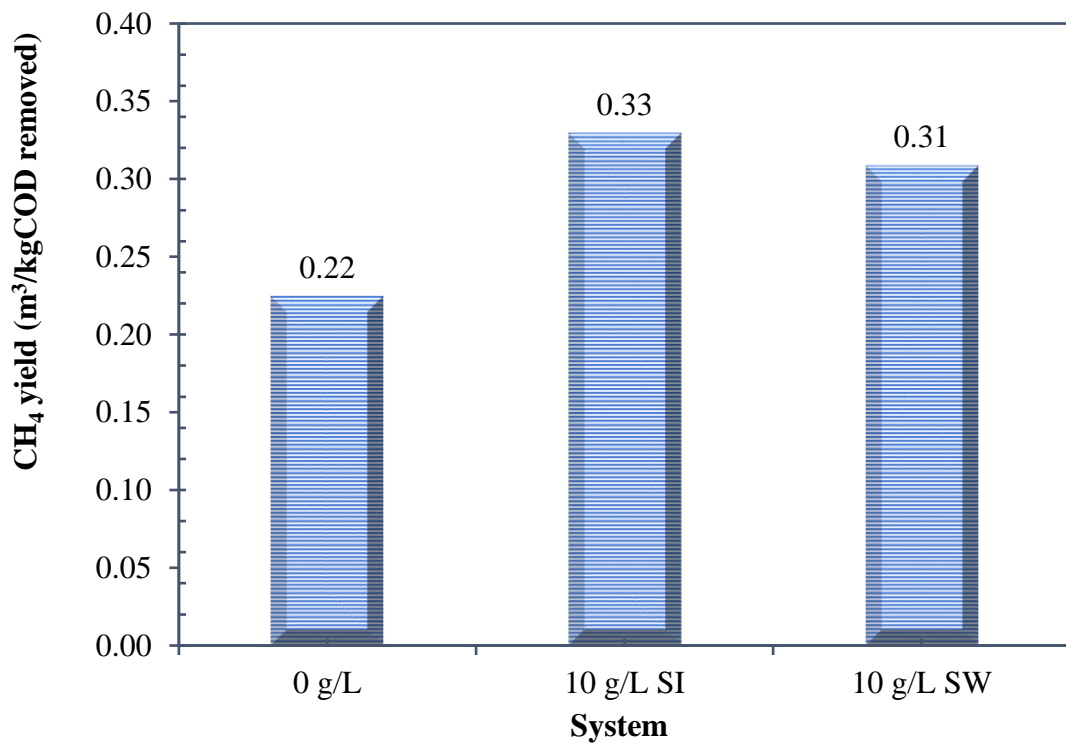
(b)

Figure 20: **Effects of Fe⁰ types on biogas production; (a) cumulative specific CH₄ yield, and (b) CH₄ yield**

However, no distinguishable difference was observed in the observed CO_2 content in the biogas between 10 g/L SI (M = 5.5%, SD = 1.4) and 10 g/L SW (M = 5.6%, SD = 1.6%), t(14) = -1.0, p > 0.05, two-tailed; (c) A significant difference was noted in the observed H_2S content between biogas produced in 0 g/L (M = 47.9 ppm, SD = 47.6 ppm) and 10 g/L SI (M = 33.8 ppm, SD = 30.4 ppm), t(14) = 4.3, p < 0.05, two-tailed, or 10 g/L SW (M = 22.6%, SD = 25.2%), t(14) = 4.2, p < 0.05, two-tailed. However, a significant difference was observed in the H_2S content in the biogas between 10 g/L SI (M = 33.8 ppm, SD = 30.4 ppm) and 10 g/L SW (M = 25.2 ppm, SD = 22.6 ppm), t(14) = 3.2, p < 0.05, two-tailed. (iv) A significant difference was found in the observed NH_3 content between biogas produced in 0 g/L (M = 38.3 ppm, SD = 36.0 ppm) and 10 g/L SI (M = 25.3 ppm, SD = 26.7 ppm), t(14) = 4.3, p < 0.05, two-tailed, or 10 g/L SW (M = 23.4%, SD = 24.3%), t(14) = 4.1, p < 0.05, two-tailed.

Conversely, a significant difference was observed in the NH_3 content in the biogas between 10 g/L SI (M = 25.3 ppm, SD = 26.7 ppm) and 10 g/L SW (M = 23.4 ppm, SD = 24.3 ppm), t(14) = 2.5, p < 0.05, two-tailed. The statistics suggest that: (a) the addition of Fe^0 materials in anaerobic digestion of domestic sewage increases the CH_4 content and decreases the CO_2, H_2S, and NH_3 contents in biogas; (b) the addition of either SI or SW materials in Fe^0-aided anaerobic digestion of domestic sewage results in the production of biogas with similar CH_4 and CO_2 but significantly different H_2S and NH_3 contents.

Biogas production with a higher CH_4 yield and content in the reactors containing Fe^0 compared to the control reactor is likely attributed to enhanced methanogenesis facilitated by Fe^0 materials (Boontian, 2015b; Ganzoury & Allam, 2015; Liu *et al.,* 2021; Ma *et al.,* 2015; Xu *et al.,* 2017; Ye *et al.,* 2021; Zhang *et al.,* 2020; Zhang *et al.,* 2020; Zhao *et al.,* 2021). For instance, in contrast to the 38.3% increase in CH_4 production reported in this study, other studies have shown that the addition of Fe^0 in anaerobic wastewater treatment increased CH_4 production by 28% in anaerobic digestion of brewery wastewater (Carpenter *et al.,* 2015), 26% in the anaerobic digestion of sulfate-rich wastewater (Paepatung *et al.,* 2020), 50% in cattle-dung slurry AD (Abdelsalam *et al.,* 2016), 58% in the AD of cassava pulp and its wastewater (Pyae *et al.,* 2019), 27%, 30%, 40.4%, 46.1%, 117%, and 120% in anaerobic digestion of sludge (Liu *et al.,* 2015; Su *et al.,* 2013a; Wang *et al.,* 2016; Wei *et al.,* 2018; Yu *et al.,* 2016), 230% in the anaerobic digestion of cheese whey (Charalambous & Vyrides, 2021), 74% in the digestion of palm oil mill wastewater (Domrongpokkaphan *et al.,* 2021), and 26.2%, 52.6%, 64.7%, and 49.9% in the digestion of potato starch processing wastewater (Antwi *et al.,* 2017).

Similarly, compared to the 12.4% increase in CH_4 content reported in this study, other research has shown that the addition of Fe^0 in wastewater treatment increased CH_4 content by 6.93% in sludge AD systems (Jia *et al.,* 2017), 5.1% to 13.2% in the digestion of wastewater sludge (Su *et al.,* 2013a), and 40% in the digestion of cassava pulp and its wastewater (Pyae *et al.,* 2019).

The generation of biogas with comparatively lower CO_2 contents in the reactors treated with Fe^0 materials, as opposed to the control reactor, can be attributed to the capability of Fe^0 materials to act as an electron donor, facilitating the reduction of CO_2 to CH_4, as explained in other studies (Abdelsalam *et al.,* 2017; Belay & Daniels, 1990; Lytras *et al.,* 2021a; Ma *et al.,* 2018). The corrosion of Fe^0 materials releases H_2 (Equation (4)), which is subsequently utilized during the conversion of CO_2 to CH_4 (Equation (3)) (Eljamal *et al.,* 2022). In contrast to the 15.2% maximum decrease in CO_2 production reported in this study with 10 g/L SI, other studies have indicated that the addition of Fe^0 in anaerobic digestion reduced CO_2 production by 58% in the anaerobic digestion of synthetic wastewater with a 5 g/L dosage of nano-scale Fe^0 (Carpenter *et al.,* 2015) and 25% in the anaerobic digestion of sulfate-rich wastewater with Fe^0 powder (Paepatung *et al.,* 2020).

The lower H_2S content observed in the biogas from Fe^0-aided reactors is possibly a result of Iron-Sulphide (FeS) precipitation (Equation (8)) or a higher pH range (7.1 – 7.8) in the reactors with Fe^0 materials compared to the pH range (6.8 – 7.3) in the control reactor (without Fe^0), as reported elsewhere (Andriamanohiarisoamanana *et al.,* 2018; Lytras *et al.,* 2021a; Ruan *et al.,* 2017; Su *et al.,* 2013a; Hvitved-Jacobsen, 2013; Zhang *et al.,* 2011). In contrast to the 48.1% maximum reduction in H_2S production observed in this study with 10 g/L SW, prior research has demonstrated that incorporating Fe^0 in anaerobic digestion led to a 98% decrease in H_2S production in the anaerobic digestion of wastewater sludge with 0.10 wt% of nano-scale Fe^0 (Zhang *et al.,* 2011) and a 50% decrease in the anaerobic digestion of wastewater containing sulfate (Zhang *et al.,* 2011).

The relatively diminished NH_3 content in the biogas from reactors treated with Fe^0 materials may be attributed to the reactors' potential to convert available nitrogen more into N_2 and N_2O rather than other forms (NH_4^+ or NH_3) (Till *et al.,* 1998) and the precipitation of nitrogen as ($FeNH_4PO_4.H_2O$) (Booker *et al.,* 1999; Bridger *et al.,* 1962; Zhou *et al.,* 2018). The lower NH_3 content in the reactor dosed with SW compared to the SI reactor is likely due to the higher reactivity of SW materials compared to SI materials (Section 4.1). In comparison to the 80% maximum reduction in NH_3 production with 10 g/L SI reported in this study, it was noted that

the addition of zero-valent Iron Scrap in the anaerobic digestion of sludge resulted in an 82% decrease in NH_3 production compared to the reactor without Fe^0 materials (Lytras *et al.,* 2021a). The presence of gaseous impurities, such as H_2S and NH_3, can pose significant challenges in AD systems due to their potential to hinder the AD process (Mutegoa *et al.,* 2020; Richard *et al.,* 2019). However, incorporating Fe^0 into the AD of domestic sewage offers a solution to this issue. This is because the addition of Fe^0 material in the AD process generates biogas with comparatively lower concentrations of gaseous impurities, specifically H_2S and NH_3, compared to the scenario where Fe^0 material is not employed.

4.3.4   Kinetic Study of Methane Production

Table 12 shows the observed and predicted cumulative CH_4 generation results and the kinetic parameters derived from average cumulative CH_4 production curves. The cumulative CH_4 production values for the 0 g/L (control reactor), 10 g/L SI, and 10 g/L SW were as follows: 422.6, 684.3, and 609.8 mLCH$_4$/gVS for the observed data; 421.6, 700.6, and 618.1 mLCH$_4$/gVS for the Gompertz model; 434.0, 706.2, and 627.9 mLCH$_4$/gVS for the Logistic model; and 432.1, 695.5, and 618.8 mLCH$_4$/gVS for the Richard model (Table 12). The higher cumulative CH_4 production observed in the Fe^0-aided reactors in both experimental and predicted results is likely attributed to the material's potential to enhance methanogenesis, as elaborated in Section 4.2.1.

Table 12 reveals that the microbial adaptation and initiation of biogas production (lag phase, λ) occur more quickly (approximately 2 days) in reactors treated with Fe^0 materials than in the control reactor (about 3 days). In the initial seven days of reactor operation, there is a comparatively minor decrease in pH in Fe^0-assisted reactors compared to the control (reactor without Fe^0 materials). Specifically, the pH decreases from 7.3 to 6.8 in the 0 g/L (control) reactor, 7.3 to 7.1 in the 10 g/L SI reactor, and 7.3 to 7.2 in the 10 g/L SW reactor.

Table 12: Kinetic parameters of average cumulative methane production curves

Parameter	Model	0 g/L	10 g/L SI	10 g/L SW
CH_4 yield. V_0 (mLCH$_4$/gVS)	Experimental	422.6	684.3	609.8
	Gompertz	421.6	700.6	618.1
CH_4 yield, A (mLCH$_4$/gVS)	Logistic	434.0	706.2	627.9
	Richards	432.1	695.5	618.8
	Gompertz	49.3	62.0	62.5
μ_m (mL/gVS/d)	Logistic	48.7	70.7	59.8
	Richards	41.1	56.6	51.7
	Gompertz	3.1	2.0	2.1
λ (days)	Logistic	3.0	2.1	2.0
	Richards	3.1	2.0	2.0
	Gompertz	–	–	–
v	Logistic	–	–	–
	Richards	2.3	2.4	2.4
	Gompertz	0.997	0.969	0.994
R^2	Logistic	0.933	0.964	0.960
	Richards	0.984	0.994	0.993
	Gompertz	0.25	2.37	1.37
Difference between V_0 and A (%)	Logistic	2.68	3.20	2.98
	Richards	2.23	1.63	1.48

The decline in pH may be attributed to two primary factors: The introduction of inoculum into the systems and acidogenesis (a second stage of anaerobic digestion). The acidogenesis is linked to the generation of volatile fatty acids (VFA), particularly butyrate, propionate, and valerate (Metcalf *et al.,* 2014; Riffat & Husnain, 2022). The accumulation of VFA has been identified as a contributor to prolonged lag phases in anaerobic digestion (Hlavínek *et al.,* 2016). Moreover, research elsewhere (Zhai *et al.,* 2015) suggests that a good buffering capacity in the initial stages of AD can mitigate the lag phase. Similarly, the initial pH has been found

to influence the latency period (λ) in the anaerobic digestion of vinasse, with optimal conditions for biogas production observed at an initial pH of 7 (Budiyono & Sumardiono, 2014).

Hence, in reactors treated with Fe^0 materials, a portion of the hydroxyl iron (OH^-) released during the anaerobic oxidation of Fe^0 (Equation (4)) undergoes neutralization. Consequently, the pH in these reactors is effectively controlled. Evidently, the pH regulation facilitated by Fe^0 materials played a role in reducing the time required for microbial adaptation and the initiation of CH_4 generation in comparison to the control reactor (0 g/L).

In the case of the control reactor (0 g/L), the variance between the observed biogas yield (V_0) and the predicted yield (A) was 0.25% according to the modified Gompertz model. This difference is lower than 2.23% for the Richards model or 2.68% for the Logistic model (Table 12). Therefore, among the models tested, the modified Gompertz model excelled in modelling CH_4 production in the anaerobic digestion of domestic sewage, as it exhibited the most minor difference between V_0 and A. Conversely, for the 10 g/L SI reactor, the disparity between the observed and predicted biogas yield was 1.63% based on the Richards model. This difference is less than 2.37% for the Gompertz model or 3.20% for the Logistic model.

Among the models examined, the Richard model demonstrated superior performance in predicting methane (CH_4) production during the anaerobic digestion of domestic sewage with Iron Scrap supplementation. Specifically, for a 10 g/L SW reactor, the difference between observed and predicted biogas yield was 1.37% for the Gompertz model, a value slightly lower than 1.48% for the Richards model and significantly less than 2.98% for the Logistic model. Consequently, in the context of the steel wool-aided anaerobic digestion of domestic sewage, the modified Gompertz model exhibited remarkable accuracy in modeling CH_4 production.

It is worth noting that a fitting error of equal to or less than 10% between observed and predicted biogas yield is generally considered favorable in various studies (Kafle *et al.,* 2013; Raposo *et al.,* 2009; Ugwu & Enweremadu, 2019). Therefore, based on the findings outlined in Table 12 and Figs. 21 and 22 all tested models (Gompertz, Logistic, and Richard) demonstrated generally good fitting errors (error < 10%) in predicting CH_4 production in Fe^0-aided anaerobic digestion of domestic sewage.

However, the Richards model consistently demonstrated the best fit for forecasting CH_4 production from Fe^0 (SI and SW)-aided anaerobic digestion of domestic sewage (Figs. 21 & 22). This is evident from its lowest fitting error, ranging from 1.63% to 1.48%, compared to

1.37% to 2.37% for the Gompertz model and 2.98% to 3.20% for the Logistic model (Table 12).

In evaluating the Gompertz, Logistic, and Richards models for predicting methane yield from anaerobic digesters dosed with Fe^0 materials, the Richards model demonstrated the highest accuracy. This conclusion is derived from the average correlation coefficients (R^2 values) for reactors dosed with either steel wool or iron scraps. Specifically, the Richards model achieved an average R^2 value of 0.994, indicating an almost perfect fit to the experimental data. In comparison, the Gompertz model had a slightly lower average R^2 value of 0.982, while the Logistic model had the lowest average R^2 value of 0.962. These results suggest that while all three models accurately predict methane yield, the Richards model is the most reliable and precise. Therefore, among the three models, for applications requiring the most accurate prediction of methane production in anaerobic digesters dosed with ZVI, the Richards model is the superior choice.
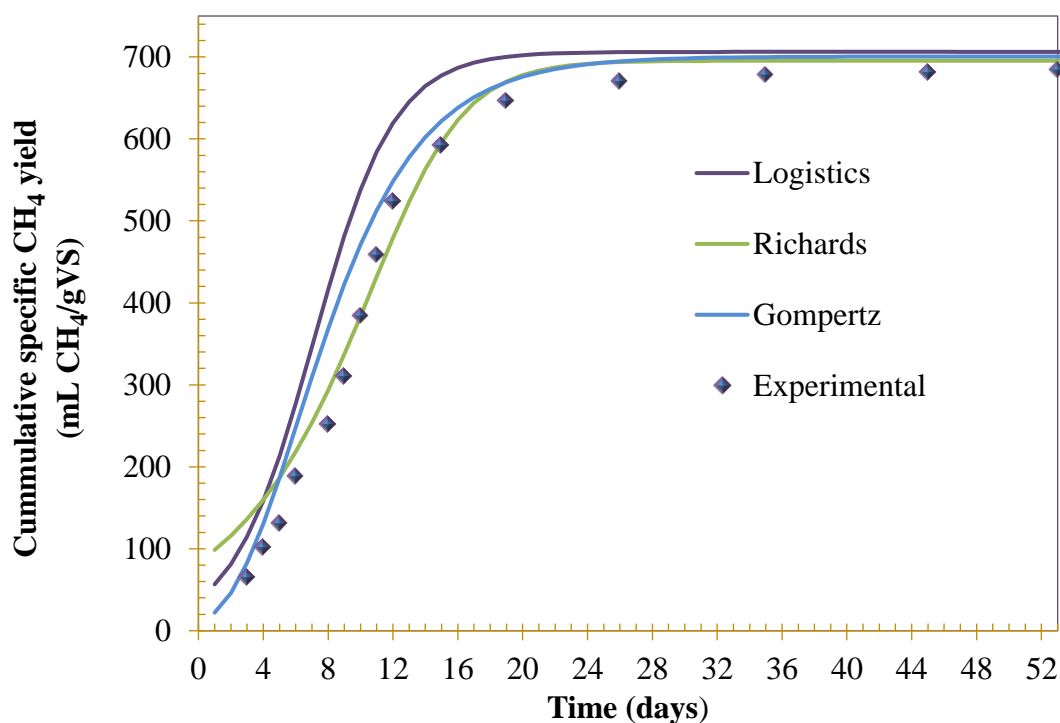
Figure 21:   Cumulative experimental methane production and their fit with models for 0 g/L reactor (control)
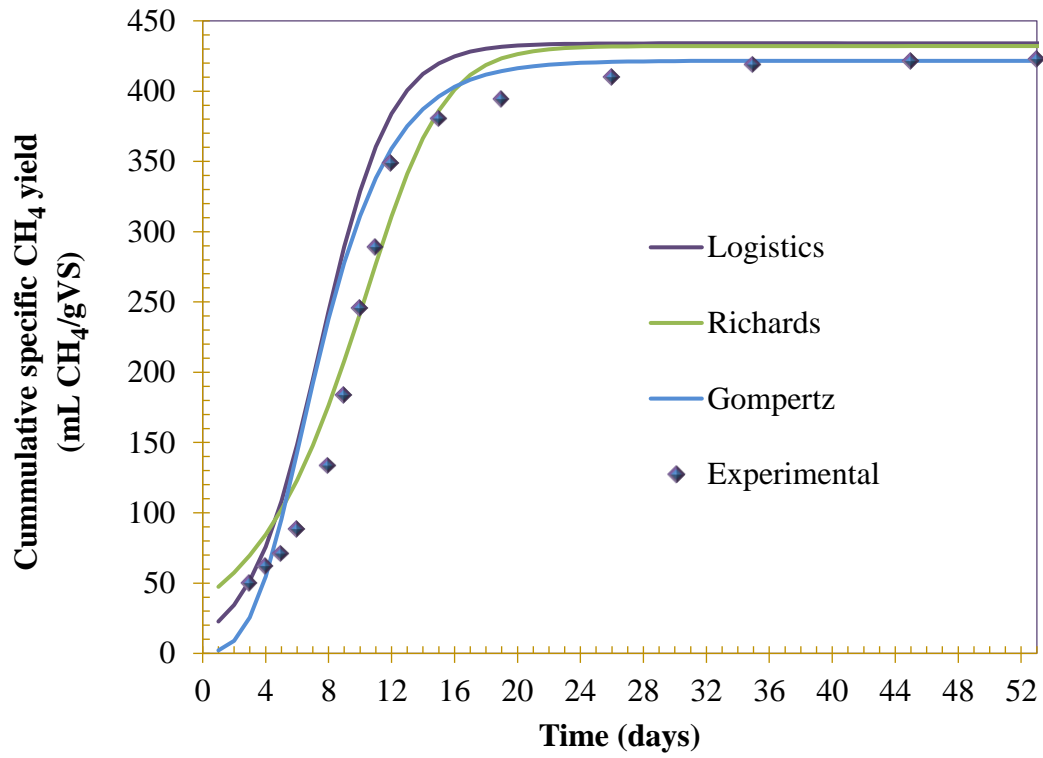
(a)
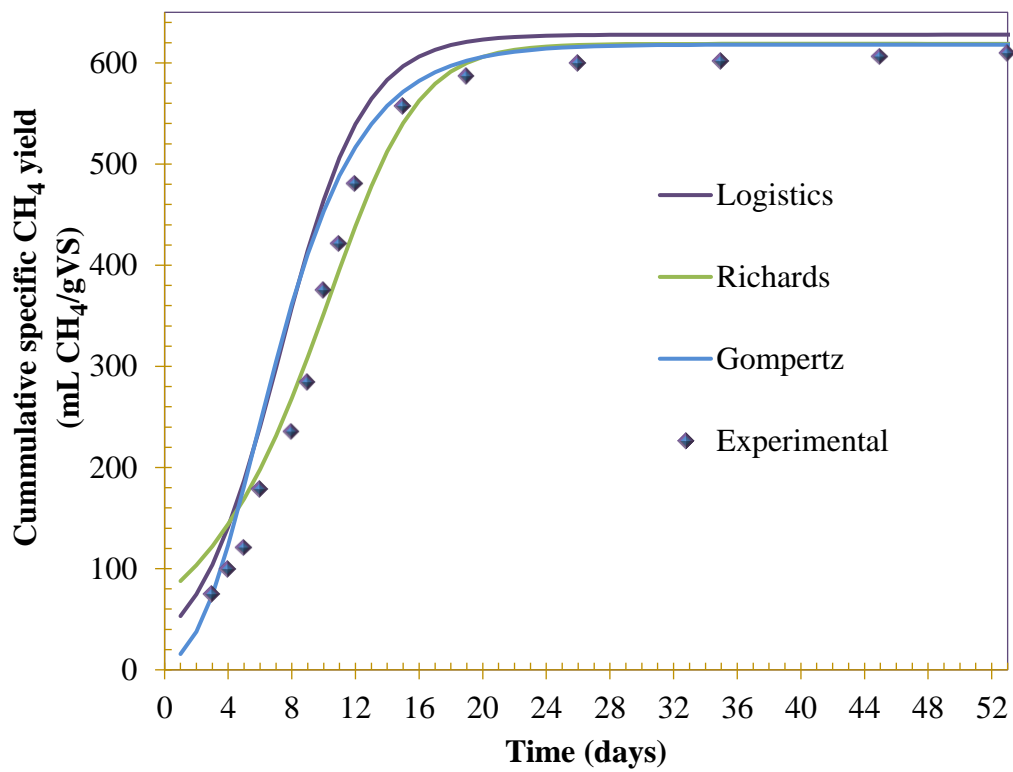
(b)

Figure 22: **Cumulative experimental methane production and their fit with models: (a) 10 g/L SI reactor, and (b) 10 g/L SW reactor**

CHAPTER FIVE

CONCLUSION AND RECOMMENDATIONS

5.1   Conclusion

This research reveals a significant improvement in anaerobic systems for the simultaneous removal of organics and nutrients from domestic sewage by incorporating Fe^0 materials. In the optimally performing reactor (10 g/L SI), minimum residual concentrations of COD (50 mg/L), $NO_3^- + NH_4^+$ (43.8 mg/L), and PO_4^{3-} (0.3 mg/L) were observed, demonstrating the potential to meet Tanzanian effluent discharge standards, which permit a maximum COD level of 60 mg/L for effluents discharged into surface waters, ensuring environmental safety. Consequently, a single anaerobic reactor incorporating Fe^0 materials can potentially achieve the required COD discharge limits, enhancing the cost-efficiency of anaerobic wastewater treatment compared to conventional methods that typically require multiple reactors. Similarly, despite the negligible performance in nutrient removal by anaerobic digestion systems, this research shows the potential to achieve a nutrient removal efficiency of 98% for PO_4^{3-} and 40% for $NO_3^- + NH_4^+$ in Fe^0-supported anaerobic digestion systems. Thus, the study suggests that iron scraps, typically considered waste, can potentially be used in these systems to simultaneously remove organics and nutrients.

Furthermore, dosing Fe^0 materials in the anaerobic digestion of domestic sewage led to a notable increase in the biogas's methane (CH_4) content. Specifically, CH_4 production increased by 12.4% using Scrap Iron materials and 11.5% with Steel Wool materials. This enhanced methane content highlights the potential for improved energy recovery from the biogas generated during the AD process with iron scraps, usually considered as wastes.

Moreover, adding ZVI materials in the anaerobic digestion of domestic sewage significantly reduced gaseous impurities in biogas, with CO_2 decreasing by more than 13%, H_2S by over 29%, and NH_3 by more than 34%. Consequently, this study indicates that iron scraps can effectively mitigate the inhibition of anaerobic digestion caused by H_2S and NH_3, producing biogas with a significantly lower percentage of gaseous impurities. Furthermore, the study found that the Richard model can effectively predict CH_4 production in domestic sewage anaerobic digestion systems dosed with Fe^0 materials.

Reactors dosed with Fe^0 materials produced sludge with relatively higher concentrations of nutrients and toxic elements. Despite the increased levels of toxic elements, these concentrations remain below the recommended ceiling limits for land application recommended by the Environmental Protection Agency (EPA), ensuring the sludge's safety for agricultural use. The Fe^0-aided anaerobic digestion of the domestic sewage also resulted in sludge with good settling properties, as indicated by a sludge volume index (SVI) of less than 100. This characteristic enhances the efficiency of solids removal. Concerning the settling behavior of solids, this study found that over 80% of the solids produced from the Fe^0-aided anaerobic digestion of domestic sewage can be effectively removed using sedimentation tanks designed with an overflow rate of 40 meters per day or less.

5.2   Recommendations

(i)   Despite the positive findings reported, this study has several limitations. It did not address factors such as reactant mixing, the impact of varying Fe^0 material sizes, effects of the trace elements found in the Fe^0 materials on the anaerobic digestion system, as indicated by the composition results monitoring of enzymatic activities and reduction-oxidation potential, the effect of Fe^0 on sludge dewaterability, the long-term implications of applying sludge containing Fe^0 corrosion products to agricultural land, and the economic aspects of using Fe^0 materials in anaerobic digestion. Moreover, Fe^0 materials were not tested in pilot or full-scale studies. The study also did not systematically compare Fe^0 materials, such as Iron Scraps and Steel Wool, based on their total exposed reactive areas, focusing instead on their concentration weight per volume. Given that IS and SW have different exposed reactive areas despite identical dosages, evaluating these materials by their reactive surface area is crucial for accurately assessing their effectiveness. Furthermore, the study did not use continuous flow reactors. Therefore, it is recommended that these limitations be recognized as key factors driving the need for further research and exploration on similar topics.

(ii)   Optimization studies for Fe^0 dosages tailored to each case are recommended to achieve the desired outcomes because the dissolution of Fe^0 material depends on the specific type of Fe^0 material and the characteristics of the dissolving media.

(iii)   Given the encouraging outcomes regarding the capacity of Fe^0 materials to reduce the concentrations of H_2S and NH_3, it is strongly advised to conduct comprehensive tests

on the application of Fe^0 in mitigating the inhibition caused by H_2S and NH_3 in anaerobic digestion systems. This recommendation is based on the potential of Fe^0 to effectively counteract the inhibitory effects of H_2S and NH_3 within anaerobic digestion processes, indicating a promising avenue for enhancing such systems' overall efficiency and stability.

REFERENCES

Abdel-Shafy, H. I., & Mansour, M. S. (2014). Biogas production as affected by heavy metals in the anaerobic digestion of sludge. *Egyptian Journal of Petroleum*, *23*(4), 409-417.

Abdelsalam, E., Samer, M., Attia, Y., Abdel-Hadi, M., Hassan, H., & Badr, Y. (2016). Comparison of nanoparticles effects on biogas and methane production from anaerobic digestion of cattle dung slurry. *Renewable Energy*, *87*, 592-598.

Abdelsalam, E., Samer, M., Attia, Y., Abdel-Hadi, M., Hassan, H., & Badr, Y. (2017). Influence of zero valent iron nanoparticles and magnetic iron oxide nanoparticles on biogas and methane production from anaerobic digestion of manure. *Energy*, *120*, 842-853.

Akteke-Ozturk, B., Koksal, G., & Weber, G. W. (2018). Nonconvex optimization of desirability functions. *Quality Engineering*, *30*(2), 293-310.

Akunna, J. C. (2018). *Anaerobic waste-wastewater treatment and biogas plants: A practical handbook*. CRC Press.

ALI, M. M., Nourou, D., BILAL, B., & Ndongo, M. (2018). Theoretical models for prediction of methane production from anaerobic digestion: A critical review. *International Journal of Physical Sciences*, *13*(13), 206-216.

Alidadi, H., Najafpoor, A., & Parvaresh, A. (2007). Determination of carbon/nitrogen ratio and heavy metals in bulking agents used for sewage composting. *Pakistan Journal of Biological Sciences*, *10*(22), 4180-4182.

Almeelbi, T., & Bezbaruah, A. (2014). Aqueous phosphate removal using nanoscale zero-valent iron. In *Nanotechnology for Sustainable Development*, 197-210. Springer International Publishing.

Alrawashdeh, K. A. B., Gul, E., Yang, Q., Yang, H., Bartocci, P., & Fantozzi, F. (2020). Effect of heavy metals in the performance of anaerobic digestion of olive mill waste. *Processes*, *8*(9), 1146.

Aly, M., Hashmi, M., Olabi, A., Benyounis, K., Messeiry, M., Hussain, A., & Abadir, E. (2012). Optimization of alkaline treatment conditions of flax fiber using Box-Behnken method. *Journal of Natural Fibers*, *9*(4), 256-276.

Andriamanohiarisoamanana, F. J., Shirai, T., Yamashiro, T., Yasui, S., Iwasaki, M., Ihara, I., Nishida, T., Tangtaweewipat, S., & Umetsu, K. (2018). Valorizing waste iron powder in biogas production: Hydrogen sulfide control and process performances. *Journal of Environmental Management*, *208*, 134-141.

An, F., Feng, X., Dang, Y., & Sun, D. (2022). Enhancing nitrate removal efficiency of micro-sized zero-valent iron by chitosan gel balls encapsulating. *Science of the Total Environment, 823,* 153641.

Antwi, P., Li, J., Boadi, P. O., Meng, J., Shi, E., Chi, X., Deng, K., & Ayivi, F. (2017). Dosing effect of zero valent iron (ZVI) on biomethanation and microbial community distribution as revealed by 16S rRNA high-throughput sequencing. *International Biodeterioration & Biodegradation*, *123*, 191-199.

Antwi, P., Zhang, D., Luo, W., Kabutey, F. T., Li, J., Su, H., Wu, M., & Liu, Z. (2020). Response of hydrolysis, methanogenesis, and microbial community structure to iron dose during anaerobic digestion of food waste leachate. *Biomass Conversion and Biorefinery*, 1-15.

Bai, H., Kang, Y., Quan, H., Han, Y., Sun, J., & Feng, Y. (2013). Bioremediation of copper-containing wastewater by sulfate reducing bacteria coupled with iron. *Journal of Environmental Management*, *129*, 350-356.

Bakraoui, M., Karouach, F., Ouhammou, B., Aggour, M., Essamri, A., & El-Bari, H. (2019). Kinetics study of the methane production from experimental recycled pulp and paper sludge by CSTR technology. *Journal of Material Cycles and Waste Management*, *21*(6), 1426-1436.

Barahmand, Z., & Samarakoon, G. (2022). Sensitivity analysis and anaerobic digestion modeling: A scoping review. *Fermentation, 8*(11), 624.

Barahmand, Z., & Samarakoon, G. (2023). Anaerobic digestion process modeling under uncertainty: A narrative review. *International Journal of Energy Production and Management, 8*(1), 41-54.

Barros, A. R., & Silva, E. L. (2012). Hydrogen and ethanol production in anaerobic fluidized bed reactors: Performance evaluation for three support materials under different operating conditions. *Biochemical Engineering Journal*, *61*, 59-65.

Belay, N., & Daniels, L. (1990). Elemental metals as electron sources for biological methane formation from CO_2. *Antonie Van Leeuwenhoek*, *57*(1), 1-7.

Bensaida, K., Eljamal, R., Sughihara, Y., & Eljamal, O. (2021). The impact of iron bimetallic nanoparticles on bulk microbial growth in wastewater. *Journal of Water Process Engineering*, *40*, 101825.

Bhanot, P., Celin, S. M., Sreekrishnan, T., Kalsi, A., Sahai, S., & Sharma, P. (2020). Application of integrated treatment strategies for explosive industry wastewater: A critical review. *Journal of Water Process Engineering*, *35*, 101232.

Booker, N., Priestley, A., & Fraser, I. (1999). Struvite formation in wastewater treatment plants: Opportunities for nutrient recovery. *Environmental Technology*, *20*(7), 777-782.

Boontian, N. (2015b). Effect of zero valent iron (ZVI) in wastewater treatment: A review. *Applied Mechanics and Materials*, *775*, 180-184.

Bridger, G., Salutsky, M. L., & Starostka, R. (1962). Micronutrient sources, metal ammonium phosphates as fertilizers. *Journal of Agricultural and Food Chemistry*, *10*(3), 181-188.

Budiyono, I. S., & Sumardiono, S. (2014). Kinetic model of biogas yield production from vinasse at various initial pH: Comparison between modified Gompertz model and first order kinetic model. *Research Journal of Applied Sciences, Engineering and Technology*, *7*(13), 2798-2805.

Carpenter, A. W., Laughton, S. N., & Wiesner, M. R. (2015). Enhanced biogas production from nanoscale zero valent iron-amended anaerobic bioreactors. *Environmental Engineering Science*, *32*(8), 647-655.

Charalambous, P., & Vyrides, I. (2021). In situ biogas upgrading and enhancement of anaerobic digestion of cheese whey by addition of scrap or powder zero-valent iron (ZVI). *Journal of Environmental Management*, *280*, 111651.

Chen, S., Chen, W., & Shih, C. (2008). Heavy metal removal from wastewater using zero-valent iron nanoparticles. *Water Science and Technology*, *58*(10), 1947-1954,

Chen, S., Tao, Z., Yao, F., Wu, B., He, L., Hou, K., Pi, Z., Fu, J., Yin, H., & Huang, Q. (2020). Enhanced anaerobic co-digestion of waste activated sludge and food waste by sulfidated microscale zerovalent iron: Insights in direct interspecies electron transfer mechanism. *Bioresource Technology*, *316*, 123901.

Chitonge, H., Mokoena, A., & Kongo, M. (2020). Water and sanitation inequality in Africa: Challenges for SDG 6. *Africa and the Sustainable Development Goals*, 207-218.

Chow, W. L., Chong, S., Lim, J. W., Chan, Y. J., Chong, M. F., Tiong, T. J., & Pan, G. T. (2020). Anaerobic co-digestion of wastewater sludge: A review of potential co-substrates and operating factors for improved methane yield. *Processes*, *8*(1), 39.

Curcio, G. M., Limonti, C., Siciliano, A., & Kabdaşlı, I. (2022). Nitrate removal by zero-valent metals: A comprehensive review. *Sustainability*, *14*(8), 4500.

Dai, C., Yang, L., Wang, J., Li, D., Zhang, Y., & Zhou, X. (2022). Enhancing anaerobic digestion of pharmaceutical industries wastewater with the composite addition of zero valent iron (ZVI) and granular activated carbon (GAC). *Bioresource Technology*, *346*, 126566. https://doi.org/10.1016/j.biortech.2021.126566.

Davis, M. L. (2010). *Water and wastewater engineering: Design principles and practice*. McGraw-Hill Education.

Deng, S., Li, D., Yang, X., Xing, W., Li, J., & Zhang, Q. (2016). Biological denitrification process based on the Fe (0)–carbon micro-electrolysis for simultaneous ammonia and nitrate removal from low organic carbon water under a microaerobic condition. *Bioresource Technology*, *219*, 677-686.

Deng, S., Peng, S., Xie, B., Yang, X., Sun, S., Yao, H., & Li, D. (2020). Influence characteristics and mechanism of organic carbon on denitrification, N2O emission and

NO2− accumulation in the iron [Fe (0)]-oxidizing supported autotrophic denitrification process. *Chemical Engineering Journal*, *393*, 124736.

Diatta, J., Waraczewska, Z., Grzebisz, W., Niewiadomska, A., & Tatuśko-Krygier, N. (2020). Eutrophication induction via N/P and P/N ratios under controlled conditions: Effects of temperature and water sources. *Water, Air, & Soil Pollution*, *231*, 1-18.

Dionisi, D. (2017). *Biological wastewater treatment processes: Mass and heat balances*. CRC Press.

Domrongpokkaphan, V., Phalakornkule, C., & Khemkhao, M. (2021). In-situ methane enrichment of biogas from anaerobic digestion of palm oil mill effluent by addition of zero valent iron (ZVI). *International Journal of Hydrogen Energy*, *46*(60), 30976-30987.

Dong, D., Aleta, P., Zhao, X., Choi, O. K., Kim, S., & Lee, J. W. (2019). Effects of nanoscale zero valent iron (nZVI) concentration on the biochemical conversion of gaseous carbon dioxide (CO2) into methane (CH4). *Bioresource Technology*, *275*, 314-320.

Donoso-Bravo, A., Mailier, J., Martin, C., Rodríguez, J., Aceves-Lara, C. A., & Wouwer, A. V. (2011). Model selection, identification and validation in anaerobic digestion: A review. *Water Research, 45*(17), 5347-5364.

Doussan, C., Ledoux, E., & Detay, M. (1998). River-Groundwater Exchanges, Bank Filtration, and Groundwater Quality. *Journal of Environmental Quality, 27*, 1418-1427.

Dykstra, C. M., & Pavlostathis, S. G. (2017). Zero-valent iron enhances biocathodic carbon dioxide reduction to methane. *Environmental Science & Technology*, *51*(21), 12956-12964.

Ekama, G., & Wentzel, M. (2008). Biological wastewater treatment: Principles, modelling and design. *IWA Publishing*.

Elena, T., Ingmar, N., Winkler-Mari, K. H., Vanrolleghem Peter, A., Sophie, B., & Smets-Ilse, Y. (2016). *Settling Tests. Experimental Methods in Wastewater Treatment.* IWA Publishing, London, UK.

97

Eljamal, R., Kahraman, I., Eljamal, O., Thompson, I. P., Maamoun, I., & Yilmaz, G. (2020). Impact of nZVI on the formation of aerobic granules, bacterial growth and nutrient removal using aerobic sequencing batch reactor. *Environmental Technology & Innovation*, *19*, 100911.

Eljamal, R., Maamoun, I., Bensaida, K., Yilmaz, G., Sugihara, Y., & Eljamal, O. (2022). A novel method to improve methane generation from waste sludge using iron nanoparticles coated with magnesium hydroxide. *Renewable and Sustainable Energy Reviews*, *158*, 112192.

Ertugay, N., Kocakaplan, N., & Malkoç, E. (2017). Investigation of pH effect by Fenton-like oxidation with ZVI in treatment of the landfill leachate. *International Journal of Mining, Reclamation and Environment*, *31*(6), 404-411.

Fang, Y., Wu, X., Dai, M., Lopez-Valdivieso, A., Raza, S., Ali, I., Peng, C., Li, J., & Naz, I. (2021). The sequestration of aqueous Cr (VI) by zero valent iron-based materials: From synthesis to practical application. *Journal of Cleaner Production*, *312*, 127678.

Farooqi, Z. H., Begum, R., Naseem, K., Wu, W., & Irfan, A. (2022). Zero valent iron nanoparticles as sustainable nanocatalysts for reduction reactions. *Catalysis Reviews*, *64*(2), 286-355.

Feng, Y., Zhang, Y., Quan, X., & Chen, S. (2014). Enhanced anaerobic digestion of waste activated sludge digestion by the addition of zero valent iron. *Water Research*, *52*, 242-250.

Florea, A. F., Lu, C., & Hansen, H. C. B. (2022). A zero-valent iron and zeolite filter for nitrate recycling from agricultural drainage water. *Chemosphere*, *287*, 131993.

Flores-Alsina, X., Solon, K., Mbamba, C. K., Tait, S., Gernaey, K. V., Jeppsson, U., & Batstone, D. J. (2016). Modelling phosphorus (P), sulfur (S) and iron (Fe) interactions for dynamic simulations of anaerobic digestion processes. *Water Research*, *95*, 370-382.

François, M., Lin, K. S., Rachmadona, N., & Khoo, K. S. (2023). Advancement of nanotechnologies in biogas production and contaminant removal: A review. *Fuel*, *340*, 127470.

Fu, F., Han, W., Tang, B., Hu, M., & Cheng, Z. (2013). Insights into environmental remediation of heavy metal and organic pollutants: Simultaneous removal of hexavalent chromium and dye from wastewater by zero-valent iron with ligand-enhanced reactivity. *Chemical Engineering Journal*, *232*, 534-540.

Ganzoury, M. A., & Allam, N. K. (2015). Impact of nanotechnology on biogas production: A mini-review. *Renewable and Sustainable Energy Reviews*, *50*, 1392-1404.

Grady, C. L., Daigger, G. T., Love, N. G., & Filipe, C. D. (2011). *Biological wastewater treatment*. CRC press.

Gray, N. F. (2004). *Biology of wastewater treatment.* World Scientific.

Günther, S., Koch, C., Hübschmann, T., Röske, I., Müller, R. A., Bley, T., Harms, H., & Müller, S. (2012). Correlation of community dynamics and process parameters as a tool for the prediction of the stability of wastewater treatment. *Environmental Science & Technology*, *46*(1), 84-92.

He, Z. W., Zou, Z. S., Ren, Y. X., Tang, C. C., Zhou, A. J., Liu, W., Wang, L., Li, Z., & Wang, A. (2022). Roles of zero-valent iron in anaerobic digestion: Mechanisms, advances and perspectives. *Science of the Total Environment*, *852*, 158420.

Henze, M., van Loosdrecht, M. C., Ekama, G. A., & Brdjanovic, D. (2008). *Biological wastewater treatment*. IWA publishing.

Hlavínek, P., Stříteský, L., Pešoutová, R., & Houdková, L. (2016). Biogas production from algal biomass from municipal wastewater treatment. *Waste and Biomass Valorization*, *7*(4), 747-752.

Hu, R., Ndé-Tchoupé, A. I., Lufingo, M., Xiao, M., Nassi, A., Noubactep, C., & Njau, K. N. (2019). The impact of selected pretreatment procedures on iron dissolution from metallic iron specimens used in water treatment. *Sustainability*, *11*(3), 671.

Hu, Y., Zang, Y., Yang, Y., Duan, A., Wang, X. C., Ngo, H. H., Li, Y. Y., & Du, R. (2020). Zero-valent iron addition in anaerobic dynamic membrane bioreactors for preconcentrated wastewater treatment: Performance and impact. *Science of the Total Environment*, *742*, 140687.

Hua, G., Salo, M. W., Schmit, C. G., & Hay, C. H. (2016). Nitrate and phosphate removal from agricultural subsurface drainage using laboratory woodchip bioreactors and recycled steel byproduct filters. *Water Research*, *102*, 180-189.

Huang, L. (2013). Optimization of a new mathematical model for bacterial growth. *Food Control*, *32*(1), 283-288.

Hussain, Z., Mishra, J., & Vanacore, E. (2020). Waste to energy and circular economy: The case of anaerobic digestion. *Journal of Enterprise Information Management*, *33*(4), 817-838.

Hvitved-Jacobsen, T., Vollertsen, J., & Nielsen, A. H. (2001). *Sewer processes: Microbial and chemical process engineering of sewer networks*. CRC Press.

Izadi, N., Ali, B. H., Shahin, M. S., & Baghdadi, M. (2022). The removal of Cr (VI) from aqueous and saturated porous media by nanoscale zero-valent iron stabilized with flaxseed gum extract: Synthesis by continuous flow injection method. *Korean Journal of Chemical Engineering*, *39*(8), 2217-2228.

Jamali, M. K., Kazi, T. G., Afridi, H. I., Arain, M. B., Jalbani, N., & Memon, A. R. (2007). Speciation of heavy metals in untreated domestic wastewater sludge by time saving BCR sequential extraction method. *Journal of Environmental Science and Health Part A*, *42*(5), 649-659.

Jia, T., Wang, Z., Shan, H., Liu, Y., & Gong, L. (2017). Effect of nanoscale zero-valent iron on sludge anaerobic digestion. *Resources, Conservation and Recycling*, *127*, 190-195.

Kafle, G. K., Kim, S. H., & Sung, K. I. (2013). Ensiling of fish industry waste for biogas production: A lab scale evaluation of biochemical methane potential (BMP) and kinetics. *Bioresource Technology*, *127*, 326-336.

Kalinowska, A., Szopińska, M., Chmiel, S., Kończak, M., Polkowska, Ż., Artichowicz, W., Jankowska, K., Nowak, A., & Łuczkiewicz, A. (2020). Heavy metals in a high arctic fiord and their introduction with the wastewater: A case study of Adventfjorden-Longyearbyen system, Svalbard. *Water*, *12*(3), 794.

Karki, R., Chuenchart, W., Surendra, K., Shrestha, S., Raskin, L., Sung, S., Hashimoto, A., & Khanal, S. K. (2021). Anaerobic co-digestion: Current status and perspectives. *Bioresource Technology*, *330*, 125001.

Koch, K., Hafner, S. D., Weinrich, S., & Astals, S. (2019). Identification of critical problems in biochemical methane potential (BMP) tests from methane production curves. *Frontiers in Environmental Science*, *7*, 178.

Konadu-Amoah, B., Hu, R., Cui, X., Tao, R., Ndé-Tchoupé, A. I., Gwenzi, W., & Noubactep, C. (2023). Understanding the process of phosphate removal in Fe0/H2O systems using the methylene blue method. *Chemical Engineering Journal*, *465*, 143042.

Konadu-Amoah, B., Hu, R., Ndé-Tchoupé, A. I., Gwenzi, W., & Noubactep, C. (2022a). Metallic iron (Fe0)-based materials for aqueous phosphate removal: A critical review. *Journal of Environmental Management*, *315*, 115157.

Konadu-Amoah, B., Ndé-Tchoupé, A. I., Hu, R., Gwenzi, W., & Noubactep, C. (2022b). Investigating the Fe0/H2O systems using the methylene blue method: Validity, applications, and future directions. *Chemosphere*, *291*, 132913.

Konaté, Y., Maiga, A. H., Casellas, C., & Picot, B. (2013). Biogas production from an anaerobic pond treating domestic wastewater in Burkina Faso. *Desalination and Water Treatment*, *51*(10-12), 2445-2452.

Kong, X., Wei, Y., Xu, S., Liu, J., Li, H., Liu, Y., & Yu, S. (2016). Inhibiting excessive acidification using zero-valent iron in anaerobic digestion of food waste at high organic load rates. *Bioresource Technology*, *211*, 65-71.

Kong, X., Yu, S., Xu, S., Fang, W., Liu, J., & Li, H. (2018). Effect of Fe0 addition on volatile fatty acids evolution on anaerobic digestion at high organic loading rates. *Waste Management*, *71*, 719-727.

Labatut, R. A., Angenent, L. T., & Scott, N. R. (2011). Biochemical methane potential and biodegradability of complex organic substrates. *Bioresource Technology*, *102*(3), 2255-2264.

Latif, M. A., Mehta, C. M., & Batstone, D. J. (2015). Low pH anaerobic digestion of waste activated sludge for enhanced phosphorous release. *Water Research*, *81*, 288-293.

Lee, J. H., Lee, J. H., Kim, S. Y., & Yoon, Y. M. (2023). Effect of Addition of Zero-Valent Iron (Fe) and Magnetite (Fe3O4) on Methane Yield and Microbial Consortium in Anaerobic Digestion of Food Wastewater. *Processes*, *11*(3), 759.

Li, J., Dou, X., Qin, H., Sun, Y., Yin, D., & Guan, X. (2019). Characterization methods of zerovalent iron for water treatment and remediation. *Water Research*, *148*, 70-85.

Li, J., Zheng, G., He, J., Chang, S., & Qin, Z. (2009). Hydrogen-producing capability of anaerobic activated sludge in three types of fermentations in a continuous stirred-tank reactor. *Biotechnology Advances*, *27*(5), 573-577.

Li, R. H., Cui, J.L., Li, X. D., & Li, X. Y. (2018). Phosphorus removal and recovery from wastewater using Fe-dosing bioreactor and cofermentation: Investigation by X-ray absorption near-edge structure spectroscopy. *Environmental Science & Technology*, *52*(24), 14119-14128.

Li, S., Ding, Y., Wang, W., & Lei, H. (2016). A facile method for determining the Fe(0) content and reactivity of zero valent iron. *Analytical Methods*, *8*(6), 1239-1248.

Li, S., Li, L., & Zhang, W. (2023). Nanoscale Zero-Valent Iron (nZVI) for Heavy Metal Wastewater Treatment: A Perspective. *Engineering, 36,* 16-20.

Li, X., Li, Y., Lv, D., Li, Y., & Wu, J. (2020). Nitrogen and phosphorus removal performance and bacterial communities in a multi-stage surface flow constructed wetland treating rural domestic sewage. *Science of the Total Environment*, *709*, 136235.

Li, Y., Guo, X., Dong, H., Luo, X., Guan, X., Zhang, X., & Xia, X. (2018). Selenite removal from groundwater by zero-valent iron (ZVI) in combination with oxidants. *Chemical Engineering Journal*, *345*, 432-440.

Lin, H., Gan, J., Rajendran, A., Reis, C. E. R., & Hu, B. (2015). Phosphorus removal and recovery from digestate after biogas production. *Biofuels-status and Perspective*. IntechOpen.

Liu, M., Wei, Y., & Leng, X. (2021). Improving biogas production using additives in anaerobic digestion: A review. *Journal of Cleaner Production*, *297*, 126666.

Liu, X., Liu, Y., Wang, M., Deng, Q., & Yang, H. (2024). Enhancing corn stalk-based anaerobic digestion with different types of zero-valent iron added during the acidification stage: Performance and mechanism. *Journal of Environmental Sciences*, *145*, 64-74.

Liu, Y., & Wang, J. (2019). Reduction of nitrate by zero valent iron (ZVI)-based materials: A review. *Science of the Total Environment*, *671*, 388-403.

Liu, Y., Wang, Q., Zhang, Y., & Ni, B.-J. (2015). Zero valent iron significantly enhances methane production from waste activated sludge by improving biochemical methane potential rather than hydrolysis rate. *Scientific Reports*, *5*(1), 1-6.

Liu, Y., Zhang, Y., & Ni, B. J. (2015). Zero valent iron simultaneously enhances methane production and sulfate reduction in anaerobic granular sludge reactors. *Water Research*, *75*, 292-300.

Liu, Y., Zhang, Y., Quan, X., Li, Y., Zhao, Z., Meng, X., & Chen, S. (2012). Optimization of anaerobic acidogenesis by adding Fe0 powder to enhance anaerobic wastewater treatment. *Chemical Engineering Journal*, *192*, 179-185.

Liu, Y., Zhang, Y., Zhao, Z., Li, Y., Quan, X., & Chen, S. (2012). Enhanced azo dye wastewater treatment in a two-stage anaerobic system with Fe0 dosing. *Bioresource Technology*, *121*, 148-153.

Lufingo, M., Ndé-Tchoupé, A. I., Hu, R., Njau, K. N., & Noubactep, C. (2019). A Novel and Facile Method to Characterize the Suitability of Metallic Iron for Water Treatment. *Water*, *11*(12), 2465.

Luo, J., Feng, L., Chen, Y., Li, X., Chen, H., Xiao, N., & Wang, D. (2014). Stimulating short-chain fatty acids production from waste activated sludge by nano zero-valent iron. *Journal of Biotechnology*, *187*, 98-105.

Lytras, N., Andronikou, M., Chrysanthou, G., Stylianou, M., Agapiou, A., & Vyrides, I. (2021a). Ex-situ biogas upgrading to methane and removal of VOCs in a system of zero valent iron and anaerobic granular sludge. *Research Square*, *PPR357882.*

Lytras, N., Andronikou, M., Chrysanthou, G., Stylianou, M., Agapiou, A., & Vyrides, I. (2021b). Ex-situ biogas upgrading to methane and removal of VOCs in a system of zero valent iron and anaerobic granular sludge. *Research Square,* 1-18.

Ma, L., Zhou, L., Mbadinga, S. M., Gu, J. D., & Mu, B. Z. (2018). Accelerated CO2 reduction to methane for energy by zero valent iron in oil reservoir production waters. *Energy*, *147*, 663-671.

Ma, L., Zhou, L., Ruan, M. Y., Gu, J. D., & Mu, B. Z. (2019). Simultaneous methanogenesis and acetogenesis from the greenhouse carbon dioxide by an enrichment culture supplemented with zero-valent iron. *Renewable Energy*, *132*, 861-870.

Ma, W., Xin, H., Zhong, D., Qian, F., Han, H., & Yuan, Y. (2015). Effects of different states of Fe on anaerobic digestion: A review. *Journal of Harbin Institute of Technology*, *22*, 69-75.

Mainardis, M., Buttazzoni, M., & Goi, D. (2020). Up-flow anaerobic sludge blanket (UASB) technology for energy recovery: A review on state-of-the-art and recent technological advances. *Bioengineering*, *7*(2), 43.

Mamais, D., Pitt, P. A., Cheng, Y. W., Loiacono, J., & Jenkins, D. (1994). Determination of ferric chloride dose to control struvite precipitation in anaerobic sludge digesters. *Water Environment Research*, *66*(7), 912-918.

Marti, N., Bouzas, A., Seco, A., & Ferrer, J. (2008). Struvite precipitation assessment in anaerobic digestion processes. *Chemical Engineering Journal*, *141*(1-3), 67-74.

Martins, R. C., Lopes, D. V., Quina, M. J., & Quinta-Ferreira, R. M. (2012). Treatment improvement of urban landfill leachates by Fenton-like process using ZVI. *Chemical Engineering Journal*, *192*, 219-225.

McCarty, P. L., Bae, J., & Kim, J. (2011). Domestic wastewater treatment as a net energy producer–can this be achieved? ACS Publications. https://doi.org/10.1021/es2014264.

Mehta, C. M., & Batstone, D. J. (2013). Nutrient solubilization and its availability following anaerobic digestion. *Water Science and Technology*, *67*(4), 756-763.

Meng, X., Sui, Q., Liu, J., Yu, D., Wang, Y., & Wei, Y. (2020). Relieving ammonia inhibition by zero-valent iron (ZVI) dosing to enhance methanogenesis in the high solid anaerobic digestion of swine manure. *Waste Management*, *118*, 452-462.

Meng, X., Zhang, Y., Li, Q., & Quan, X. (2013). Adding Fe0 powder to enhance the anaerobic conversion of propionate to acetate. *Biochemical Engineering Journal*, *73*, 80-85.

Metcalf, Eddy, Abu-Orf, M., Bowden, G., Burton, F. L., Pfrang, W., Stensel, H. D., Tchobanoglous, G., Tsuchihashi, R., & AECOM. (2014). *Wastewater engineering: Treatment and resource recovery*. McGraw Hill Education.

Mohamed, M. A., Nourou, D., Boudy, B., & Mamoudou, N. (2018). Theoretical models for prediction of methane production from anaerobic digestion: A critical review. *International Journal of Physical Sciences*, *13*(13), 206-216.

Moran, S. (2018). *An applied guide to water and effluent treatment plant design*. Butterworth-Heinemann.

Mu, L., Zhang, L., Zhu, K., Ma, J., Ifran, M., & Li, A. (2020). Anaerobic co-digestion of sewage sludge, food waste and yard waste: Synergistic enhancement on process stability and biogas production. *Science of the Total Environment*, *704*, 135429.

Mucha, N. R. (2016). *Electrospun Carbon Nanofibers with Surface Attached Zero Valent Iron Nanoparticles for Heavy Metal Remediation in Ground and Wastewater* (Master's thesis, North Carolina Agricultural and Technical State University).

Mudhoo, A., & Kumar, S. (2013). Effects of heavy metals as stress factors on anaerobic digestion processes and biogas production from biomass. *International Journal of Environmental Science and Technology*, *10*(6), 1383-1398.

Mutegoa, E., Hilonga, A., & Njau, K. N. (2020). Approaches to the mitigation of ammonia inhibition during anaerobic digestion: A review. *Water Practice and Technology*, *15*(3), 551-570.

Narayanasamydamodaran, S., Zuo, J. e., Ren, H., & Kumar, N. (2021). Scrap Iron Filings assisted nitrate and phosphate removal in low C/N waters using mixed microbial culture. *Frontiers of Environmental Science & Engineering*, *15*, 1-14.

Nguyen, V. K., Chaudhary, D. K., Dahal, R. H., Trinh, N. H., Kim, J., Chang, S. W., Hong, Y., La, D. D., Nguyen, X. C., & Ngo, H. H. (2021). Review on pretreatment techniques to improve anaerobic digestion of sewage sludge. *Fuel*, *285*, 119105.

Niu, C., Cai, T., Lu, X., Zhen, G., Pan, Y., Ren, X., Qin, X., Li, W., Tang, Y., & Zhi, Z. (2021). Nano zero-valent iron regulates the enrichment of organics-degrading and hydrogenotrophic microbes to stimulate methane bioconversion of waste activated sludge. *Chemical Engineering Journal*, *418*, 129511.

Niu, J., Kong, X., Li, Q., Zhang, Y., Yuan, J., Liu, J., & Zhang, Y. (2023). Deciphering different effects of ZVI and NaOH on metabolic characteristics in the process of methanogenesis recovery from VFA suppression. *Journal of Environmental Management*, *336*, 117686.

Noubactep, C. (2010). The fundamental mechanism of aqueous contaminant removal by metallic iron. *Water Sa*, *36*(5), 663-670.

Noubactep, C. (2011). On the mechanism of microbe inactivation by metallic iron. *Journal of Hazardous Materials*, *198*, 383-386.

Orbuleţ, O. D., Dăncilă, A. M., Căprărescu, S., Modrogan, C., & Purcar, V. (2022). Nitrates Removal from Simulated Groundwater Using Nano Zerovalent Iron Supported by Polystyrenic Gel. *Polymers*, *15*(1), 61.

Ou, C., Shen, J., Zhang, S., Mu, Y., Han, W., Sun, X., Li, J., & Wang, L. (2016). Coupling of iron shavings into the anaerobic system for enhanced 2, 4-dinitroanisole reduction in wastewater. *Water Research*, *101*, 457-466.

Paepatung, N., Songkasiri, W., Yasui, H., & Phalakornkule, C. (2020). Enhancing methanogenesis in fed-batch anaerobic digestion of high-strength sulfate-rich wastewater using zero-valent scrap iron. *Journal of Environmental Chemical Engineering*, *8*(6), 104508.

Paranjpe, A., Saxena, S., & Jain, P. (2023). A review on performance improvement of anaerobic digestion using co-digestion of food waste and sewage sludge. *Journal of Environmental Management*, *338*, 117733.

Part, C. (1994). EPA Land Application of Sewage Sludge.

Pereira, M. A., & Marques, R. C. (2021). Sustainable water and sanitation for all: Are we there yet? *Water Research*, *207*, 117765.

Pererva, Y., Miller, C. D., & Sims, R. C. (2020). Existing empirical kinetic models in biochemical methane potential (BMP) testing, their selection and numerical solution. *Water*, *12*(6), 1831.

Piro, P., Carbone, M., Penna, N., & Marsalek, J. (2011). Characterization of the settling process for wastewater from a combined sewer system. *Water Research*, *45*(20), 6615-6624.

Pullen, T. (2015). *Anaerobic Digestion-Making Biogas-Making Energy: The Earthscan Expert Guide*. Routledge.

Puyol, D., Flores-Alsina, X., Segura, Y., Molina, R., Padrino, B., Fierro, J., Gernaey, K., Melero, J., & Martinez, F. (2018). Exploring the effects of ZVI addition on resource recovery in the anaerobic digestion process. *Chemical Engineering Journal*, *335*, 703-711.

Pyae, H. A., Aye, W. W., Yossapol, C., & Dararatana, S. (2019). Micro-Particle ZVI Inhibition Threshold in Cassava Pulp Bio-Methanation. *Environment Asia*, *12*, 64-73.

Qasim, S. R., & Zhu, G. (2017). *Wastewater treatment and reuse, theory and design examples, volume 1: Principles and basic treatment*. CRC press.

Raposo, F., Borja, R., Martín, M., Martín, A., De-la-Rubia, M., & Rincón, B. (2009). Influence of inoculum-substrate ratio on the anaerobic digestion of sunflower oil cake in batch mode: Process stability and kinetic evaluation. *Chemical Engineering Journal*, *149*(1-3), 70-77.

Ren, N., Chua, H., Chan, S., Tsang, Y. F., Wang, Y., & Sin, N. (2007). Assessing optimal fermentation type for bio-hydrogen production in continuous-flow acidogenic reactors. *Bioresource Technology*, *98*(9), 1774-1780.

Richard, E. N., Hilonga, A., Machunda, R. L., & Njau, K. N. (2019). A review on strategies to optimize metabolic stages of anaerobic digestion of municipal solid wastes towards enhanced resources recovery. *Sustainable Environment Research*, *29*(1), 1-13.

Riffat, R., & Husnain, T. (2013). *Fundamentals of wastewater treatment and engineering*. CRC Press.

Riffat, R., & Husnain, T. (2022). *Fundamentals of wastewater treatment and engineering*. CRC Press.

Romero-Güiza, M., Vila, J., Mata-Alvarez, J., Chimenos, J., & Astals, S. (2016). The role of additives on anaerobic digestion: A review. *Renewable and Sustainable Energy Reviews*, *58*, 1486-1499.

Ruan, R., Cao, J., Li, C., Zheng, D., & Luo, J. (2017). The influence of micro-oxygen addition on desulfurization performance and microbial communities during waste-activated sludge digestion in a rusty scrap iron-loaded anaerobic digester. *Energies*, *10*(2), 258.

Schädler, S., Burkhardt, C., Hegler, F., Straub, K., Miot, J., Benzerara, K., & Kappler, A. (2009). Formation of cell-iron-mineral aggregates by phototrophic and nitrate-reducing anaerobic Fe (II)-oxidizing bacteria. *Geomicrobiology Journal*, *26*(2), 93-103.

Schievano, A., D'Imporzano, G., Salati, S., & Adani, F. (2011). On-field study of anaerobic digestion full-scale plants (Part I): An on-field methodology to determine mass, carbon and nutrients balance. *Bioresource Technology*, *102*(17), 7737-7744.

Shah, F. A., Mahmood, Q., Rashid, N., Pervez, A., Raja, I. A., & Shah, M. M. (2015). Co-digestion, pretreatment and digester design for enhanced methanogenesis. *Renewable and Sustainable Energy Reviews*, *42*, 627-642.

Sharma, Y., Manro, B., Thakur, P., Khera, A., Dey, P., Gupta, D., Khajuria, A., Jaiswal, P. K., Barnwal, R. P., & Singh, G. (2023). Nanotechnology as a vital science in accelerating biofuel production, a boon or bane. *Biofuels, Bioproducts and Biorefining*, *17*(3), 616-663.

Shi, Y., Liu, T., Chen, S., & Quan, X. (2022). Accelerating anaerobic hydrolysis acidification of dairy wastewater in integrated floating-film and activated sludge (IFFAS) by using

zero-valent iron (ZVI) composite carriers. *Biochemical Engineering Journal*, *177*, 108226.

Show, K. Y., & Lee, D. J. (2017). Anaerobic treatment versus aerobic treatment. *Current Developments in Biotechnology and Bioengineering*, 205-230.

Sleiman, N., Deluchat, V., Wazne, M., Mallet, M., Courtin-Nomade, A., Kazpard, V., & Baudu, M. (2017). Phosphate removal from aqueous solutions using zero valent iron (ZVI): influence of solution composition and ZVI aging. *Colloids and Surfaces A: Physicochemical and Engineering Aspects*, *514*, 1-10.

Sperling, M. V., & De-Lemos-Chernicharo, C. A. (2005). *Biological Wastewater Treatment in Warm Climate Regions*, *1*, 810-810.

Stazi, V., & Tomei, M. C. (2018). Enhancing anaerobic treatment of domestic wastewater: State of the art, innovative technologies and future perspectives. *Science of the Total Environment*, *635*, 78-91.

Su, L., Shi, X., Guo, G., Zhao, A., & Zhao, Y. (2013a). Stabilization of sewage sludge in the presence of nanoscale zero-valent iron (nZVI): Abatement of odor and improvement of biogas production. *Journal of Material Cycles and Waste Management*, *15*(4), 461-468.

Su, L., Shi, X., Guo, G., Zhao, A., & Zhao, Y. (2013b). Stabilization of sewage sludge in the presence of nanoscale zero-valent iron (nZVI): Abatement of odor and improvement of biogas production. *Journal of Material Cycles and Waste Management*, *15*, 461-468.

Subbarao, P. M., D'Silva, T. C., Adlak, K., Kumar, S., Chandra, R., & Vijay, V. K. (2023). Anaerobic digestion as a sustainable technology for efficiently utilizing biomass in the context of carbon neutrality and circular economy. *Environmental Research*, *234*, 116286.

Summer, D., Schöftner, P., Watzinger, A., & Reichenauer, T. G. (2020). Inhibition and stimulation of two perchloroethene degrading bacterial cultures by nano-and micro-scaled zero-valent iron particles. *Science of the Total Environment*, *722*, 137802.

Sun, Y., Li, J., Huang, T., & Guan, X. (2016). The influences of iron characteristics, operating conditions and solution chemistry on contaminants removal by zero-valent iron: A review. *Water Research*, *100*, 277-295.

Tchobanoglous, G., Stensel, H. D., Tsuchihashi, R., Burton, F., Abu-Orf, M., Bowden, G., & Pfrang, W. (2014). *Wastewater Engineering: Treatment and Resource Recovery*. McGraw-Hill Education.

Till, B. A., Weathers, L. J., & Alvarez, P. J. (1998). Fe (0)-supported autotrophic denitrification. *Environmental Science & Technology*, *32*(5), 634-639.

Ugwu, S. N., & Enweremadu, C. C. (2019). Biodegradability and kinetic studies on biomethane production from okra (*Abelmoschus esculentus*) waste. *South African Journal of Science*, *115*(7-8), 1-5.

USEPA. (1994). A Guide for Land Appliers on the Requirements of the Federal Standards for the Use or Disposal of Sewage Sludge. *40 CFR Part 503*, 105.

Wainaina, S., Awasthi, M. K., Sarsaiya, S., Chen, H., Singh, E., Kumar, A., & Taherzadeh, M. J. (2020). Resource recovery and circular economy from organic solid waste using aerobic and anaerobic digestion technologies. *Bioresource Technology*, *301*, 122778.

Wang, Q., Liao, Z., Yao, D., Yang, Z., Wu, Y., & Tang, C. (2021). Phosphorus immobilization in water and sediment using iron-based materials: A review. *Science of the Total Environment*, *767*, 144246.

Wang, T., Zhang, D., Dai, L., Chen, Y., & Dai, X. (2016). Effects of metal nanoparticles on methane production from waste-activated sludge and microorganism community shift in anaerobic granular sludge. *Scientific Reports*, *6*(1), 1-10.

Wang, Y., Wang, D., & Fang, H. (2018). Comparison of enhancement of anaerobic digestion of waste activated sludge through adding nano-zero valent iron and zero valent iron. *RSC Advances*, *8*(48), 27181-27190.

Wang, Y., Wei, W., Wu, S. L., & Ni, B. J. (2020). Zerovalent iron effectively enhances medium-chain fatty acids production from waste activated sludge through improving

sludge biodegradability and electron transfer efficiency. *Environmental Science & Technology*, *54*(17), 10904-10915.

Ware, A., & Power, N. (2017). Modelling methane production kinetics of complex poultry slaughterhouse wastes using sigmoidal growth functions. *Renewable Energy*, *104*, 50-59.

Wei, W., Cai, Z., Fu, J., Xie, G. J., Li, A., Zhou, X., Ni, B. J., Wang, D., & Wang, Q. (2018). Zero valent iron enhances methane production from primary sludge in anaerobic digestion. *Chemical Engineering Journal*, *351*, 1159-1165.

Weiner, R., Matthews, R., & Vesilind, P. A. (2003). *Environmental Engineering*. Elsevier.

Wilkin, R. T., & McNeil, M. S. (2003). Laboratory evaluation of zero-valent iron to treat water impacted by acid mine drainage. *Chemosphere*, *53*(7), 715-725.

Wiśniowska, E., Grobelak, A., Kokot, P., & Kacprzak, M. (2019a). Sludge legislation-comparison between different countries. *Industrial and Municipal Sludge*, 201-224.

Wu, D., Zheng, S., Ding, A., Sun, G., & Yang, M. (2015). Performance of a zero valent iron-based anaerobic system in swine wastewater treatment. *Journal of Hazardous Materials*, *286*,1-6.

Wu, Y., Zhang, J., Tong, Y., & Xu, X. (2009). Chromium (VI) reduction in aqueous solutions by Fe3O4-stabilized Fe0 nanoparticles. *Journal of Hazardous Materials*, *172*(2-3), 1640-1645.

Xiao, M., Hu, R., Ndé-Tchoupé, A. I., Gwenzi, W., & Noubactep, C. (2022). Metallic iron for water remediation: Plenty of room for collaboration and convergence to advance the science. *Water*, *14*(9), 1492.

Xu, H., Che, L., Liu, Y., Tian, Q., Cao, X., Wei, R., Song, X., & Yang, B. (2021). Core-shell ZVI@ carbon composites reduce phosphate inhibition of ZVI dissolution and enhance methane production in an anaerobic sewage treatment. *Water Research*, *199*, 117197.

Xu, R., Xu, S., Zhang, L., Florentino, A. P., Yang, Z., & Liu, Y. (2019). Impact of zero valent iron on blackwater anaerobic digestion. *Bioresource Technology*, *285*, 121351.

Xu, Y., Wang, C., Hou, J., Wang, P., You, G., Miao, L., Lv, B., Yang, Y., & Zhang, F. (2017). Application of zero valent iron coupling with biological process for wastewater treatment: A review. *Reviews in Environmental Science and Biotechnology*, *16*(4), 667-693.

Yamada, C., Kato, S., Ueno, Y., Ishii, M., & Igarashi, Y. (2015). Conductive iron oxides accelerate thermophilic methanogenesis from acetate and propionate. *Journal of Bioscience and Bioengineering*, *119*(6), 678-682.

Yang, Y., Guo, J., & Hu, Z. (2013). Impact of nano zero valent iron (NZVI) on methanogenic activity and population dynamics in anaerobic digestion. *Water Research*, *47*(17), 6790-6800.

Yang, Y., Wang, J., & Zhou, Y. (2019). Enhanced anaerobic digestion of swine manure by the addition of zero-valent iron. *Energy & Fuels*, *33*(12), 12441-12449.

Yang, Y., Yang, F., Huang, W., Huang, W., Li, F., Lei, Z., & Zhang, Z. (2018). Enhanced anaerobic digestion of ammonia-rich swine manure by zero-valent iron: With special focus on the enhancement effect on hydrogenotrophic methanogenesis activity. *Bioresource Technology*, *270*, 172-179.

Ye, W., Lu, J., Ye, J., & Zhou, Y. (2021). The effects and mechanisms of zero-valent iron on anaerobic digestion of solid waste: A mini-review. *Journal of Cleaner Production*, *278*, 123567.

Yin, W., Wu, J., Li, P., Wang, X., Zhu, N., Wu, P., & Yang, B. (2012). Experimental study of zero-valent iron induced nitrobenzene reduction in groundwater: The effects of pH, iron dosage, oxygen and common dissolved anions. *Chemical Engineering Journal*, *184*, 198-204.

You, G., Wang, P., Hou, J., Wang, C., Xu, Y., Miao, L., Lv, B., Yang, Y., & Zhang, F. (2017). The use of zero-valent iron (ZVI)-microbe technology for wastewater treatment with special attention to the factors influencing performance: A critical review. *Critical Reviews in Environmental Science and Technology*, *47*(10), 877-907.

You, Y., Han, J., Chiu, P. C., & Jin, Y. (2005). Removal and inactivation of waterborne viruses using zerovalent iron. *Environmental Science & Technology*, *39*(23), 9263-9269.

Yu, B., Huang, X., Zhang, D., Lou, Z., Yuan, H., & Zhu, N. (2016). Response of sludge fermentation liquid and microbial community to nano zero-valent iron exposure in a mesophilic anaerobic digestion system. *RSC Advances*, *6*(29), 24236-24244.

Yuan, T., Bian, S., Ko, J. H., Liu, J., Shi, X., & Xu, Q. (2020). Exploring the roles of zero-valent iron in two-stage food waste anaerobic digestion. *Waste Management*, *107*, 91-100.

Zang, Y., Yang, Y., Hu, Y., Ngo, H. H., Wang, X. C., & Li, Y. Y. (2020). Zero-valent iron enhanced anaerobic digestion of pre-concentrated domestic wastewater for bioenergy recovery: Characteristics and mechanisms. *Bioresource Technology*, *310*, 123441.

Zhai, N., Zhang, T., Yin, D., Yang, G., Wang, X., Ren, G., & Feng, Y. (2015). Effect of initial pH on anaerobic co-digestion of kitchen waste and cow manure. *Waste Management*, *38*, 126-131.

Zhang, B., Wang, L., & Li, Y. (2019). Fractionation and identification of iron-phosphorus compounds in sewage sludge. *Chemosphere*, *223*, 250-256.

Zhang, J., Chen, Z., Liu, Y., Wei, W., & Ni, B. J. (2022). Phosphorus recovery from wastewater and sewage sludge as vivianite. *Journal of Cleaner Production*, 133439.

Zhang, J., Qu, Y., Qi, Q., Zhang, P., Zhang, Y., Tong, Y. W., & He, Y. (2020). The bio-chemical cycle of iron and the function induced by ZVI addition in anaerobic digestion: A review. *Water Research*, *186*, 116405.

Zhang, J., Zhang, Y., Quan, X., Liu, Y., An, X., Chen, S., & Zhao, H. (2011). Bioaugmentation and functional partitioning in a zero valent iron-anaerobic reactor for sulfate-containing wastewater treatment. *Chemical Engineering Journal*, *174*(1), 159-165.

Zhang, L., Kuroki, A., & Tong, Y. W. (2020). A mini-review on in situ biogas upgrading technologies via enhanced hydrogenotrophic methanogenesis to improve the quality of biogas from anaerobic digesters. *Frontiers in Energy Research*, *8*, 69.

Zhang, Q. Q., Feng, Z. T., Zhou, J. M., Ma, X., Sun, Y. J., Liu, J. Z., Zhao, J. Q., & Jin, R. C. (2023). Roles of Fe (II), Fe (III) and Fe0 in denitrification and anammox process:

Mechanisms, advances and perspectives. *Journal of Water Process Engineering*, *53*, 103746.

Zhang, Y., Feng, Y., & Quan, X. (2015). Zero-valent iron enhanced methanogenic activity in anaerobic digestion of waste activated sludge after heat and alkali pretreatment. *Waste Management*, *38*, 297-302.

Zhang, Y., Jing, Y., Quan, X., Liu, Y., & Onu, P. (2011). A built-in zero valent iron anaerobic reactor to enhance treatment of azo dye wastewater. *Water Science and Technology*, *63*(4), 741-746.

Zhang, Z., Ping, Q., Gao, D., Vanrolleghem, P. A., & Li, Y. (2021). Effects of ferric-phosphate forms on phosphorus release and the performance of anaerobic fermentation of waste activated sludge. *Bioresource Technology*, *323*, 124622.

Zhao, C., Mu, H., Zhao, Y., Wang, L., & Zuo, B. (2018). Microbial characteristics analysis and kinetic studies on substrate composition to methane after microbial and nutritional regulation of fruit and vegetable wastes anaerobic digestion. *Bioresource Technology*, *249*, 315-321.

Zhao, J., Li, Y., & Dong, R. (2021). Recent progress towards in-situ biogas upgrading technologies. *Science of the Total Environment*, *800*, 149667.

Zhao, L., Ji, Y., Kong, D., Lu, J., Zhou, Q., & Yin, X. (2016). Simultaneous removal of bisphenol A and phosphate in zero-valent iron activated persulfate oxidation process. *Chemical Engineering Journal*, *303*, 458-466.

Zhao, Z., Zhang, Y., Li, Y., Quan, X., & Zhao, Z. (2018). Comparing the mechanisms of ZVI and Fe3O4 for promoting waste-activated sludge digestion. *Water Research*, *144*, 126-133.

Zhong, Y., He, J., Zhang, P., Zou, X., Pan, X., & Zhang, J. (2022). Effects of different particle size of zero-valent iron (ZVI) during anaerobic digestion: Performance and mechanism from genetic level. *Chemical Engineering Journal*, *435*, 134977.

Zhou, J., You, X., Niu, B., Yang, X., Gong, L., Zhou, Y., Wang, J., & Zhang, H. (2020). Enhancement of methanogenic activity in anaerobic digestion of high solids sludge by nano zero-valent iron. *Science of the Total Environment*, *703*, 135532.

Zhou, K., Wu, B., Dai, X., & Chai, X. (2018). Development of polymeric iron/zirconium-pillared clinoptilolite for simultaneous removal of multiple inorganic contaminants from wastewater. *Chemical Engineering Journal*, *347*, 819-827.

Zhou, S., Xu, J., Yang, G., & Zhuang, L. (2014). Methanogenesis affected by the co-occurrence of iron (III) oxides and humic substances. *FEMS Microbiology Ecology*, *88*(1), 107-120.

Zwietering, M. H., Jongenburger, I., Rombouts, F. M., & Van't Riet, K. (1990). Modeling of the bacterial growth curve. *Applied and Environmental Microbiology*, *56*(6), 1875-1881. https://doi.org/10.1128/aem.56.6.1875-1881.1990.

RESEARCH OUTPUTS

(i)   Research Papers

Bakari, O., Njau, K. N., & Noubactep, C. (2022). Fe^0-Supported Anaerobic Digestion for Organics and Nutrients Removal from Domestic Sewage. *Water*, *14*(10), 1623.

Bakari, O., Njau, K. N., & Noubactep, C. (2023). Effects of zero-valent iron on sludge and methane production in anaerobic digestion of domestic wastewater. *Case Studies in Chemical and Environmental Engineering*, *8*, 100377.

Cao, V., Bakari, O., Kenmogne-Tchidjo, J. F., Gatcha-Bandjun, N., Ndé-Tchoupé, A. I., Gwenzi, W., ... & Noubactep, C. (2022). Conceptualizing the Fe^0/H_2O System: A Call for Collaboration to Mark the 30th Anniversary of the Fe^0-Based Permeable Reactive Barrier Technology. *Water*, *14*(19), 3120.

(ii)   Poster Presentation

Poster Presentation

POTENTIAL USE OF ZERO-VALENT IRON IN ENHANCING PERFORMANCE AND RESOURCE RECOVERY DURING THE ANAEROBIC DIGESTION OF DOMESTIC SEWAGE

Omari Bakari, Prof. Karoli Njau, and Prof. Chicgoua Noubactep

The Nelson Mandela African Institution of Science and Technology (NM-AIST)

BACKGROUND

Effluents from anaerobic digestion (AD) often need further treatment to meet regulatory standards due to residual COD and the presence of nitrogen (N) and phosphorus (P). Despite AD's effectiveness, significant COD levels remain, necessitating additional treatment. Secondary AD struggles with N and P removal, risking eutrophication. Tertiary treatments like constructed wetlands and SBRs require substantial space and funding, highlighting the need to enhance AD systems. Incorporating zero-valent iron (Fe^0) into anaerobic digesters shows promise for simultaneously removing COD and nutrient from domestic sewage (DS), but systematic studies on its effectiveness are lacking. Existing studies focus on single contaminants at high concentrations, complicating comparisons. Comprehensive evaluations of predictive models for methane (CH_4) yields in Fe^0-supported AD systems are also missing. This study assesses different types and dosages of Fe0 in removing organics (COD) and nutrients (PO_4^{3-} and NO_3^- + NH_4^+), characterizes solids and biogas generated during Fe^0-aided anaerobic digestion, and evaluates performance of models (Logistic, modified Gompertz, and Richard) for predicting CH_4

METHODS

Two distinct experiments were conducted at various scales. In the first experiment, nine lab-scale reactors with DS received varying Fe^0 dosages (0 to 30 g/L) over 32 runs for 76 days at $37 \pm 0.5°C$ to optimize Fe^0 dosages. In the second experiment, bench-scale reactors with DS were fed Fe^0 and operated over 15 runs for 53 days at $24 \pm 3°C$ to assess the impact of Fe^0 on sludge and biogas composition. Iron scraps (SI) and steel wool (SW) were used as Fe^0 sources, with a control experiment receiving no Fe^0 conducted in each case.

RESULTS

The optimal (10 g/L Fe^0 SI) achieved an 88.0% reduction in COD, 98.0% removal of PO_4^{3-}, and 40.0% reduction in NH_4^+ + NO_3^- in AD systems. Reactors dosed with Fe^0 produced nutrient-rich sludge with elevated but safe levels of toxic elements below EPA's limits for agricultural use. Dosing Fe^0 increased methane content by 12.4% with scrap iron and 11.5% with steel wool, enhancing energy recovery from biogas. It also reduced CO_2 by over 13%, H_2S by over 29%, and NH_3 by over 34%. The Richards model, with an average R^2 of 0.994, was the most accurate for predicting methane yield from Fe^0-dosed AD, outperforming the Gompertz (R^2 = 0.982) and

CONCLUSION

Iron scraps, often considered waste, can enhance AD systems by effectively removing organics and nutrients from DS and increasing methane content in biogas, thereby improving energy recovery. The produced sludge has potential for improving soil fertility, exhibits good settling properties, and is practically removable through sedimentation. The Richard model is the most accurate for simulating methane production in Fe0-supported AD systems, surpassing the Logistic and Gompertz models.